



Exclusive dielectron production in ultraperipheral Pb+Pb collisions at $\sqrt{s_{\text{NN}}} = 5.02$ TeV with ATLAS

The ATLAS Collaboration

Exclusive production of dielectron pairs, $\gamma\gamma \rightarrow e^+e^-$, is studied using $\mathcal{L}_{\text{int}} = 1.72 \text{ nb}^{-1}$ of data from ultraperipheral collisions of lead nuclei at $\sqrt{s_{\text{NN}}} = 5.02$ TeV recorded by the ATLAS detector at the LHC. The process of interest proceeds via photon–photon interactions in the strong electromagnetic fields of relativistic lead nuclei. Dielectron production is measured in the fiducial region defined by following requirements: electron transverse momentum $p_{\text{T}}^e > 2.5$ GeV, absolute electron pseudorapidity $|\eta^e| < 2.5$, dielectron invariant mass $m_{ee} > 5$ GeV, and dielectron transverse momentum $p_{\text{T}}^{ee} < 2$ GeV. Differential cross-sections are measured as a function of m_{ee} , average p_{T}^e , absolute dielectron rapidity $|y_{ee}|$, and scattering angle in the dielectron rest frame, $|\cos \theta^*|$, in the inclusive sample, and also with a requirement of no activity in the forward direction. The total integrated fiducial cross-section is measured to be $215 \pm 1(\text{stat.}) \pm_{-20}^{+23}(\text{syst.}) \pm 4(\text{lumi.}) \mu\text{b}$. Within experimental uncertainties the measured integrated cross-section is in good agreement with the QED predictions from the Monte Carlo programs STARLIGHT and SUPERCHIC, confirming the broad features of the initial photon fluxes. The differential cross-sections show systematic differences from these predictions which are more pronounced at high $|y_{ee}|$ and $|\cos \theta^*|$ values.

Contents

1	Introduction	2
2	ATLAS detector	4
3	Data and Monte Carlo simulation samples	5
4	Signal selection and detector corrections	6
5	Background contributions	8
6	Analysis	12
7	Systematic uncertainties	13
8	Results	14
9	Conclusions	17

1 Introduction

Collisions of ultrarelativistic heavy ions provide an opportunity to study not only the strong interactions between nucleons but also processes involving electromagnetic (EM) interactions. This is due to the presence of intense EM fields associated with the ultrarelativistic ions. The EM interactions become dominant at large impact parameters, $b > 2R_A$, where R_A is the ion radius. Such collisions are usually referred to as ultraperipheral collisions (UPC). Comprehensive reviews of UPC physics can be found in Refs. [1, 2].

The EM fields associated with the ultrarelativistic nuclei can be treated as fluxes of quasi-real photons according to the equivalent photon approximation (EPA) formalism [3, 4]. In this approach, the total cross-section for a given process is calculated as a convolution of the photon flux with the elementary production cross-section. Although the same approach is also valid for proton–proton (pp) collisions, the expected cross-sections are strongly enhanced in the heavy-ion (HI) collisions. The photon flux from each nucleus is enhanced by a factor of Z^2 , where Z is the atomic number. That results in a Z^4 enhancement of the cross-sections. For lead (Pb, $Z = 82$), this Z^4 enhancement is 4.5×10^7 . Another advantage of studying photon-induced interactions in UPC HI collisions is the relatively low number of interactions per LHC bunch crossing. The mean number of simultaneous hadronic interactions, μ , is typically at the subpercent level. This provides a clean environment, facilitating the detection of the interaction products, and little contamination from unrelated interactions in the same crossing. With the centre-of-mass energy per nucleon pair available at the Large Hadron Collider (LHC), $\sqrt{s_{NN}} = 5.02$ TeV, the initial photons can reach energies up to 75–100 GeV in the Pb+Pb centre-of-mass system.

Among the possible set of photon-induced reactions, the exclusive production of dielectron pairs from photon–photon collisions, i.e. $\gamma\gamma \rightarrow e^+e^-$, is one of the cleanest elementary processes. This process, also referred to as the Breit–Wheeler process [5], is a non-resonant two-photon scattering to opposite-charge electron pairs. The outgoing nuclei may be excited, due to incoherent emission of photons participating in

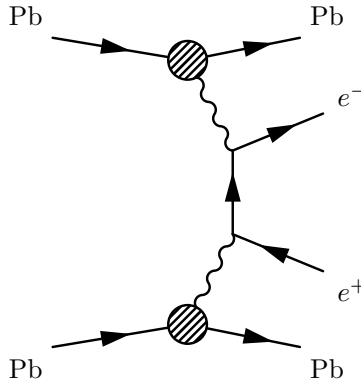


Figure 1: Feynman diagram of the leading-order $\gamma\gamma \rightarrow e^+e^-$ process.

$\gamma\gamma \rightarrow e^+e^-$ process or via photonuclear reactions, occurring when an additional photon is exchanged. [6, 7]. A Feynman diagram of the leading-order $\gamma\gamma \rightarrow e^+e^-$ reaction is shown in Figure 1. Even for large $\gamma\gamma$ invariant masses, the relatively large cross-section associated with this process allows precise differential measurements to be made. Thus, this process is a particularly effective tool for studying the modelling of photon fluxes and elementary production cross-sections, as well as for studying the effects of nuclear break-up induced by additional photon exchanges, whose probability is strongly correlated with the internuclear impact parameter [2]. Nuclear break-up gives rise to forward neutron production, and the fraction of events with such activity is larger at smaller impact parameters.

Exclusive dilepton production, via both electron-pair and muon-pair final states, has been measured by ATLAS and CMS in pp collisions at $\sqrt{s} = 7$ TeV [8–10] and $\sqrt{s} = 13$ TeV [11–13]. The ALICE Collaboration has measured exclusive production of electron pairs in Pb+Pb collisions at $\sqrt{s_{NN}} = 2.76$ TeV [14] over a limited kinematic range. The STAR and PHENIX experiments at RHIC have measured exclusive dileptons at lower invariant masses at $\sqrt{s_{NN}} = 200$ GeV for both Au+Au and U+U collisions [15–17]. With the higher centre-of-mass energy of $\sqrt{s_{NN}} = 5.02$ TeV, ATLAS has performed differential measurements of $\gamma\gamma \rightarrow \mu^+\mu^-$ production in UPC Pb+Pb collisions [18]. Both STAR and ATLAS have observed substantial broadening of angular distributions for exclusive dileptons from $\gamma\gamma$ interactions in events where the nuclei overlapped and interacted hadronically [15, 19]. Finally, CMS has observed that angular correlations in exclusive dimuon events are broadened significantly as a function of the impact parameter [20], as inferred by the amount of forward neutron production.

Exclusive dielectron production is an important reference process for other measurements. References [21] and [22] propose using it in the context of $\gamma\gamma \rightarrow \tau^+\tau^-$ production, in order to reduce the impact of correlated systematic uncertainties for the measurement of the τ -lepton anomalous magnetic moment. It is also an important background for light-by-light scattering, which proceeds via loop diagrams and thus has a much lower cross-section. This has been assessed in several publications on light-by-light scattering by ATLAS [23–25] and CMS [26].

This paper presents a measurement of the exclusive production of dielectrons with the ATLAS detector at the LHC. It uses Pb+Pb data collected in 2018, which have an integrated luminosity three times larger than the sample used in the ATLAS dimuon measurement [18]. Dielectron production is measured in the fiducial region defined by the following requirements: electron transverse momentum $p_T^e > 2.5$ GeV, electron pseudorapidity $|\eta^e| < 2.5$, dielectron invariant mass $m_{ee} > 5$ GeV, and dielectron transverse momentum $p_T^{ee} < 2$ GeV. Compared to the dimuon measurement discussed in Ref. [18], this fiducial

region has wider coverage in lepton p_T and dilepton invariant mass, with the minimum values lowered by 1.5 GeV and 5 GeV, respectively. The backgrounds originating from single-dissociative processes, $\Upsilon(nS)$ production, and exclusive τ -lepton pair production, $\gamma\gamma \rightarrow \tau^+\tau^-$, are estimated and subtracted. Differential cross-sections are measured as a function of m_{ee} , average electron transverse momentum $\langle p_T^e \rangle$, absolute dielectron rapidity $|y_{ee}|$, and scattering angle in the dielectron rest frame, $|\cos\theta^*|$. The cross-sections are extracted both inclusively in forward neutron activity and exclusively in $\gamma\gamma \rightarrow e^+e^-$ events without activity in the forward direction. The latter is a unique feature of this paper.

2 ATLAS detector

The ATLAS detector [27] at the LHC covers nearly the entire solid angle around the collision point. It consists of an inner tracking detector surrounded by a thin superconducting solenoid, electromagnetic and hadronic calorimeters, and a muon spectrometer incorporating three large superconducting toroidal magnets with eight coils each.

The inner detector (ID) is immersed in a 2 T axial magnetic field and provides charged-particle tracking in the pseudorapidity range $|\eta| < 2.5$.¹ The high-granularity silicon pixel (Pixel) detector covers the vertex region and typically provides four measurements per track, with the first hit normally being in the insertable B-layer (IBL) [28], which was installed at the mean distance of 3.3 cm from the beam axis before the start of Run 2. It is followed by the silicon microstrip tracker (SCT), which usually provides four two-dimensional measurement points per track. These silicon detectors are complemented by the transition radiation tracker, which enables radially extended track reconstruction up to $|\eta| = 2.0$.

The calorimeter system covers the pseudorapidity range $|\eta| < 4.9$. Within the region $|\eta| < 3.2$, electromagnetic calorimetry is provided by barrel and endcap lead/liquid-argon (LAr) calorimeters (high granularity for $|\eta| < 2.5$), with an additional thin LAr presampler covering $|\eta| < 1.8$ to correct for energy loss in material upstream of the calorimeters. Hadronic calorimetry is provided by the steel/scintillator-tile calorimeter, which is segmented into three barrel structures within $|\eta| < 1.7$, and two copper/LAr hadronic endcap calorimeters. The solid angle coverage is completed with forward copper/LAr and tungsten/LAr calorimeter modules (FCal) optimised for electromagnetic and hadronic measurements respectively.

The muon spectrometer (MS) comprises separate trigger and high-precision tracking chambers measuring the deflection of muons in a magnetic field generated by the superconducting air-core toroids. The precision chamber system covers the region $|\eta| < 2.7$ with three layers of monitored drift tubes, complemented by cathode strip chambers in the forward region, where the background is highest. The muon trigger system covers the range $|\eta| < 2.4$ with resistive plate chambers in the barrel, and thin gap chambers in the endcap regions.

The zero-degree calorimeters (ZDC) consist of four longitudinal compartments on each side of the IP, each with one nuclear interaction length of tungsten absorber, with Cherenkov light read out by 1.5-mm-diameter quartz rods. The detectors are located 140 m from the nominal IP in both directions, covering $|\eta| > 8.3$, and are well suited to measuring neutral particles originating from the collision. In Pb+Pb collisions the

¹ ATLAS uses a right-handed coordinate system with its origin at the nominal interaction point (IP) in the centre of the detector and the z -axis along the beam pipe. The x -axis points from the IP to the centre of the LHC ring, and the y -axis points upwards. Cylindrical coordinates (r, ϕ) are used in the transverse plane, ϕ being the azimuthal angle around the z -axis. The pseudorapidity is defined in terms of the polar angle θ as $\eta = -\ln \tan(\theta/2)$. Angular distance is measured in units of $\Delta R \equiv \sqrt{(\Delta\eta)^2 + (\Delta\phi)^2}$. The photon (electron) transverse energy is $E_T = E/\cosh(\eta)$, where E is its energy.

ZDC detects individual neutrons originating from the incoming nuclei. The ZDC calibration is performed in each set of four modules using photonuclear processes that deposit one or more neutrons on one side, and a single neutron, carrying the full per-nucleon beam energy, on the other. Time-dependent weights are determined for each module in short time intervals to minimise the variance around the nominal per-nucleon beam energy. Energy resolutions achieved are typically around $\Delta E/E \approx 16\%$.

The ATLAS trigger system [29, 30] consists of a first-level (L1) trigger implemented using a combination of dedicated electronics and programmable logic, and a software-based high-level trigger (HLT). An extensive software suite [31] is used in the reconstruction and analysis of real and simulated data, in detector operations, and in the trigger and data acquisition systems of the experiment.

3 Data and Monte Carlo simulation samples

The data used in this measurement are from Pb+Pb collisions with a centre-of-mass energy of $\sqrt{s_{\text{NN}}} = 5.02$ TeV, recorded in 2018 with the ATLAS detector at the LHC. The full data set corresponds to an integrated luminosity of 1.72 nb^{-1} . Only high-quality data [32] with all detectors operating normally are analysed.

Monte Carlo (MC) simulated events for the $\gamma\gamma \rightarrow e^+e^-$ signal process were generated at leading order (LO) using STARLIGHT v3.13 [33]. In this approach, the cross-section is computed by convolving the Pb+Pb photon flux with the LO calculation of the elementary $\gamma\gamma \rightarrow e^+e^-$ process. The photon spectrum is calculated in impact parameter space by integrating the photon number density over all impact parameters while assuming that the beam projectiles do not interact hadronically. This is done by utilising a simple Glauber model [34] which provides an impact-parameter-dependent probability of inelastic processes. STARLIGHT also requires that the dilepton pairs are not formed within either nucleus. Several signal samples were produced for exclusive m_{ee} intervals within the range $4.5 < m_{ee} < 200$ GeV. An alternative sample for the signal $\gamma\gamma \rightarrow e^+e^-$ process uses the SUPERCHIC v3.05 [35] program. The difference between the nominal and alternative signal prediction is mainly in the implementation of the initial photon flux. The STARLIGHT generator relies on flux from point-like sources restricted to impact parameters larger than nuclear radius ($b > R_A$), while SUPERCHIC generator implements flux calculations down to $b = 0$ and takes the nuclear form factor into account.

Backgrounds from $\gamma\gamma \rightarrow \tau^+\tau^-$ and $Y(nS) \rightarrow e^+e^-$ were simulated using STARLIGHT v3.13. All generated events utilised PYTHIA 8 (Py8) [36] to model QED final-state radiation (FSR) from the outgoing leptons.

Incoherent emission of photons participating in $\gamma\gamma \rightarrow e^+e^-$ process contribute to background in the dielectron production sample. In such a process either one (single dissociation) or both (double dissociation) nuclei interact inelastically and dissociate. Simulation of this process is not available in any MC generator, however a similar process in pp collisions is modelled using SUPERCHIC v4.0 (SC4) [37]. The sample generated with SC4 was interfaced to PYTHIA 8 for showering and hadronisation. A data-driven approach, discussed in detail in Section 5, is used in the analysis to utilise this sample in Pb+Pb collisions.

Apart from the alternative signal sample, all generated events are processed with a detector simulation [38] based on GEANT4 [39] and are reconstructed with the standard ATLAS reconstruction software [31]. The alternative signal sample is used for comparisons with the measured differential cross-sections discussed in Section 8.

4 Signal selection and detector corrections

Candidate dielectron events were recorded using a dedicated trigger for events with moderate activity in the calorimeter but little additional activity in the entire detector. A logical OR of two L1 trigger conditions was required: (1) at least one EM cluster with $E_T > 1$ GeV in coincidence with a total E_T of 4–200 GeV registered in the calorimeter, or (2) at least two EM clusters with $E_T > 1$ GeV and a total E_T below 50 GeV registered in the calorimeter. At the HLT, the total E_T on each side of the FCal detector was required to be below 3 GeV. Additionally, a veto condition on the maximum activity in the Pixel detector, hereafter referred to as the Pixel-veto, had to be satisfied at the HLT. The number of hits was required to be at most 15 to be compatible with low-multiplicity UPC events.

Electrons are reconstructed from EM clusters in the calorimeter and tracking information provided by the ID [40]. Selection requirements are applied to remove EM clusters with a large amount of energy from poorly functioning calorimeter cells, and a timing requirement is made to reject out-of-time candidates. An energy calibration specifically optimised for electrons and photons [40] is applied to the candidates to account for upstream energy loss and both lateral and longitudinal shower leakage. The calibration is derived for nominal pp collisions with dedicated factors applied to account for the much lower contribution from multiple Pb+Pb collisions in the same bunch crossing.

The electron identification in this analysis is based on a ‘loose’ cut-based working point [40] which is defined using selections on the shower-shape and tracking variables. Only electrons with $p_T^e > 2.5$ GeV and $|\eta^e| < 2.47$, excluding the calorimeter transition region $1.37 < |\eta^e| < 1.52$, are considered. The minimum p_T^e requirement is driven by the electron reconstruction efficiency, which drops below 20% for p_T^e values below this threshold.

Preselected events are required to have exactly two opposite-charge electrons satisfying the above selection criteria, with a dielectron invariant mass, m_{ee} , greater than 5 GeV. To suppress non-exclusive backgrounds, only two charged-particle tracks [41, 42] each with $p_T > 100$ MeV, $|\eta| < 2.5$, at least seven hits in the Pixel and SCT detectors in total and at most two silicon sensors without a hit, and associated with the dielectron are allowed. To reject non-collision backgrounds such as cosmic-ray muons, the event must not have a track in the MS. Finally, the total p_T of the dielectron, p_T^{ee} , is required to be less than 2 GeV. Low p_T^{ee} values are a key feature of the purely EM process, which involves initial-state photons with very low p_T .

Each of the events satisfying the $\gamma\gamma \rightarrow e^+e^-$ criteria can be further classified into one of three categories based on the observed activity in the ZDC detector: 1) no neutron is registered in either ZDC (‘0n0n’), 2) one or more forward neutrons registered in one ZDC and none in the other (‘Xn0n’), and 3) one or more forward neutrons detected in both ZDC arms (‘XnXn’). The observed fractions of events falling into these categories are: $f_{0n0n} = (62.9 \pm 0.3)\%$, $f_{Xn0n} = (29.7 \pm 0.3)\%$, and $f_{XnXn} = (7.4 \pm 0.2)\%$. Due to the relatively large instantaneous luminosity of Pb+Pb collisions, which peaked around $7 \times 10^{27} \text{ cm}^{-2}\text{s}^{-1}$, additional neutrons might be generated per bunch crossing by single and mutual dissociation processes and detected in one or both arms of the ZDC, but they are not associated with the exclusive dielectron process. This leads to an outflow of events from the 0n0n and Xn0n categories to both the Xn0n and XnXn categories. This effect is accounted for using the method established in Ref. [18]. A matrix equation with two fundamental parameters representing probabilities for single and mutual dissociation is built. The corrected fractions are measured in four bins of m_{ee} , with boundaries at 5, 10, 20, and 40 GeV, and three bins of $|y_{ee}|$, with boundaries at 0, 0.8, 1.6, and 2.4, and also in the sample integrated over m_{ee} and $|y_{ee}|$. On average, in the 0n0n category, they are about 13% larger than the observed fractions. Figure 2 shows the fractions of events in the 0n0n category as a function of m_{ee} in three bins of $|y_{ee}|$, corrected for the

presence of additional neutrons. These fractions tend to drop with increasing mass, and are in general larger for higher $|y_{ee}|$ values. For the rapidity range of $|y_{ee}| < 0.8$, which has the largest number of events, the f_{0n0n} values drop from about 78% in the lowest mass bin to about 57% in the highest mass bin. The systematic uncertainties in the fractions of events in the 0n0n category originate from several sources: uncertainties in the exclusive single and double EM dissociation cross-sections measured by the ALICE Collaboration [43], and their extrapolation from $\sqrt{s_{NN}} = 2.76$ TeV to 5.02 TeV as evaluated in Ref. [18]; the uncertainty in the dissociative background contribution as discussed in Section 5; and the uncertainty in the ZDC efficiency.

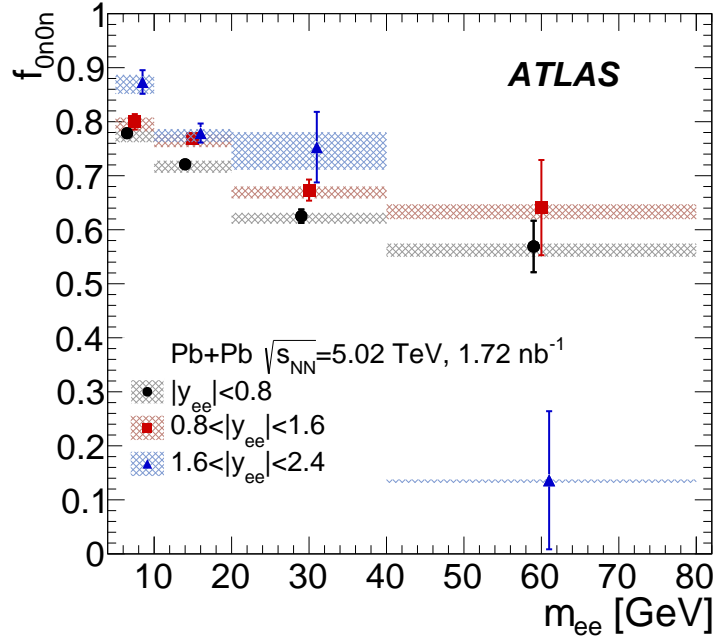


Figure 2: Fractions of events in the 0n0n category evaluated from data in three bins of $|y_{ee}|$, corrected for the presence of additional neutrons. Error bars represent statistical uncertainties, while shaded boxes represent systematic uncertainties. Points for $|y_{ee}| < 0.8$ and $1.6 < |y_{ee}| < 2.4$ are displaced horizontally for better visibility.

The efficiency of the primary physics trigger (ϵ_T) is determined as $\epsilon_T = \epsilon_{L1} \cdot \epsilon_{\text{PixVeto}} \cdot \epsilon_{\text{FCal}}$, where ϵ_{L1} is the efficiency of the L1 EM trigger to register the moderate calorimeter activity characteristic of the signal process, $\epsilon_{\text{PixVeto}}$ is the efficiency of the trigger to reject events with large numbers of Pixel detector hits, and ϵ_{FCal} is the efficiency of the FCal selection to reject events with large energy depositions on either side. Individual efficiencies are evaluated in a sample of $\gamma\gamma \rightarrow e^+e^-$ events collected with a set of dedicated supporting triggers that do not use the condition under study in the primary physics trigger to reject any events. The ϵ_{L1} value rises with the sum of the transverse energies of the two electron clusters and reaches 100% for $\Sigma E_T > 8$ GeV. The Pixel-veto efficiency and its uncertainties are measured as a function of the dielectron rapidity in the dedicated dielectron sample collected by the supporting trigger requiring at least two tracks with p_T above 1 GeV and without veto requirement on the number of Pixel hits. The efficiency is evaluated as a ratio of events passing the Pixel-veto requirement to all selected events. It is just over 80% for $|y_{ee}| \sim 0$ and falls to about 50% for $|y_{ee}| > 2$. The dependence on $|y_{ee}|$ originates from the growing number of Pixel-detector layers in the forward direction that a dielectron pair

has to pass through. The average number of Pixel hits for the signal process is 10 in the central region, and it increases to 14 in the forward direction. The systematic uncertainties are evaluated by repeating the efficiency measurement on the dielectron sample selected by varying requirements on p_T^e and m_{ee} , and acoplanarity ($\alpha = 1 - |\Delta\phi|/\pi$, where $\Delta\phi$ is the azimuthal angle between the two electrons). They are at the level of 0.5%, while the statistical uncertainty ranges between 1 and 2%. Finally, the FCal veto efficiency is measured to be $(99.1 \pm 0.6)\%$, and it is constant for the entire range in ΣE_T . The total uncertainty in the trigger efficiency is determined by increasing and decreasing all of the individual components by their respective total uncertainties. They amount to about 3%–4% for the primary calorimeter pair trigger, driven mainly by the limited number of dielectron events collected by an independent ZDC-based trigger used to measure ε_{L1} , and less than a percent for the other contributions.

The total electron efficiency is the product of the electron reconstruction efficiency and the ‘loose’ electron identification efficiency [40]. This is determined in data using a sample of events triggered by the presence of EM clusters, limited total E_T , and a maximal number of Pixel hits, on which a tag-and-probe procedure is performed. The tag is a well-reconstructed, high-purity electron candidate with $E_T > 2.5$ GeV, and the probe is an opposite-charge track built from at least three hits in the Pixel detector (referred to as a ‘Pixel-track’). Pixel tracks are required to have $p_T > 50$ MeV. The invariant mass of the tag-and-probe system must exceed 5 GeV and the acoplanarity has to be less than 0.1. The extracted mass distribution is found to agree well with a reconstructed sample of STARLIGHT events. The reconstruction efficiency is defined as the fraction of probes which are reconstructed electrons, while the identification efficiency is the fraction of reconstructed electrons which are identified as ‘loose’ electrons. The reconstruction efficiency has large variations with both p_T and Pixel-track η , and ranges from about 30% at $p_T = 2.5$ GeV to 95% above 15 GeV. The identification efficiency is found to vary more weakly with Pixel-track η , ranging between 80% and 90%. Then, the overall reconstruction scale factors are extracted as the ratio of efficiencies measured in data and MC simulation. They vary between 0.9 and 1.2, with the largest deviations from unity being in the forward direction for Pixel-track $|\eta| > 1.1$. Systematic uncertainties in the scale factors are evaluated using tighter selection criteria for the tag and probe candidates, as well as reducing a potential contribution from background processes by limiting the measurement to the 0n0n category or to a narrow acoplanarity region, $\alpha < 0.01$. In particular the requirement on maximum α reduces the contribution from the exclusive $\tau^+\tau^-$ production to 0.25% level. The total systematic uncertainty is at the level of 5% for central Pixel-tracks with $|\eta| < 1$, and grows to 10% in the forward direction. In the forward region, the statistical and systematic uncertainties are of similar size.

5 Background contributions

There are three primary sources of background considered in this analysis, presented in order of decreasing contributions: dissociative $\gamma\gamma \rightarrow e^+e^-$ production; Υ -meson production; and exclusive τ -lepton pair ($\tau^+\tau^-$) production.

The largest background originates from $\gamma\gamma \rightarrow e^+e^-$ production with nuclear dissociation. In this process one (or both) of the initial photons originates from the substructure of the nucleon, rather than from the exterior EM field of the nuclei as a whole. The photon interaction that produces the e^+e^- pair is thus accompanied by the dissociation of the emitting nucleus, whose remnants are produced in the forward direction and are typically captured by the ZDC detector.

The contribution from dissociative events is estimated using a template-fitting approach applied to the acoplanarity distribution. The signal template is simulated with STARLIGHT + PYTHIA 8 and it is peaked at

$\alpha \approx 0$, with some contribution in the tail originating from events with FSR. The background template shape is taken from the single-dissociative events simulated in pp collisions with SUPERCHIC v4.0 interfaced with PYTHIA 8. These events have a much wider α distribution than the signal. The acoplanarity shape is strongly correlated with the transverse momentum of the $\gamma\gamma$ system, which is driven by the transverse momenta of the initial photons. For the photons emitted coherently from the nucleus, the transverse momentum is of order $\hbar c/R_A \approx 30$ MeV, while typical p_T scale for dissociative events is of order GeV. In the case of dilepton production in pp collisions, the typical initial p_T scale is about 200 MeV. The convolution of photon fluxes originating from either proton or ion with photons emitted from nucleon substructure is always dominated by the harder spectrum of the latter. Therefore, the shape of the acoplanarity distribution for dissociative dielectron production in Pb+Pb collisions can be described by the simulation of this process in pp collisions. The fit to the data is performed in the same intervals of m_{ee} and $|y_{ee}|$ as in the study of the fractions of events in the 0n0n, Xn0n and XnXn categories. In each bin, a binned maximum-likelihood fitting procedure is performed separately in three ZDC categories. The normalisation of the relative background contribution, f_{bkg} , is taken to be a free parameter of the fit. The signal fraction is thus $(1 - f_{\text{bkg}})$. For the inclusive sample, f_{bkg} is a weighted sum of the results for the 0n0n, Xn0n, and XnXn categories. The f_{bkg} fraction accounts for contributions from dissociative production and exclusive $\tau^+\tau^-$ production, $\gamma\gamma \rightarrow \tau^+\tau^-$. The latter may contribute to the electron background, especially when both τ -leptons decay in the electron channel. The $\tau^+\tau^-$ contribution is estimated using a dedicated MC sample from STARLIGHT. The resulting background fraction of $\gamma\gamma \rightarrow \tau^+\tau^-$ events in the full data sample amounts to 0.1%. It is found that the shape of the α distribution for the exclusive $\tau^+\tau^-$ events is similar to the α distribution for the pure dissociative component. However, the origin of this shape in $\tau^+\tau^-$ events is due to the presence of the neutrino in τ -lepton decay. The dissociative contribution, f_{diss} , is therefore determined as the background fraction obtained from the fitting procedure, then reduced by the $\tau^+\tau^-$ background fraction.

The results of the fitting procedure for the data from the $10 < m_{ee} < 20$ GeV and $|y_{ee}| < 0.8$ interval are presented in Figure 3 for three ZDC categories as well as for the inclusive sample. The f_{bkg} fraction amounts to $(0.3 \pm 0.2)\%$, $(9.9 \pm 0.6)\%$, $(13 \pm 1)\%$ and $(4.3 \pm 0.3)\%$ for the 0n0n, Xn0n, XnXn categories, and the inclusive sample, respectively and increases with m_{ee} and $|y_{ee}|$.

The contribution from Y -meson production is estimated using the dedicated STARLIGHT + PYTHIA 8 samples. Three Y states, $Y(1S)$, $Y(2S)$, and $Y(3S)$ are considered. This background is significant only for m_{ee} below 14 GeV and amounts to 2.4% of events satisfying the selection criteria for the $\gamma\gamma \rightarrow e^+e^-$ process. The α distribution of the dielectron candidates from Y decays is peaked at zero, similarly to the signal shape. It does not contribute to f_{bkg} because the resulting fraction is not sensitive to a 2.4% change in the acoplanarity peak. Hence, the Y contribution is subtracted separately from the data.

A background contribution originating from photonuclear processes occurring in ultraperipheral heavy-ion collisions is largely suppressed by the trigger requirement limiting the maximum E_T deposited in the FCal to 3 GeV per side. The validity of this assumption was tested by examining the multiplicity distribution of Pixel-tracks. The fraction of events that have more than two Pixel-tracks is 1.3% and consistent with simulations of $\gamma\gamma \rightarrow e^+e^-$ events. This also confirms that the pileup contribution from additional low- p_T $\gamma\gamma \rightarrow e^+e^-$ interactions, which should be below 1%, can be neglected in the selected data sample.

Figure 4 shows control distributions for reconstructed and uncorrected values of m_{ee} , $\langle p_T^e \rangle$, y_{ee} , $|\cos \theta^*| = |\tanh(\Delta\eta_{ee}/2)|$, and α for the inclusive data sample compared with MC predictions including the signal and background processes. The trigger decision is not simulated in the MC events. Instead, the distributions are weighted event-by-event by the parameterised trigger efficiency and by electron scale factors. The signal, Y decay and $\tau^+\tau^-$ MC prediction is normalised to the integrated luminosity in data. The dissociative contribution is scaled to constitute the f_{diss} fraction (determined for the inclusive sample) of the data. In

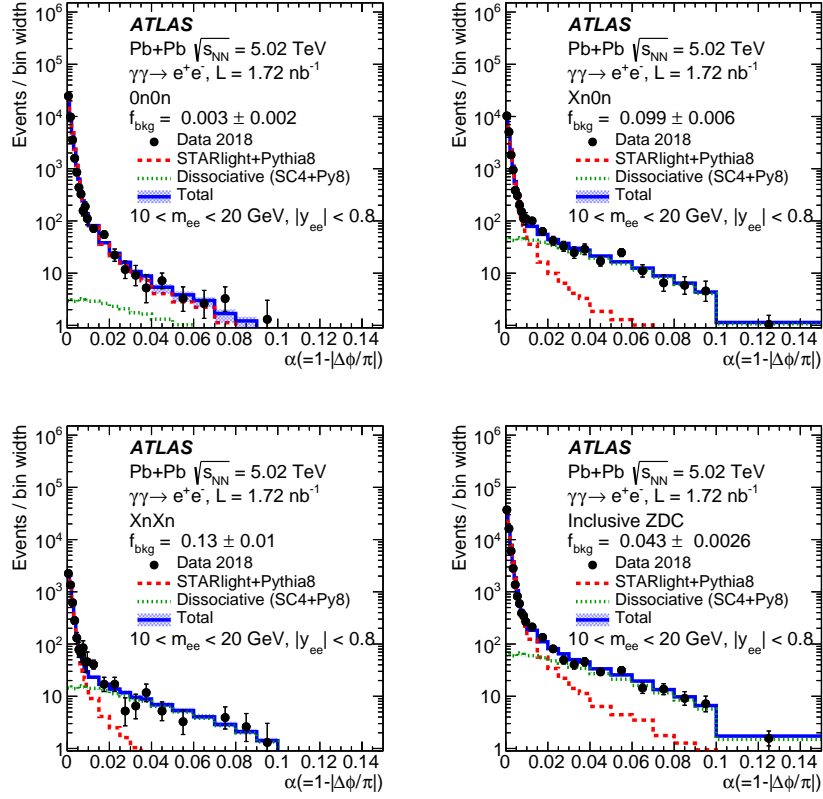


Figure 3: Acoplanarity distribution in the data sample (markers) of $\gamma\gamma \rightarrow e^+e^-$ candidates selected with $10 < m_{ee} < 20$ GeV and $|y_{ee}| < 0.8$ requirements. The sample is split into 0n0n (top left), Xn0n (top right), XnXn (bottom left) and inclusive (bottom right) categories. The fitted dissociative background in each category is shown with the green dashed line, while the prediction for the signal process is shown by the red line. The sum of the two components is shown with the solid blue line. The resulting estimate of the background fraction in the data, f_{bkg} , is given in the legend. The shaded area represents the total uncertainty of the sum of signal and background components.

general, good agreement between data and the sum of the predictions for signal and background processes is found. On average, the observed discrepancies are at the level of 10%–15% with some exceptions which are discussed further. In the m_{ee} distribution the data excess is more strongly pronounced for m_{ee} between 10 and 20 GeV, where the difference between data and MC simulation is 10%–20%. The data-to-MC ratio drops below unity for masses above 40 GeV. The same features are observed in the $\langle p_T^e \rangle$ distribution, with the largest deviations from unity in the range 5–10 GeV. In the y_{ee} distribution, the data excess is smaller, up to 10%, in the range from -1.2 to 1.2 , with larger discrepancies for higher $|y_{ee}|$ values. The data-to-MC ratio in the $|\cos\theta^*|$ distribution drops slowly from 1.2 for $|\cos\theta^*| = 0$ to unity at $|\cos\theta^*| = 0.75$, and then falls more steeply, to 0.5 for the largest values of $|\cos\theta^*|$. In the α distribution, a difference in the overall shape is observed in the full range. This can be explained by a sensitivity of the results to the p_T spectrum assumed by STARLIGHT, since this spectrum determines the width of the α distribution. In general, all these discrepancies tend to be consistent with the observations made in the ATLAS $\gamma\gamma \rightarrow \mu^+\mu^-$ measurement [18], where the STARLIGHT predictions were found to underestimate the measured integrated fiducial cross-sections by about 10%.

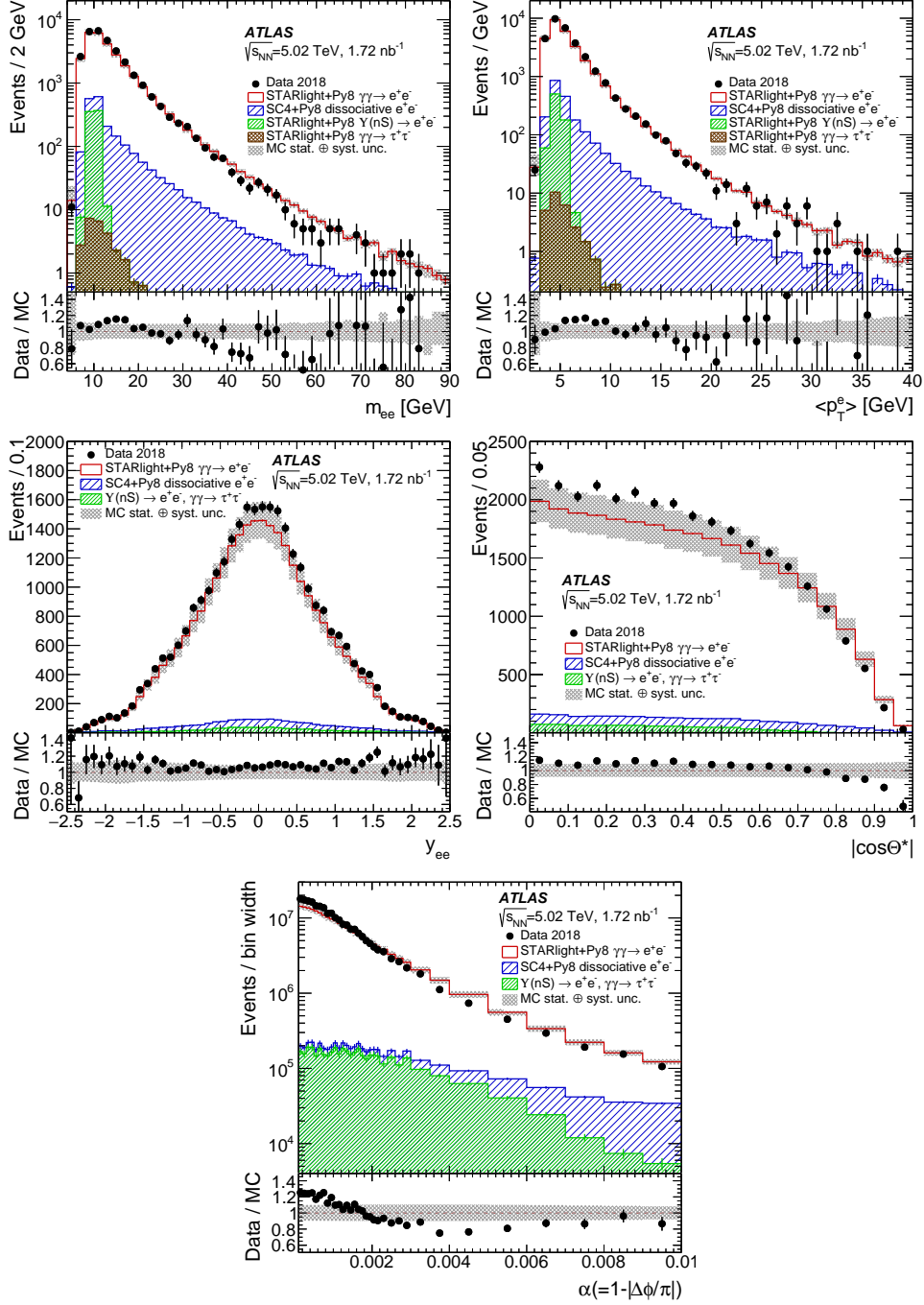


Figure 4: Distributions of m_{ee} (top left), $\langle p_T^e \rangle$ (top right), y_{ee} (middle left), $|\cos \theta^*|$ (middle right), and α (bottom) for the inclusive sample in data and the MC predictions for signal and background processes. The lower panels show the ratio of data to MC simulation. Error bars represent statistical uncertainties. The shaded area represents the overall uncertainty of the total MC prediction. In the y_{ee} , $|\cos \theta^*|$, and α distributions, the Υ and $\tau^+\tau^-$ contributions are shown together. The dissociative contribution is scaled to constitute the f_{diss} fraction from the data fit.

6 Analysis

The integrated fiducial cross-section for exclusive dielectron production is calculated using the following formula:

$$\sigma^{\text{fid}} = \frac{N_{\text{data}} - N_{\text{bkg}}}{C \cdot A \cdot L},$$

where:

- N_{data} and N_{bkg} refer to the number of events in data after event selection and the expected number of background events in this selected sample, respectively;
- C is a correction factor accounting for detector inefficiencies (including the trigger), calculated as $N_{\text{MC, reco}}^{\text{fid, cut}} / N_{\text{MC, gen}}^{\text{fid, cut}}$ where $N_{\text{MC, gen}}^{\text{fid, cut}}$ is the number of generated events passing fiducial requirements of the analysis, while $N_{\text{MC, reco}}^{\text{fid, cut}}$ is the number of simulated signal events that also pass the reconstruction-level selection;
- A is the acceptance correction, used to correct the result for the exclusion of the calorimeter transition region and extrapolation from $|\eta^e| < 2.47$ to $|\eta^e| < 2.5$; and is calculated as $N_{\text{MC, gen}}^{\text{fid, cut}} / N_{\text{MC, gen}}^{\text{fid}}$, where $N_{\text{MC, gen}}^{\text{fid}}$ is the number of generated events passing all fiducial requirements of the analysis, except the requirement to exclude the calorimeter transition region;
- L is the total integrated luminosity.

Both $N_{\text{MC, gen}}^{\text{fid, cut}}$ and $N_{\text{MC, gen}}^{\text{fid}}$ are extracted with respect to the generator-level electrons before FSR. The fiducial region is defined by the following requirements: $p_{\text{T}}^e > 2.5$ GeV, $|\eta^e| < 2.5$, $m_{ee} > 5$ GeV, and $p_{\text{T}}^{ee} < 2$ GeV. The number of events passing the fiducial selection is $N_{\text{data}} = 30456$. The dissociative and $\tau^+\tau^-$ background fraction obtained from the fit amounts to 4.5%. The Υ background amounts to 2.4% of all events satisfying the selection criteria.

The selected data sample is corrected in a few subsequent steps in order to compare it with the theoretical predictions. In the first step the backgrounds are subtracted. Distributions in the data are reweighted event-by-event by the factor $(1 - f_{\text{bkg}})$ where f_{bkg} is the fraction of background (inclusive in ZDC) from the fit in a given m_{ee} and $|y_{ee}|$ range. For masses above 40 GeV, the fraction obtained from the fit in the full $|y_{ee}| < 2.4$ range is taken. For events with m_{ee} below 40 GeV, the fraction as a function of $|y_{ee}|$ is used. If $|y_{ee}|$ exceeds 2.4, the fraction from the $1.6 < |y_{ee}| < 2.4$ bin is applied. In the next step, the background expected from $\Upsilon(nS)$ decays is subtracted.

For differential cross-section measurement, the data are corrected with fiducial correction factors defined as the fraction of events in each bin which fall into the fiducial region at generator level. These factors correct for the events that are reconstructed within the fiducial region, but fall outside it at the generator level. They are parameterised using the reconstructed kinematic variables. They deviate from unity at the subpercent level, so their impact is marginal. After this, the reconstructed data are unfolded using a Bayesian-inspired iterative procedure [44] with one iteration for all distributions implemented in the RooUnfold package [45], using response matrices derived from signal MC samples. The number of iterations is chosen to minimise the resulting statistical uncertainty and at the same time provide good closure. A closure test based on the signal MC samples is performed to validate the unfolding procedure. The signal sample is split into two parts. The first part is used to fill the response matrices, while the second one is unfolded. The ratio of the unfolded yields to the generated yields deviates from unity by 1% at most.

Finally, the distributions are divided by the luminosity as well as the product of correction factors, $C \times A$, which account for detector inefficiencies as well as acceptance losses. They are determined for each bin of the unfolded distribution as the fraction of events that pass the fiducial requirements at reconstruction level, in events that pass them at generator level. The $C \times A$ factors are parameterised using generator-level kinematics, but then weighted by trigger and reconstruction efficiency scale factors, evaluated at reconstruction level. The average C and A factors amount to 0.087 and 0.878, respectively.

7 Systematic uncertainties

The following systematic uncertainties are considered in the cross-section measurement. The total scale factors for the electron reconstruction and identification efficiency [40] are varied upwards and downwards coherently over the full kinematic range, as a conservative estimate. The data-driven trigger efficiency, which is the product of the L1 efficiency, the Pixel-veto efficiency, and the forward transverse energy requirement efficiency, is increased and decreased by its total uncertainty. To assess known uncertainties in the EM energy scale and energy resolution, the calibrations are varied by factors determined in 13 TeV pp collisions [40]. The background contributions are increased and decreased by their total uncertainties. The dissociative backgrounds are dominated by their statistical uncertainties from the fit. The systematic uncertainties are also evaluated, and the largest contribution is related to the shape of the signal template. This is estimated using data from the 0n0n category as a signal distribution for the Xn0n and XnXn categories. The background template shape uncertainty is estimated by adding the double dissociative component. The uncertainty in the expected Υ yields is dominated by both the efficiency scale factors and the EM energy scale. Given the small contribution from Υ production, the theoretical uncertainties of its cross-section are considered to have negligible impact on the final measurement.

For the differential cross-sections, additional systematic uncertainties are related to the unfolding procedures. The MC sample is split in two, with one subsample used to determine the response matrix and the other treated as a simulated data set. The differences between the generated and unfolded yields are treated as a systematic uncertainty. Similarly, the sensitivity to the Bayesian prior is tested by reweighting the simulated data set to agree with the reconstructed data. Again, the differences between simulated and reconstructed yields in this closure test are applied as an uncertainty. While the primary unfolding is evaluated in one dimension rather than two, a cross-check is performed using the response in two dimensions. For each of the unfolded variables, every other one is used in the second dimension, but with the number of bins reduced to four (three) for m_{ee} and $\langle p_T^e \rangle$ ($|y_{ee}|$ and $|\cos \theta^*|$) to compensate for the limited number of events in the MC sample. The three resulting two-dimensional cross-sections are projected to one dimension and compared with the nominal results for each unfolded variable. The largest variations in each bin are included as an uncertainty. Finally, the spectra are evaluated in the 0n0n category, using the fractions determined in Section 4, but evaluated for generator-level m_{ee} and $|y_{ee}|$ (as opposed to the reconstructed values). The differences are found to be within 1%–2%.

The uncertainty in the integrated luminosity of the data sample is 2.0%. It is derived from the calibration of the luminosity scale using x – y beam-separation scans, following a methodology similar to that detailed in Ref. [46], and using the LUCID-2 detector for the baseline luminosity measurements [47].

A summary of the systematic uncertainties as a function of m_{ee} and $|y_{ee}|$ is shown in Figure 5. The dominant source of uncertainty arises from the uncertainties in the electron scale factors. They are at the level of 10%–11% in the whole range of m_{ee} , and rise from 9% at $|y_{ee}| \approx 0$ to about 15% for $|y_{ee}|$ close to 2. The systematic uncertainty from the trigger efficiency is approximately 2% for m_{ee} above 10 GeV and

$|y_{ee}|$ below 1.6. It rises to 4% for smaller m_{ee} , and to 6% for the highest $|y_{ee}|$ values. The uncertainty related to the energy scale and resolution is below 1% in the whole range of $|y_{ee}|$, but exceeds this value in some m_{ee} bins, reaching approximately 5% for the lowest m_{ee} values. The background uncertainties are within 1%–3% and increase slightly with increasing m_{ee} and $|y_{ee}|$. Uncertainties related to unfolding procedures do not exhibit such clear dependencies in m_{ee} and $|y_{ee}|$. They are mostly within the 2%–3% range but exceed this value, up to 5%, at intermediate m_{ee} and $|y_{ee}|$.

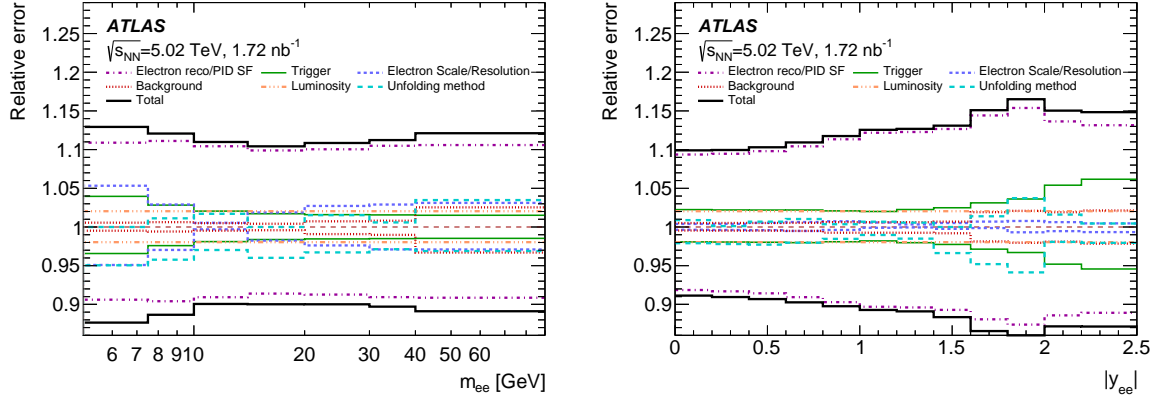


Figure 5: Breakdown of relative systematic uncertainties in the differential cross-section as a function of m_{ee} (left) and $|y_{ee}|$ (right).

8 Results

The total integrated fiducial cross-section is measured to be $215 \pm 1(\text{stat.})^{+23}_{-20}(\text{syst.}) \pm 4(\text{lumi.}) \mu\text{b}$. The STARLIGHT prediction for the total integrated fiducial cross-section is $196.9 \mu\text{b}$, while the SUPERCHIC prediction is $235.1 \mu\text{b}$. Both predictions are statistically compatible with the measurement.

The differential cross-sections for exclusive dielectron production are presented as a function of m_{ee} , $\langle p_T^e \rangle$, $|y_{ee}|$, and $|\cos \theta^*|$ in Figure 6. The cross-sections are measured inclusively in the ZDC categories. The results are corrected for detector inefficiency and resolution effects, and are compared with STARLIGHT v3.13 and SUPERCHIC v3.05 predictions for the signal $\gamma\gamma \rightarrow e^+e^-$ process. The bottom panel in each plot shows the ratio of the unfolded data to MC predictions. On average the STARLIGHT predictions underestimate the data by about 10%–15%, while SUPERCHIC predictions are higher by about the same amount. The STARLIGHT and SUPERCHIC predictions tend to have very similar shapes. The difference in the absolute normalisation of the two predictions is due to different approaches in the calculation of the initial photon flux. The predictions describe the shape of the data well, except at high $|y_{ee}|$ and high $|\cos \theta^*|$. The differences are more pronounced for m_{ee} between 10 and 20 GeV, and for $\langle p_T^e \rangle$ between 5 and 10 GeV. The ratio of data to STARLIGHT rises from about 1.1 to 1.2 as $|y_{ee}|$ increases from 0 to 2.5. For $|\cos \theta^*|$ close to 0, the data-to-STARLIGHT ratio reaches its largest value, around 1.15, and then slowly decreases to about 1.05 for $|\cos \theta^*| = 0.8$. The ratio falls more steeply in the last two bins of $|\cos \theta^*|$ and drops below unity to 0.75 and 0.65 for STARLIGHT and SUPERCHIC respectively. The measured cross-section in the highest $|\cos \theta^*|$ bin is 1.8 (2.7) standard deviations below the theory prediction from STARLIGHT (SUPERCHIC). There is a plausible proposal that higher-order scattering processes (involving more than

two photons in the initial state) are relevant and would tend to reduce the predicted cross-sections by the observed discrepancies [48].

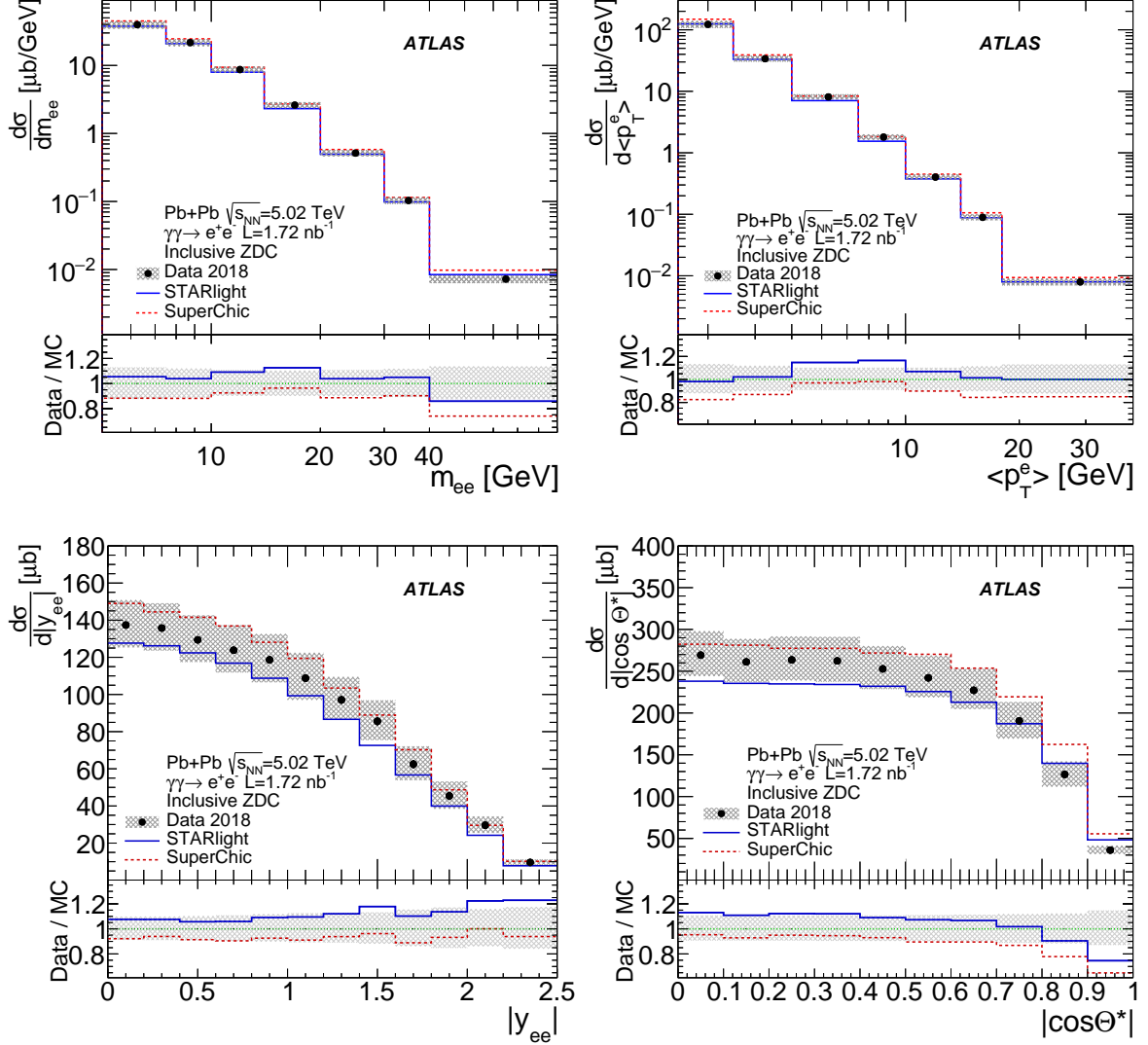


Figure 6: Fully corrected differential cross-sections measured inclusively in ZDC categories for exclusive dielectron production, $\gamma\gamma \rightarrow e^+e^-$, as a function of m_{ee} , $\langle p_T^e \rangle$, $|y_{ee}|$ and $|\cos\theta^*|$ for data (dots) and MC predictions from STARLIGHT (solid blue) and SUPERCHIC (dashed red). Bottom panels present the ratios of data to MC predictions. The shaded area represents the total uncertainty of the data, excluding the 2% luminosity uncertainty.

The differential cross-sections as a function of m_{ee} , $\langle p_T^e \rangle$, $|y_{ee}|$ and $|\cos\theta^*|$ for the 0n0n category are presented in Figure 7. They are compared with the MC predictions from STARLIGHT v3.13 and SUPERCHIC v3.05. Both simulated samples were produced inclusively and reweighted to the 0n0n category using the measured fractions presented in Fig. 2. The reweighting was performed event-by-event based on the generator level values of m_{ee} and $|y_{ee}|$. Each theory prediction is represented by two curves reflecting the systematic variations of the measured 0n0n fractions. STARLIGHT can also generate a prediction conditional on the presence of neutron emission in one or both directions. These dedicated predictions

from STARLIGHT for the 0n0n category are shown in the same plots. That prediction agrees well with the shape of the inclusive STARLIGHT prediction corrected for the measured 0n0n fractions, but is systematically lower by 2%–3% for $|y_{ee}| < 1.4$. The general conclusions from this comparison between MC predictions and data are consistent with the inclusive case. Agreement between data and MC events is generally better for lower $|y_{ee}|$ and $|\cos \theta^*|$ values, i.e. involving lower-energy initial-state photons.

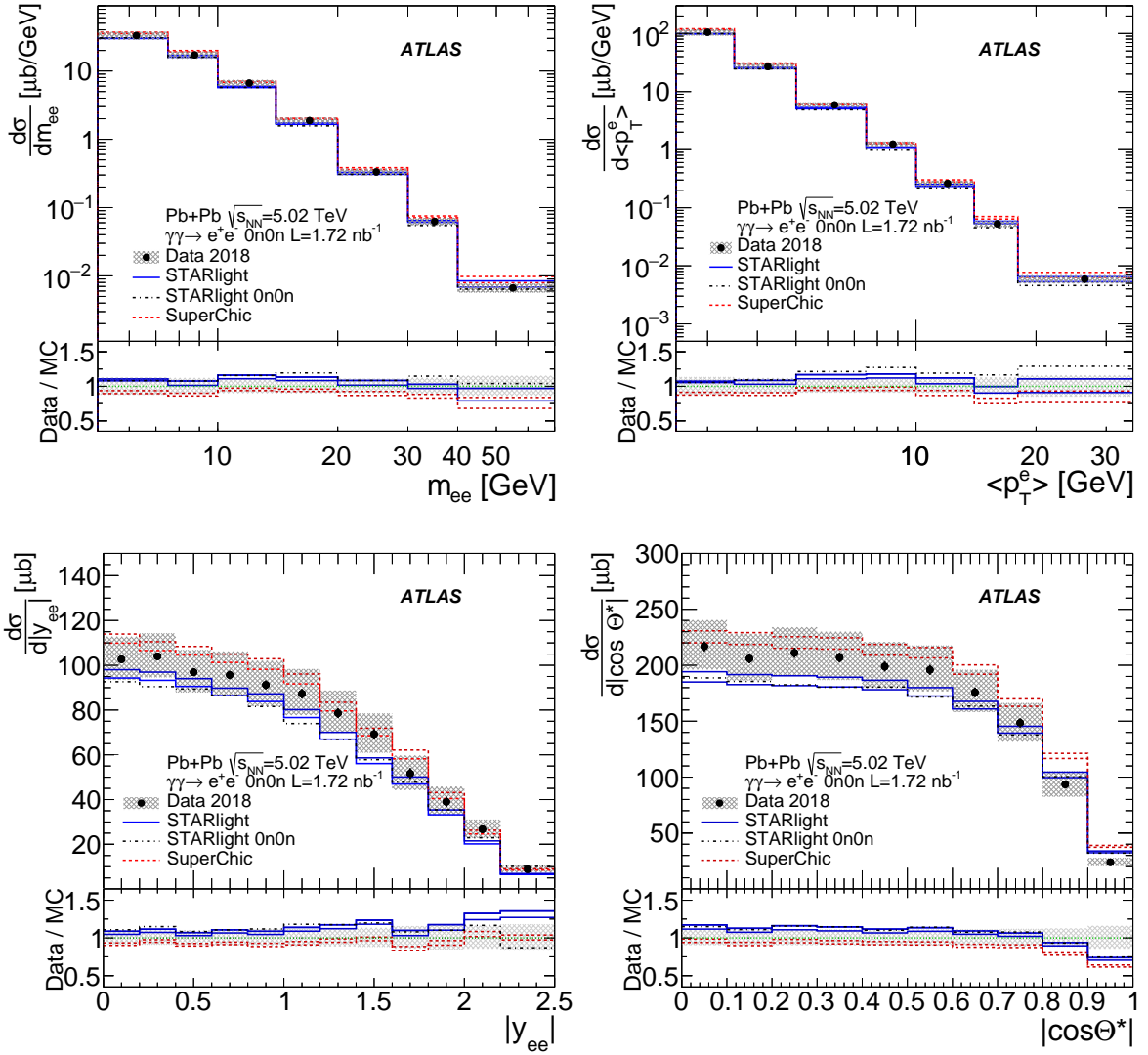


Figure 7: Fully corrected differential cross-sections measured for the 0n0n category for exclusive dielectron production as a function of m_{ee} , $\langle p_T^e \rangle$, $|y_{ee}|$ and $|\cos \theta^*|$. The cross-sections are compared with MC predictions from STARLIGHT (solid blue) and SUPERCHIC v3.05 (dashed red), each represented by two lines reflecting systematic variations. Also, a dedicated prediction from STARLIGHT for the 0n0n category (dashed-dotted black) is shown. The bottom panels show the ratios of data to predictions. The shaded area represents the total uncertainty of the data, excluding the 2% luminosity uncertainty.

9 Conclusions

A measurement of the cross-section for exclusive dielectron production, $\gamma\gamma \rightarrow e^+e^-$, is performed using $\mathcal{L}_{\text{int}} = 1.72 \text{ nb}^{-1}$ of ultraperipheral Pb+Pb collision data at $\sqrt{s_{\text{NN}}} = 5.02 \text{ TeV}$ recorded by the ATLAS detector at the LHC. The cross-section is corrected for detector efficiency, acceptance losses, and background contributions. The backgrounds from dissociative processes, Υ decays, and $\tau^+\tau^-$ production are subtracted, with the first contribution estimated using a template fit to the acoplanarity distribution. After all corrections, the integrated cross-section for the $\gamma\gamma \rightarrow e^+e^-$ process in the fiducial region, defined by $p_{\text{T}}^e > 2.5 \text{ GeV}$, $|\eta^e| < 2.5$, $m_{ee} > 5 \text{ GeV}$, and $p_{\text{T}}^{ee} < 2 \text{ GeV}$ requirements, is measured to be $215 \pm 1(\text{stat.})_{-20}^{+23}(\text{syst.}) \pm 4(\text{lumi.}) \mu\text{b}$. Within experimental uncertainties the data are in good agreement with the QED predictions from STARLIGHT v3.13 and SUPERCHIC v3.05. The differential cross-sections are presented as a function of m_{ee} , $\langle p_{\text{T}}^e \rangle$, $|y_{ee}|$ and $|\cos \theta^*|$, both with and without requirements on forward neutron activity. The differential results are compared with the predictions from STARLIGHT v3.13, which are generally lower than measured cross-sections, and from SUPERCHIC v3.05, which tend to be higher. In general, the shapes of the distributions agree well, but some systematic differences are observed. In particular, the discrepancy between data and the STARLIGHT prediction rises with higher $|y_{ee}|$, similarly to what ATLAS observed previously in $\gamma\gamma \rightarrow \mu^+\mu^-$ production. For $|\cos \theta^*| \approx 1$, the measured cross-section is 1.8 (2.7) standard deviations below the theory prediction from STARLIGHT (SUPERCHIC). Agreement between data and MC simulation is generally better for lower $|y_{ee}|$ and $|\cos \theta^*|$ values.

Acknowledgements

We thank CERN for the very successful operation of the LHC, as well as the support staff from our institutions without whom ATLAS could not be operated efficiently.

We acknowledge the support of ANPCyT, Argentina; YerPhI, Armenia; ARC, Australia; BMWFW and FWF, Austria; ANAS, Azerbaijan; CNPq and FAPESP, Brazil; NSERC, NRC and CFI, Canada; CERN; ANID, Chile; CAS, MOST and NSFC, China; Minciencias, Colombia; MEYS CR, Czech Republic; DNRF and DNSRC, Denmark; IN2P3-CNRS and CEA-DRF/IRFU, France; SRNSFG, Georgia; BMBF, HGF and MPG, Germany; GSRI, Greece; RGC and Hong Kong SAR, China; ISF and Benoziyo Center, Israel; INFN, Italy; MEXT and JSPS, Japan; CNRST, Morocco; NWO, Netherlands; RCN, Norway; MEiN, Poland; FCT, Portugal; MNE/IFA, Romania; MESTD, Serbia; MSSR, Slovakia; ARRS and MIZŠ, Slovenia; DSI/NRF, South Africa; MICINN, Spain; SRC and Wallenberg Foundation, Sweden; SERI, SNSF and Cantons of Bern and Geneva, Switzerland; MOST, Taiwan; TENMAK, Türkiye; STFC, United Kingdom; DOE and NSF, United States of America. In addition, individual groups and members have received support from BCKDF, CANARIE, Compute Canada and CRC, Canada; PRIMUS 21/SCI/017 and UNCE SCI/013, Czech Republic; COST, ERC, ERDF, Horizon 2020 and Marie Skłodowska-Curie Actions, European Union; Investissements d’Avenir Labex, Investissements d’Avenir Idex and ANR, France; DFG and AvH Foundation, Germany; Herakleitos, Thales and Aristeia programmes co-financed by EU-ESF and the Greek NSRF, Greece; BSF-NSF and MINERVA, Israel; Norwegian Financial Mechanism 2014-2021, Norway; NCN and NAWA, Poland; La Caixa Banking Foundation, CERCA Programme Generalitat de Catalunya and PROMETEO and GenT Programmes Generalitat Valenciana, Spain; Göran Gustafssons Stiftelse, Sweden; The Royal Society and Leverhulme Trust, United Kingdom.

The crucial computing support from all WLCG partners is acknowledged gratefully, in particular from CERN, the ATLAS Tier-1 facilities at TRIUMF (Canada), NDGF (Denmark, Norway, Sweden), CC-IN2P3

(France), KIT/GridKA (Germany), INFN-CNAF (Italy), NL-T1 (Netherlands), PIC (Spain), ASGC (Taiwan), RAL (UK) and BNL (USA), the Tier-2 facilities worldwide and large non-WLCG resource providers. Major contributors of computing resources are listed in Ref. [\[49\]](#).

References

- [1] A. J. Baltz et al., *The physics of ultraperipheral collisions at the LHC*, *Phys. Rep.* **458** (2008) 1, ISSN: 0370-1573, URL: <https://www.sciencedirect.com/science/article/pii/S0370157307004462>.
- [2] S. R. Klein and P. Steinberg, *Photonuclear and Two-photon Interactions at High-Energy Nuclear Colliders*, *Ann. Rev. Nucl. Part. Sci.* **70** (2020) 323, arXiv: 2005.01872 [nucl-ex].
- [3] E. Fermi, *On the theory of collisions between atoms and electrically charged particles*, *Nuovo Cim.* **2** (1925) 143, arXiv: hep-th/0205086 [hep-th].
- [4] E. J. Williams, *Nature of the High Energy Particles of Penetrating Radiation and Status of Ionization and Radiation Formulae*, *Phys. Rev.* **45** (1934) 729.
- [5] G. Breit and J. A. Wheeler, *Collision of Two Light Quanta*, *Phys. Rev.* **46** (1934) 1087.
- [6] I. A. Pshenichnov, *Electromagnetic excitation and fragmentation of ultrarelativistic nuclei*, *Phys. Part. Nucl.* **42** (2011) 215.
- [7] A. Veyssiere, H. Beil, R. Bergere, P. Carlos and A. Lepretre, *Photoneutron cross sections of ^{208}Pb and ^{197}Au* , *Nucl. Phys. A* **159** (1970) 561, ISSN: 0375-9474, URL: <https://www.sciencedirect.com/science/article/pii/037594747090727X>.
- [8] ATLAS Collaboration, *Measurement of exclusive $\gamma\gamma \rightarrow \ell^+\ell^-$ production in proton-proton collisions at $\sqrt{s} = 7$ TeV with the ATLAS detector*, *Phys. Lett. B* **749** (2015) 242, arXiv: 1506.07098 [hep-ex].
- [9] CMS Collaboration, *Search for Exclusive or Semi-Exclusive Photon Pair Production and Observation of Exclusive and Semi-Exclusive Electron Pair Production in pp Collisions at $\sqrt{s} = 7$ TeV*, *JHEP* **11** (2012) 080, arXiv: 1209.1666 [hep-ex].
- [10] CMS Collaboration, *Exclusive photon-photon production of muon pairs in proton-proton collisions at $\sqrt{s} = 7$ TeV*, *JHEP* **01** (2012) 052, arXiv: 1111.5536 [hep-ex].
- [11] ATLAS Collaboration, *Measurement of the exclusive $\gamma\gamma \rightarrow \mu^+\mu^-$ process in proton-proton collisions at $\sqrt{s} = 13$ TeV with the ATLAS detector*, *Phys. Lett. B* **777** (2018) 303, arXiv: 1708.04053 [hep-ex].
- [12] ATLAS Collaboration, *Observation and Measurement of Forward Proton Scattering in Association with Lepton Pairs Produced via the Photon Fusion Mechanism at ATLAS*, *Phys. Rev. Lett.* **125** (2020) 261801, arXiv: 2009.14537 [hep-ex].
- [13] CMS and TOTEM Collaborations, *Observation of proton-tagged, central (semi)exclusive production of high-mass lepton pairs in pp collisions at 13 TeV with the CMS-TOTEM precision proton spectrometer*, *JHEP* **07** (2018) 153, arXiv: 1803.04496 [hep-ex].
- [14] ALICE Collaboration, *Charmonium and e^+e^- pair photoproduction at mid-rapidity in ultra-peripheral Pb-Pb collisions at $\sqrt{s_{NN}}=2.76$ TeV*, *Eur. Phys. J. C* **73** (2013) 2617, arXiv: 1305.1467 [nucl-ex].

- [15] STAR Collaboration, *Low- p_T e^+e^- pair production in Au+Au collisions at $\sqrt{s_{NN}} = 200$ GeV and U+U collisions at $\sqrt{s_{NN}} = 193$ GeV at STAR*, *Phys. Rev. Lett.* **121** (2018) 132301, arXiv: [1806.02295 \[hep-ex\]](#).
- [16] STAR Collaboration, *Measurement of e^+e^- Momentum and Angular Distributions from Linearly Polarized Photon Collisions*, *Phys. Rev. Lett.* **127** (2021) 052302, arXiv: [1910.12400 \[nucl-ex\]](#).
- [17] P. Collaboration, *Photoproduction of J/Ψ and of high mass e^+e^- in ultra-peripheral Au+Au collisions at $\sqrt{s_{NN}} = 200$ GeV*, *Phys. Lett. B* **679** (2009) 321, arXiv: [0903.2041 \[nucl-ex\]](#).
- [18] ATLAS Collaboration, *Exclusive dimuon production in ultraperipheral Pb+Pb collisions at $\sqrt{s_{NN}} = 5.02$ TeV with ATLAS*, *Phys. Rev. C* **104** (2021) 024906, arXiv: [2011.12211 \[nucl-ex\]](#).
- [19] ATLAS Collaboration, *Observation of centrality-dependent acoplanarity for muon pairs produced via two-photon scattering in Pb+Pb collisions at $\sqrt{s_{NN}} = 5.02$ TeV with the ATLAS detector*, *Phys. Rev. Lett.* **121** (2018) 212301, arXiv: [1806.08708 \[nucl-ex\]](#).
- [20] CMS Collaboration, *Observation of Forward Neutron Multiplicity Dependence of Dimuon Acoplanarity in Ultraperipheral Pb-Pb Collisions at $\sqrt{s_{NN}}=5.02$ TeV*, *Phys. Rev. Lett.* **127** (2021) 122001, arXiv: [2011.05239 \[hep-ex\]](#).
- [21] M. Dyndał, M. Kłusek-Gawenda, A. Szczurek and M. Schott, *Anomalous electromagnetic moments of τ lepton in $\gamma\gamma \rightarrow \tau^+\tau^-$ reaction in Pb+Pb collisions at the LHC*, *Phys. Lett. B* **809** (2020) 135682, ISSN: 0370-2693.
- [22] L. Beresford and J. Liu, *New physics and tau $g - 2$ using LHC heavy ion collisions*, *Phys. Rev. D* **102** (2020) 113008, URL: <https://link.aps.org/doi/10.1103/PhysRevD.102.113008>.
- [23] ATLAS Collaboration, *Evidence for light-by-light scattering in heavy-ion collisions with the ATLAS detector at the LHC*, *Nature Phys.* **13** (2017) 852, arXiv: [1702.01625 \[hep-ex\]](#).
- [24] ATLAS Collaboration, *Observation of light-by-light scattering in ultraperipheral Pb+Pb collisions with the ATLAS detector*, *Phys. Rev. Lett.* **123** (2019) 052001, arXiv: [1904.03536 \[hep-ex\]](#).
- [25] ATLAS Collaboration, *Measurement of light-by-light scattering and search for axion-like particles with 2.2 nb^{-1} of Pb+Pb data with the ATLAS detector*, *JHEP* **11** (2021) 050, arXiv: [2008.05355 \[hep-ex\]](#).
- [26] CMS Collaboration, *Evidence for light-by-light scattering and searches for axion-like particles in ultraperipheral PbPb collisions at $\sqrt{s_{NN}} = 5.02$ TeV*, *Phys. Lett. B* **797** (2019) 134826, arXiv: [1810.04602 \[hep-ex\]](#).
- [27] ATLAS Collaboration, *The ATLAS experiment at the CERN Large Hadron Collider*, *JINST* **3** (2008) S08003.
- [28] ATLAS Collaboration, *ATLAS Insertable B-Layer Technical Design Report*, (2010), URL: <https://cds.cern.ch/record/1291633>.
- [29] ATLAS Collaboration, *Performance of the ATLAS Trigger System in 2015*, *Eur. Phys. J. C* **77** (2017) 317, arXiv: [1611.09661 \[hep-ex\]](#).
- [30] ATLAS Collaboration, *Operation of the ATLAS trigger system in Run 2*, *JINST* **15** (2020) P10004, arXiv: [2007.12539 \[hep-ex\]](#).

- [31] ATLAS Collaboration, *The ATLAS Collaboration Software and Firmware*, ATL-SOFT-PUB-2021-001, 2021, URL: <https://cds.cern.ch/record/2767187>.
- [32] ATLAS Collaboration, *ATLAS data quality operations and performance for 2015–2018 data-taking*, *JINST* **15** (2020) P04003, arXiv: 1911.04632 [physics.ins-det].
- [33] S. R. Klein, J. Nystrand, J. Seger, Y. Gorbunov and J. Butterworth, *STARlight: A Monte Carlo simulation program for ultra-peripheral collisions of relativistic ions*, *Comput. Phys. Commun.* **212** (2017) 258, arXiv: 1607.03838 [hep-ph].
- [34] M. L. Miller, K. Reygers, S. J. Sanders and P. Steinberg, *Glauber Modeling in High-Energy Nuclear Collisions*, *Ann. Rev. Nucl. Part. Sci.* **57** (2007) 205, URL: <https://doi.org/10.1146/annurev.nucl.57.090506.123020>.
- [35] L. A. Harland-Lang, V. A. Khoze and M. G. Ryskin, *Exclusive LHC physics with heavy ions: SuperChic 3*, *Eur. Phys. J. C* **79** (2019) 39, URL: <https://doi.org/10.1140/epjc/s10052-018-6530-5>.
- [36] T. Sjöstrand et al., *An introduction to PYTHIA 8.2*, *Comput. Phys. Commun.* **191** (2015) 159, arXiv: 1410.3012 [hep-ph].
- [37] L. A. Harland-Lang, M. Tasevsky, V. A. Khoze and M. G. Ryskin, *A new approach to modelling elastic and inelastic photon-initiated production at the LHC: SuperChic 4*, *Eur. Phys. J. C* **80** (2020) 925, arXiv: 2007.12704 [hep-ph].
- [38] ATLAS Collaboration, *The ATLAS Simulation Infrastructure*, *Eur. Phys. J. C* **70** (2010) 823, arXiv: 1005.4568 [physics.ins-det].
- [39] GEANT4 Collaboration, S. Agostinelli et al., *GEANT4: A Simulation toolkit*, *Nucl. Instrum. Meth. A* **506** (2003) 250.
- [40] ATLAS Collaboration, *Electron and photon performance measurements with the ATLAS detector using the 2015–2017 LHC proton-proton collision data*, *JINST* **14** (2019) P12006, arXiv: 1908.00005 [hep-ex].
- [41] ATLAS Collaboration, *Early Inner Detector Tracking Performance in the 2015 Data at $\sqrt{s} = 13$ TeV*, ATL-PHYS-PUB-2015-051, 2015, URL: <https://cds.cern.ch/record/2110140>.
- [42] ATLAS Collaboration, *Performance of the ATLAS track reconstruction algorithms in dense environments in LHC Run 2*, *Eur. Phys. J. C* **77** (2017) 673, arXiv: 1704.07983 [hep-ex].
- [43] ALICE Collaboration, B. Abelev et al., *Measurement of the Cross Section for Electromagnetic Dissociation with Neutron Emission in Pb-Pb Collisions at $\sqrt{s_{NN}} = 2.76$ TeV*, *Phys. Rev. Lett.* **109** (2012) 252302, arXiv: 1203.2436 [nucl-ex].
- [44] G. D’Agostini, *A multidimensional unfolding method based on Bayes’ theorem*, *Nucl. Instrum. Meth. A* **362** (1995) 487, ISSN: 0168-9002, URL: <https://www.sciencedirect.com/science/article/pii/016890029500274X>.
- [45] T. Adye, ‘Unfolding algorithms and tests using RooUnfold’, *Proceedings, 2011 Workshop on Statistical Issues Related to Discovery Claims in Search Experiments and Unfolding (PHYSTAT 2011)* (CERN, Geneva, Switzerland, 17th–20th Jan. 2011) 313, arXiv: 1105.1160 [physics.data-an].

- [46] ATLAS Collaboration,
Luminosity determination in pp collisions at $\sqrt{s} = 8$ TeV using the ATLAS detector at the LHC,
Eur. Phys. J. C **76** (2016) 653, arXiv: [1608.03953 \[hep-ex\]](#).
- [47] G. Avoni et al., *The new LUCID-2 detector for luminosity measurement and monitoring in ATLAS*,
JINST **13** (2018) P07017.
- [48] W. Zha and Z. Tang,
Discovery of higher-order quantum electrodynamics effect for the vacuum pair production,
JHEP **08** (2021) 083, arXiv: [2103.04605 \[hep-ph\]](#).
- [49] ATLAS Collaboration, *ATLAS Computing Acknowledgements*, ATL-SOFT-PUB-2021-003, 2021,
URL: <https://cds.cern.ch/record/2776662>.

The ATLAS Collaboration

G. Aad ¹⁰¹, B. Abbott ¹¹⁹, D.C. Abbott ¹⁰², K. Abeling ⁵⁵, S.H. Abidi ²⁹, A. Aboulhorma ^{35e}, H. Abramowicz ¹⁵⁰, H. Abreu ¹⁴⁹, Y. Abulaiti ¹¹⁶, A.C. Abusleme Hoffman ^{136a}, B.S. Acharya ^{68a,68b,p}, B. Achkar ⁵⁵, L. Adam ⁹⁹, C. Adam Bourdarios ⁴, L. Adamczyk ^{84a}, L. Adamek ¹⁵⁴, S.V. Addepalli ²⁶, J. Adelman ¹¹⁴, A. Adiguzel ^{21c}, S. Adorni ⁵⁶, T. Adye ¹³³, A.A. Affolder ¹³⁵, Y. Afik ³⁶, M.N. Agaras ¹³, J. Agarwala ^{72a,72b}, A. Aggarwal ⁹⁹, C. Agheorghiesei ^{27c}, J.A. Aguilar-Saavedra ^{129f}, A. Ahmad ³⁶, F. Ahmadov ^{38,z}, W.S. Ahmed ¹⁰³, S. Ahuja ⁹⁴, X. Ai ⁴⁸, G. Aielli ^{75a,75b}, I. Aizenberg ¹⁶⁸, M. Akbiyik ⁹⁹, T.P.A. Åkesson ⁹⁷, A.V. Akimov ³⁷, K. Al Khoury ⁴¹, G.L. Alberghi ^{23b}, J. Albert ¹⁶⁴, P. Albicocco ⁵³, M.J. Alconada Verzini ⁸⁹, S. Alderweireldt ⁵², M. Aleksa ³⁶, I.N. Aleksandrov ³⁸, C. Alexa ^{27b}, T. Alexopoulos ¹⁰, A. Alfonsi ¹¹³, F. Alfonsi ^{23b}, M. Alhroob ¹¹⁹, B. Ali ¹³¹, S. Ali ¹⁴⁷, M. Aliev ³⁷, G. Alimonti ^{70a}, C. Allaire ³⁶, B.M.M. Allbrooke ¹⁴⁵, P.P. Allport ²⁰, A. Aloisio ^{71a,71b}, F. Alonso ⁸⁹, C. Alpigiani ¹³⁷, E. Alunno Camelia ^{75a,75b}, M. Alvarez Estevez ⁹⁸, M.G. Alvigi ^{71a,71b}, Y. Amaral Coutinho ^{81b}, A. Ambler ¹⁰³, C. Amelung ³⁶, C.G. Ames ¹⁰⁸, D. Amidei ¹⁰⁵, S.P. Amor Dos Santos ^{129a}, S. Amoroso ⁴⁸, K.R. Amos ¹⁶², C.S. Amrouche ⁵⁶, V. Ananiev ¹²⁴, C. Anastopoulos ¹³⁸, N. Andari ¹³⁴, T. Andeen ¹¹, J.K. Anders ¹⁹, S.Y. Andrean ^{47a,47b}, A. Andreazza ^{70a,70b}, S. Angelidakis ⁹, A. Angerami ^{41,ac}, A.V. Anisenkov ³⁷, A. Annovi ^{73a}, C. Antel ⁵⁶, M.T. Anthony ¹³⁸, E. Antipov ¹²⁰, M. Antonelli ⁵³, D.J.A. Antrim ^{17a}, F. Anulli ^{74a}, M. Aoki ⁸², J.A. Aparisi Pozo ¹⁶², M.A. Aparo ¹⁴⁵, L. Aperio Bella ⁴⁸, C. Appelt ¹⁸, N. Aranzabal ³⁶, V. Araujo Ferraz ^{81a}, C. Arcangeletti ⁵³, A.T.H. Arce ⁵¹, E. Arena ⁹¹, J-F. Arguin ¹⁰⁷, S. Argyropoulos ⁵⁴, J.-H. Arling ⁴⁸, A.J. Armbruster ³⁶, O. Arnaez ¹⁵⁴, H. Arnold ¹¹³, Z.P. Arrubarrena Tame ¹⁰⁸, G. Artoni ^{74a,74b}, H. Asada ¹¹⁰, K. Asai ¹¹⁷, S. Asai ¹⁵², N.A. Asbah ⁶¹, E.M. Asimakopoulou ¹⁶⁰, J. Assahsah ^{35d}, K. Assamagan ²⁹, R. Astalos ^{28a}, R.J. Atkin ^{33a}, M. Atkinson ¹⁶¹, N.B. Atlay ¹⁸, H. Atmani ^{62b}, P.A. Atmasiddha ¹⁰⁵, K. Augsten ¹³¹, S. Auricchio ^{71a,71b}, A.D. Auriol ²⁰, V.A. Austrup ¹⁷⁰, G. Avner ¹⁴⁹, G. Avolio ³⁶, K. Axiotis ⁵⁶, M.K. Ayoub ^{14c}, G. Azuelos ^{107,ag}, D. Babal ^{28a}, H. Bachacou ¹³⁴, K. Bachas ^{151,s}, A. Bachi ³⁴, F. Backman ^{47a,47b}, A. Badea ⁶¹, P. Bagnaia ^{74a,74b}, M. Bahmani ¹⁸, A.J. Bailey ¹⁶², V.R. Bailey ¹⁶¹, J.T. Baines ¹³³, C. Bakalis ¹⁰, O.K. Baker ¹⁷¹, P.J. Bakker ¹¹³, E. Bakos ¹⁵, D. Bakshi Gupta ⁸, S. Balaji ¹⁴⁶, R. Balasubramanian ¹¹³, E.M. Baldin ³⁷, P. Balek ¹³², E. Ballabene ^{70a,70b}, F. Balli ¹³⁴, L.M. Baltes ^{63a}, W.K. Balunas ³², J. Balz ⁹⁹, E. Banas ⁸⁵, M. Bandieramonte ¹²⁸, A. Bandyopadhyay ²⁴, S. Bansal ²⁴, L. Barak ¹⁵⁰, E.L. Barberio ¹⁰⁴, D. Barberis ^{57b,57a}, M. Barbero ¹⁰¹, G. Barbour ⁹⁵, K.N. Barends ^{33a}, T. Barillari ¹⁰⁹, M-S. Barisits ³⁶, J. Barkeloo ¹²², T. Barklow ¹⁴², R.M. Barnett ^{17a}, P. Baron ¹²¹, D.A. Baron Moreno ¹⁰⁰, A. Baroncelli ^{62a}, G. Barone ²⁹, A.J. Barr ¹²⁵, L. Barranco Navarro ^{47a,47b}, F. Barreiro ⁹⁸, J. Barreiro Guimarães da Costa ^{14a}, U. Barron ¹⁵⁰, M.G. Barros Teixeira ^{129a}, S. Barsov ³⁷, F. Bartels ^{63a}, R. Bartoldus ¹⁴², A.E. Barton ⁹⁰, P. Bartos ^{28a}, A. Basalae ⁴⁸, A. Basan ⁹⁹, M. Baselga ⁴⁹, I. Bashta ^{76a,76b}, A. Bassalat ^{66,b}, M.J. Basso ¹⁵⁴, C.R. Basson ¹⁰⁰, R.L. Bates ⁵⁹, S. Batlamous ^{35e}, J.R. Batley ³², B. Batool ¹⁴⁰, M. Battaglia ¹³⁵, M. Bauge ^{74a,74b}, P. Bauer ²⁴, A. Bayirli ^{21a}, J.B. Beacham ⁵¹, T. Beau ¹²⁶, P.H. Beauchemin ¹⁵⁷, F. Becherer ⁵⁴, P. Bechtel ²⁴, H.P. Beck ^{19,r}, K. Becker ¹⁶⁶, C. Becot ⁴⁸, A.J. Beddall ^{21d}, V.A. Bednyakov ³⁸, C.P. Bee ¹⁴⁴, L.J. Beemster ¹⁵, T.A. Beermann ³⁶, M. Begalli ^{81d}, M. Begel ²⁹, A. Behera ¹⁴⁴, J.K. Behr ⁴⁸, C. Beirao Da Cruz E Silva ³⁶, J.F. Beirer ^{55,36}, F. Beisiegel ²⁴, M. Belfkir ¹⁵⁸, G. Bella ¹⁵⁰, L. Bellagamba ^{23b}, A. Bellerive ³⁴, P. Bellos ²⁰, K. Beloborodov ³⁷, K. Belotskiy ³⁷, N.L. Belyaev ³⁷, D. Benckekroun ^{35a},

F. Bendebba ^{35a}, Y. Benhammou ¹⁵⁰, D.P. Benjamin ²⁹, M. Benoit ²⁹, J.R. Bensinger ²⁶,
 S. Bentvelsen ¹¹³, L. Beresford ³⁶, M. Beretta ⁵³, D. Berge ¹⁸, E. Bergeaas Kuutmann ¹⁶⁰,
 N. Berger ⁴, B. Bergmann ¹³¹, J. Beringer ^{17a}, S. Berlendis ⁷, G. Bernardi ⁵, C. Bernius ¹⁴²,
 F.U. Bernlochner ²⁴, T. Berry ⁹⁴, P. Berta ¹³², A. Berthold ⁵⁰, I.A. Bertram ⁹⁰,
 O. Bessidskaia Bylund ¹⁷⁰, S. Bethke ¹⁰⁹, A. Betti ^{74a,74b}, A.J. Bevan ⁹³, M. Bhamjee ^{33c},
 S. Bhatta ¹⁴⁴, D.S. Bhattacharya ¹⁶⁵, P. Bhattarai ²⁶, V.S. Bhopatkar ⁶, R. Bi ¹²⁸, R. Bi ^{29,aj},
 R.M. Bianchi ¹²⁸, O. Biebel ¹⁰⁸, R. Bielski ¹²², M. Biglietti ^{76a}, T.R.V. Billoud ¹³¹, M. Bindi ⁵⁵,
 A. Bingul ^{21b}, C. Bini ^{74a,74b}, S. Biondi ^{23b,23a}, A. Biondini ⁹¹, C.J. Birch-sykes ¹⁰⁰,
 G.A. Bird ^{20,133}, M. Birman ¹⁶⁸, T. Bisanz ³⁶, E. Bisceglie ^{43b,43a}, D. Biswas ^{169,1},
 A. Bitadze ¹⁰⁰, K. Bjørke ¹²⁴, I. Bloch ⁴⁸, C. Blocker ²⁶, A. Blue ⁵⁹, U. Blumenschein ⁹³,
 J. Blumenthal ⁹⁹, G.J. Bobbink ¹¹³, V.S. Bobrovnikov ³⁷, M. Boehler ⁵⁴, D. Bogavac ³⁶,
 A.G. Bogdanchikov ³⁷, C. Bohm ^{47a}, V. Boisvert ⁹⁴, P. Bokan ⁴⁸, T. Bold ^{84a}, M. Bomben ⁵,
 M. Bona ⁹³, M. Boonekamp ¹³⁴, C.D. Booth ⁹⁴, A.G. Borbély ⁵⁹, H.M. Borecka-Bielska ¹⁰⁷,
 L.S. Borgna ⁹⁵, G. Borissov ⁹⁰, D. Bortoletto ¹²⁵, D. Boscherini ^{23b}, M. Bosman ¹³,
 J.D. Bossio Sola ³⁶, K. Bouaouda ^{35a}, J. Boudreau ¹²⁸, E.V. Bouhova-Thacker ⁹⁰,
 D. Boumediene ⁴⁰, R. Bouquet ⁵, A. Boveia ¹¹⁸, J. Boyd ³⁶, D. Boye ²⁹, I.R. Boyko ³⁸,
 J. Bracinik ²⁰, N. Brahimy ^{62d,62c}, G. Brandt ¹⁷⁰, O. Brandt ³², F. Braren ⁴⁸, B. Brau ¹⁰²,
 J.E. Brau ¹²², W.D. Breaden Madden ⁵⁹, K. Brendlinger ⁴⁸, R. Brenner ¹⁶⁸, L. Brenner ³⁶,
 R. Brenner ¹⁶⁰, S. Bressler ¹⁶⁸, B. Brickwedde ⁹⁹, D. Britton ⁵⁹, D. Britzger ¹⁰⁹, I. Brock ²⁴,
 G. Brooijmans ⁴¹, W.K. Brooks ^{136f}, E. Brost ²⁹, P.A. Bruckman de Renstrom ⁸⁵, B. Brüers ⁴⁸,
 D. Bruncko ^{28b,*}, A. Bruni ^{23b}, G. Bruni ^{23b}, M. Bruschi ^{23b}, N. Brusino ^{74a,74b},
 L. Bryngemark ¹⁴², T. Buanes ¹⁶, Q. Buat ¹³⁷, P. Buchholz ¹⁴⁰, A.G. Buckley ⁵⁹,
 I.A. Budagov ^{38,*}, M.K. Bugge ¹²⁴, O. Bulekov ³⁷, B.A. Bullard ⁶¹, S. Burdin ⁹¹,
 C.D. Burgard ⁴⁸, A.M. Burger ⁴⁰, B. Burghgrave ⁸, J.T.P. Burr ³², C.D. Burton ¹¹,
 J.C. Burzynski ¹⁴¹, E.L. Busch ⁴¹, V. Büscher ⁹⁹, P.J. Bussey ⁵⁹, J.M. Butler ²⁵, C.M. Buttar ⁵⁹,
 J.M. Butterworth ⁹⁵, W. Buttinger ¹³³, C.J. Buxo Vazquez ¹⁰⁶, A.R. Buzykaev ³⁷, G. Cabras ^{23b},
 S. Cabrera Urbán ¹⁶², D. Caforio ⁵⁸, H. Cai ¹²⁸, Y. Cai ^{14a,14d}, V.M.M. Cairo ³⁶, O. Cakir ^{3a},
 N. Calace ³⁶, P. Calafiura ^{17a}, G. Calderini ¹²⁶, P. Calfayan ⁶⁷, G. Callea ⁵⁹, L.P. Caloba ^{81b},
 D. Calvet ⁴⁰, S. Calvet ⁴⁰, T.P. Calvet ¹⁰¹, M. Calvetti ^{73a,73b}, R. Camacho Toro ¹²⁶,
 S. Camarda ³⁶, D. Camarero Munoz ⁹⁸, P. Camarri ^{75a,75b}, M.T. Camerlingo ^{76a,76b},
 D. Cameron ¹²⁴, C. Camincher ¹⁶⁴, M. Campanelli ⁹⁵, A. Camplani ⁴², V. Canale ^{71a,71b},
 A. Canesse ¹⁰³, M. Cano Bret ⁷⁹, J. Cantero ¹⁶², Y. Cao ¹⁶¹, F. Capocasa ²⁶, M. Capua ^{43b,43a},
 A. Carbone ^{70a,70b}, R. Cardarelli ^{75a}, J.C.J. Cardenas ⁸, F. Cardillo ¹⁶², T. Carli ³⁶,
 G. Carlino ^{71a}, B.T. Carlson ^{128,t}, E.M. Carlson ^{164,155a}, L. Carminati ^{70a,70b}, M. Carnesale ^{74a,74b},
 S. Caron ¹¹², E. Carquin ^{136f}, S. Carrá ^{70a,70b}, G. Carratta ^{23b,23a}, F. Carrio Argos ^{33g},
 J.W.S. Carter ¹⁵⁴, T.M. Carter ⁵², M.P. Casado ^{13,i}, A.F. Casha ¹⁵⁴, E.G. Castiglia ¹⁷¹,
 F.L. Castillo ^{63a}, L. Castillo Garcia ¹³, V. Castillo Gimenez ¹⁶², N.F. Castro ^{129a,129e},
 A. Catinaccio ³⁶, J.R. Catmore ¹²⁴, V. Cavaliere ²⁹, N. Cavalli ^{23b,23a}, V. Cavasinni ^{73a,73b},
 E. Celebi ^{21a}, F. Celli ¹²⁵, M.S. Centonze ^{69a,69b}, K. Cerny ¹²¹, A.S. Cerqueira ^{81a}, A. Cerri ¹⁴⁵,
 L. Cerrito ^{75a,75b}, F. Cerutti ^{17a}, A. Cervelli ^{23b}, S.A. Cetin ^{21d}, Z. Chadi ^{35a},
 D. Chakraborty ¹¹⁴, M. Chala ^{129f}, J. Chan ¹⁶⁹, W.S. Chan ¹¹³, W.Y. Chan ¹⁵²,
 J.D. Chapman ³², B. Chargeishvili ^{148b}, D.G. Charlton ²⁰, T.P. Charman ⁹³, M. Chatterjee ¹⁹,
 S. Chekanov ⁶, S.V. Chekulaev ^{155a}, G.A. Chelkov ^{38,a}, A. Chen ¹⁰⁵, B. Chen ¹⁵⁰, B. Chen ¹⁶⁴,
 C. Chen ^{62a}, H. Chen ^{14c}, H. Chen ²⁹, J. Chen ^{62c}, J. Chen ²⁶, S. Chen ¹⁵², S.J. Chen ^{14c},
 X. Chen ^{62c}, X. Chen ^{14b,af}, Y. Chen ^{62a}, C.L. Cheng ¹⁶⁹, H.C. Cheng ^{64a}, A. Cheplakov ³⁸,
 E. Cheremushkina ⁴⁸, E. Cherepanova ¹¹³, R. Cherkaoui El Moursli ^{35e}, E. Cheu ⁷, K. Cheung ⁶⁵,
 L. Chevalier ¹³⁴, V. Chiarella ⁵³, G. Chiarelli ^{73a}, N. Chiedde ¹⁰¹, G. Chiodini ^{69a},

A.S. Chisholm ^{id20}, A. Chitan ^{id27b}, Y.H. Chiu ^{id164}, M.V. Chizhov ^{id38}, K. Choi ^{id11},
 A.R. Chomont ^{id74a,74b}, Y. Chou ^{id102}, E.Y.S. Chow ^{id113}, T. Chowdhury ^{id33g}, L.D. Christopher ^{id33g},
 K.L. Chu ^{id64a}, M.C. Chu ^{id64a}, X. Chu ^{id14a,14d}, J. Chudoba ^{id130}, J.J. Chwastowski ^{id85}, D. Cieri ^{id109},
 K.M. Ciesla ^{id84a}, V. Cindro ^{id92}, A. Ciocio ^{id17a}, F. Cirotto ^{id71a,71b}, Z.H. Citron ^{id168,m}, M. Citterio ^{id70a},
 D.A. Ciubotaru ^{id27b}, B.M. Ciungu ^{id154}, A. Clark ^{id56}, P.J. Clark ^{id52}, J.M. Clavijo Columbie ^{id48},
 S.E. Clawson ^{id100}, C. Clement ^{id47a,47b}, J. Clercx ^{id48}, L. Clissa ^{id23b,23a}, Y. Coadou ^{id101},
 M. Cobal ^{id68a,68c}, A. Coccaro ^{id57b}, R.F. Coelho Barrue ^{id129a}, R. Coelho Lopes De Sa ^{id102},
 S. Coelli ^{id70a}, H. Cohen ^{id150}, A.E.C. Coimbra ^{id70a,70b}, B. Cole ^{id41}, J. Collot ^{id60},
 P. Conde Muiño ^{id129a,129g}, M.P. Connell ^{id33c}, S.H. Connell ^{id33c}, I.A. Connelly ^{id59}, E.I. Conroy ^{id125},
 F. Conventi ^{id71a,ah}, H.G. Cooke ^{id20}, A.M. Cooper-Sarkar ^{id125}, F. Cormier ^{id163}, L.D. Corpe ^{id36},
 M. Corradi ^{id74a,74b}, E.E. Corrigan ^{id97}, F. Corriveau ^{id103,y}, A. Cortes-Gonzalez ^{id18}, M.J. Costa ^{id162},
 F. Costanza ^{id4}, D. Costanzo ^{id138}, B.M. Cote ^{id118}, G. Cowan ^{id94}, J.W. Cowley ^{id32}, K. Cranmer ^{id116},
 S. Crépe-Renaudin ^{id60}, F. Crescioli ^{id126}, M. Cristinziani ^{id140}, M. Cristoforetti ^{id77a,77b,d}, V. Croft ^{id157},
 G. Crosetti ^{id43b,43a}, A. Cueto ^{id36}, T. Cuhadar Donszelmann ^{id159}, H. Cui ^{id14a,14d}, Z. Cui ^{id7},
 A.R. Cukierman ^{id142}, W.R. Cunningham ^{id59}, F. Curcio ^{id43b,43a}, P. Czodrowski ^{id36}, M.M. Czurylo ^{id63b},
 M.J. Da Cunha Sargedas De Sousa ^{id62a}, J.V. Da Fonseca Pinto ^{id81b}, C. Da Via ^{id100}, W. Dabrowski ^{id84a},
 T. Dado ^{id49}, S. Dahbi ^{id33g}, T. Dai ^{id105}, C. Dallapiccola ^{id102}, M. Dam ^{id42}, G. D'amen ^{id29},
 V. D'Amico ^{id76a,76b}, J. Damp ^{id99}, J.R. Dandoy ^{id127}, M.F. Daneri ^{id30}, M. Danninger ^{id141}, V. Dao ^{id36},
 G. Darbo ^{id57b}, S. Darmora ^{id6}, S.J. Das ^{id29,aj}, A. Dattagupta ^{id122}, S. D'Auria ^{id70a,70b}, C. David ^{id155b},
 T. Davidek ^{id132}, D.R. Davis ^{id51}, B. Davis-Purcell ^{id34}, I. Dawson ^{id93}, K. De ^{id8}, R. De Asmundis ^{id71a},
 M. De Beurs ^{id113}, S. De Castro ^{id23b,23a}, N. De Groot ^{id112}, P. de Jong ^{id113}, H. De la Torre ^{id106},
 A. De Maria ^{id14c}, A. De Salvo ^{id74a}, U. De Sanctis ^{id75a,75b}, A. De Santo ^{id145},
 J.B. De Vivie De Regie ^{id60}, D.V. Dedovich ^{id38}, J. Degens ^{id113}, A.M. Deiana ^{id44}, F. Del Corso ^{id23b,23a},
 J. Del Peso ^{id98}, F. Del Rio ^{id63a}, F. Deliot ^{id134}, C.M. Delitzsch ^{id49}, M. Della Pietra ^{id71a,71b},
 D. Della Volpe ^{id56}, A. Dell'Acqua ^{id36}, L. Dell'Asta ^{id70a,70b}, M. Delmastro ^{id4}, P.A. Delsart ^{id60},
 S. Demers ^{id171}, M. Demichev ^{id38}, S.P. Denisov ^{id37}, L. D'Eramo ^{id114}, D. Derendarz ^{id85},
 F. Derue ^{id126}, P. Dervan ^{id91}, K. Desch ^{id24}, K. Dette ^{id154}, C. Deutsch ^{id24}, P.O. Deviveiros ^{id36},
 F.A. Di Bello ^{id74a,74b}, A. Di Ciaccio ^{id75a,75b}, L. Di Ciaccio ^{id4}, A. Di Domenico ^{id74a,74b},
 C. Di Donato ^{id71a,71b}, A. Di Girolamo ^{id36}, G. Di Gregorio ^{id73a,73b}, A. Di Luca ^{id77a,77b},
 B. Di Micco ^{id76a,76b}, R. Di Nardo ^{id76a,76b}, C. Diaconu ^{id101}, F.A. Dias ^{id113}, T. Dias Do Vale ^{id141},
 M.A. Diaz ^{id136a,136b}, F.G. Diaz Capriles ^{id24}, M. Didenko ^{id162}, E.B. Diehl ^{id105}, L. Diehl ^{id54},
 S. Díez Cornell ^{id48}, C. Diez Pardos ^{id140}, C. Dimitriadi ^{id24,160}, A. Dimitrievska ^{id17a}, W. Ding ^{id14b},
 J. Dingfelder ^{id24}, I-M. Dinu ^{id27b}, S.J. Dittmeier ^{id63b}, F. Dittus ^{id36}, F. Djama ^{id101}, T. Djobava ^{id148b},
 J.I. Djuvsland ^{id16}, D. Dodsworth ^{id26}, C. Doglioni ^{id100,97}, J. Dolejsi ^{id132}, Z. Dolezal ^{id132},
 M. Donadelli ^{id81c}, B. Dong ^{id62c}, J. Donini ^{id40}, A. D'Onofrio ^{id14c}, M. D'Onofrio ^{id91}, J. Dopke ^{id133},
 A. Doria ^{id71a}, M.T. Dova ^{id89}, A.T. Doyle ^{id59}, M.A. Draguet ^{id125}, E. Drechsler ^{id141}, E. Dreyer ^{id168},
 I. Drivas-koulouris ^{id10}, A.S. Drobac ^{id157}, D. Du ^{id62a}, T.A. du Pree ^{id113}, F. Dubinin ^{id37},
 M. Dubovsky ^{id28a}, E. Duchovni ^{id168}, G. Duckeck ^{id108}, O.A. Ducu ^{id36}, D. Duda ^{id109}, A. Dudarev ^{id36},
 M. D'uffizi ^{id100}, L. Dufflot ^{id66}, M. Dührssen ^{id36}, C. Dülsen ^{id170}, A.E. Dumitriu ^{id27b}, M. Dunford ^{id63a},
 S. Dungs ^{id49}, K. Dunne ^{id47a,47b}, A. Duperrin ^{id101}, H. Duran Yildiz ^{id3a}, M. Düren ^{id58},
 A. Durglishvili ^{id148b}, B.L. Dwyer ^{id114}, G.I. Dyckes ^{id17a}, M. Dyndal ^{id84a}, S. Dysch ^{id100},
 B.S. Dziedzic ^{id85}, Z.O. Earnshaw ^{id145}, B. Eckerova ^{id28a}, M.G. Eggleston ^{id51},
 E. Egidio Purcino De Souza ^{id81b}, L.F. Ehrke ^{id56}, G. Eigen ^{id16}, K. Einsweiler ^{id17a}, T. Ekelof ^{id160},
 P.A. Ekman ^{id97}, Y. El Ghazali ^{id35b}, H. El Jarrari ^{id35e,147}, A. El Moussaouy ^{id35a}, V. Ellajosyula ^{id160},
 M. Ellert ^{id160}, F. Ellinghaus ^{id170}, A.A. Elliot ^{id93}, N. Ellis ^{id36}, J. Elmsheuser ^{id29}, M. Elsing ^{id36},
 D. Emelianov ^{id133}, A. Emerman ^{id41}, Y. Enari ^{id152}, I. Ene ^{id17a}, S. Epari ^{id13}, J. Erdmann ^{id49},
 A. Ereditato ^{id19}, P.A. Erland ^{id85}, M. Errenst ^{id170}, M. Escalier ^{id66}, C. Escobar ^{id162}, E. Etzion ^{id150},

G. Evans [ID129a](#), H. Evans [ID67](#), M.O. Evans [ID145](#), A. Ezhilov [ID37](#), S. Ezzarqtouni [ID35a](#), F. Fabbri [ID59](#), L. Fabbri [ID23b,23a](#), G. Facini [ID95](#), V. Fadeyev [ID135](#), R.M. Fakhruddinov [ID37](#), S. Falciano [ID74a](#), P.J. Falke [ID24](#), S. Falke [ID36](#), J. Faltova [ID132](#), Y. Fan [ID14a](#), Y. Fang [ID14a,14d](#), G. Fanourakis [ID46](#), M. Fanti [ID70a,70b](#), M. Faraj [ID68a,68b](#), A. Farbin [ID8](#), A. Farilla [ID76a](#), T. Farooque [ID106](#), S.M. Farrington [ID52](#), F. Fassi [ID35e](#), D. Fassouliotis [ID9](#), M. Fauci Giannelli [ID75a,75b](#), W.J. Fawcett [ID32](#), L. Fayard [ID66](#), O.L. Fedin [ID37,a](#), G. Fedotov [ID37](#), M. Feickert [ID161](#), L. Feligioni [ID101](#), A. Fell [ID138](#), D.E. Fellers [ID122](#), C. Feng [ID62b](#), M. Feng [ID14b](#), Z. Feng [ID113](#), M.J. Fenton [ID159](#), A.B. Fenyuk [ID37](#), L. Ferencz [ID48](#), S.W. Ferguson [ID45](#), J. Ferrando [ID48](#), A. Ferrari [ID160](#), P. Ferrari [ID113](#), R. Ferrari [ID72a](#), D. Ferrere [ID56](#), C. Ferretti [ID105](#), F. Fiedler [ID99](#), A. Filipčič [ID92](#), E.K. Filmer [ID1](#), F. Filthaut [ID112](#), M.C.N. Fiolhais [ID129a,129c,c](#), L. Fiorini [ID162](#), F. Fischer [ID140](#), W.C. Fisher [ID106](#), T. Fitschen [ID20,66](#), I. Fleck [ID140](#), P. Fleischmann [ID105](#), T. Flick [ID170](#), L. Flores [ID127](#), M. Flores [ID33d,ad](#), L.R. Flores Castillo [ID64a](#), F.M. Follega [ID77a,77b](#), N. Fomin [ID16](#), J.H. Foo [ID154](#), B.C. Forland [ID67](#), A. Formica [ID134](#), A.C. Forti [ID100](#), E. Fortin [ID101](#), A.W. Fortman [ID61](#), M.G. Foti [ID17a](#), L. Fountas [ID9,j](#), D. Fournier [ID66](#), H. Fox [ID90](#), P. Francavilla [ID73a,73b](#), S. Francescato [ID61](#), M. Franchini [ID23b,23a](#), S. Franchino [ID63a](#), D. Francis [ID36](#), L. Franco [ID112](#), L. Franconi [ID19](#), M. Franklin [ID61](#), G. Frattari [ID26](#), A.C. Freegard [ID93](#), P.M. Freeman [ID20](#), W.S. Freund [ID81b](#), N. Fritzsche [ID50](#), A. Froch [ID54](#), D. Froidevaux [ID36](#), J.A. Frost [ID125](#), Y. Fu [ID62a](#), M. Fujimoto [ID117](#), E. Fullana Torregrosa [ID162,*](#), J. Fuster [ID162](#), A. Gabrielli [ID23b,23a](#), A. Gabrielli [ID36](#), P. Gadow [ID48](#), G. Gagliardi [ID57b,57a](#), L.G. Gagnon [ID17a](#), G.E. Gallardo [ID125](#), E.J. Gallas [ID125](#), B.J. Gallop [ID133](#), R. Gamboa Goni [ID93](#), K.K. Gan [ID118](#), S. Ganguly [ID152](#), J. Gao [ID62a](#), Y. Gao [ID52](#), F.M. Garay Walls [ID136a,136b](#), B. Garcia [ID29,aj](#), C. García [ID162](#), J.E. García Navarro [ID162](#), J.A. García Pascual [ID14a](#), M. Garcia-Sciveres [ID17a](#), R.W. Gardner [ID39](#), D. Garg [ID79](#), R.B. Garg [ID142,q](#), S. Gargiulo [ID54](#), C.A. Garner [ID154](#), V. Garonne [ID29](#), S.J. Gasiorowski [ID137](#), P. Gaspar [ID81b](#), G. Gaudio [ID72a](#), V. Gautam [ID13](#), P. Gauzzi [ID74a,74b](#), I.L. Gavrilenko [ID37](#), A. Gavrilyuk [ID37](#), C. Gay [ID163](#), G. Gaycken [ID48](#), E.N. Gazis [ID10](#), A.A. Geanta [ID27b](#), C.M. Gee [ID135](#), J. Geisen [ID97](#), M. Geisen [ID99](#), C. Gemme [ID57b](#), M.H. Genest [ID60](#), S. Gentile [ID74a,74b](#), S. George [ID94](#), W.F. George [ID20](#), T. Geralis [ID46](#), L.O. Gerlach [ID55](#), P. Gessinger-Befurt [ID36](#), M. Ghasemi Bostanabad [ID164](#), M. Ghneimat [ID140](#), A. Ghosal [ID140](#), A. Ghosh [ID159](#), A. Ghosh [ID7](#), B. Giacobbe [ID23b](#), S. Giagu [ID74a,74b](#), N. Giangiacomi [ID154](#), P. Giannetti [ID73a](#), A. Giannini [ID62a](#), S.M. Gibson [ID94](#), M. Gignac [ID135](#), D.T. Gil [ID84b](#), A.K. Gilbert [ID84a](#), B.J. Gilbert [ID41](#), D. Gillberg [ID34](#), G. Gilles [ID113](#), N.E.K. Gillwald [ID48](#), L. Ginabat [ID126](#), D.M. Gingrich [ID2,ag](#), M.P. Giordani [ID68a,68c](#), P.F. Giraud [ID134](#), G. Giugliarelli [ID68a,68c](#), D. Giugni [ID70a](#), F. Giuli [ID36](#), I. Gkialas [ID9,j](#), L.K. Gladilin [ID37](#), C. Glasman [ID98](#), G.R. Gledhill [ID122](#), M. Glisic [ID122](#), I. Gnesi [ID43b,f](#), Y. Go [ID29,aj](#), M. Goblirsch-Kolb [ID26](#), D. Godin [ID107](#), S. Goldfarb [ID104](#), T. Golling [ID56](#), M.G.D. Gololo [ID33g](#), D. Golubkov [ID37](#), J.P. Gombas [ID106](#), A. Gomes [ID129a,129b](#), G. Gomes Da Silva [ID140](#), A.J. Gomez Delegido [ID162](#), R. Goncalves Gama [ID55](#), R. Gonçalves [ID129a,129c](#), G. Gonella [ID122](#), L. Gonella [ID20](#), A. Gongadze [ID38](#), F. Gonnella [ID20](#), J.L. Gonski [ID41](#), R.Y. González Andana [ID52](#), S. González de la Hoz [ID162](#), S. Gonzalez Fernandez [ID13](#), R. Gonzalez Lopez [ID91](#), C. Gonzalez Renteria [ID17a](#), R. Gonzalez Suarez [ID160](#), S. Gonzalez-Sevilla [ID56](#), G.R. Gonzalvo Rodriguez [ID162](#), L. Goossens [ID36](#), N.A. Gorasia [ID20](#), P.A. Gorbounov [ID37](#), B. Gorini [ID36](#), E. Gorini [ID69a,69b](#), A. Gorišek [ID92](#), A.T. Goshaw [ID51](#), M.I. Gostkin [ID38](#), C.A. Gottardo [ID36](#), M. Goughri [ID35b](#), V. Goumarre [ID48](#), A.G. Goussiou [ID137](#), N. Govender [ID33c](#), C. Goy [ID4](#), I. Grabowska-Bold [ID84a](#), K. Graham [ID34](#), E. Gramstad [ID124](#), S. Grancagnolo [ID18](#), M. Grandi [ID145](#), V. Gratchev [ID37,*](#), P.M. Gravila [ID27f](#), F.G. Gravili [ID69a,69b](#), H.M. Gray [ID17a](#), M. Greco [ID69a,69b](#), C. Grefe [ID24](#), I.M. Gregor [ID48](#), P. Grenier [ID142](#), C. Grieco [ID13](#), A.A. Grillo [ID135](#), K. Grimm [ID31,n](#), S. Grinstein [ID13,v](#), J.-F. Grivaz [ID66](#), E. Gross [ID168](#), J. Grosse-Knetter [ID55](#), C. Grud [ID105](#), A. Grummer [ID111](#), J.C. Grundy [ID125](#), L. Guan [ID105](#), W. Guan [ID169](#), C. Gubbels [ID163](#), J.G.R. Guerrero Rojas [ID162](#), G. Guerrieri [ID68a,68b](#), F. Guescini [ID109](#), R. Gugel [ID99](#), J.A.M. Guhit [ID105](#), A. Guida [ID48](#), T. Guillemain [ID4](#), E. Guilloton [ID166,133](#), S. Guindon [ID36](#), F. Guo [ID14a,14d](#), J. Guo [ID62c](#), L. Guo [ID66](#), Y. Guo [ID105](#),

R. Gupta ⁴⁸, S. Gurbuz ²⁴, S.S. Gurdasani ⁵⁴, G. Gustavino ³⁶, M. Guth ⁵⁶, P. Gutierrez ¹¹⁹, L.F. Gutierrez Zagazeta ¹²⁷, C. Gutschow ⁹⁵, C. Guyot ¹³⁴, C. Gwenlan ¹²⁵, C.B. Gwilliam ⁹¹, E.S. Haaland ¹²⁴, A. Haas ¹¹⁶, M. Habedank ⁴⁸, C. Haber ^{17a}, H.K. Hadavand ⁸, A. Hadeif ⁹⁹, S. Hadzic ¹⁰⁹, M. Haleem ¹⁶⁵, J. Haley ¹²⁰, J.J. Hall ¹³⁸, G.D. Hallowell ¹⁰¹, L. Halser ¹⁹, K. Hamano ¹⁶⁴, H. Hamdaoui ^{35e}, M. Hamer ²⁴, G.N. Hamity ⁵², J. Han ^{62b}, K. Han ^{62a}, L. Han ^{14c}, L. Han ^{62a}, S. Han ^{17a}, Y.F. Han ¹⁵⁴, K. Hanagaki ⁸², M. Hance ¹³⁵, D.A. Hangal ^{41,ac}, M.D. Hank ³⁹, R. Hankache ¹⁰⁰, J.B. Hansen ⁴², J.D. Hansen ⁴², P.H. Hansen ⁴², K. Hara ¹⁵⁶, D. Harada ⁵⁶, T. Harenberg ¹⁷⁰, S. Harkusha ³⁷, Y.T. Harris ¹²⁵, N.M. Harrison ¹¹⁸, P.F. Harrison ¹⁶⁶, N.M. Hartman ¹⁴², N.M. Hartmann ¹⁰⁸, Y. Hasegawa ¹³⁹, A. Hasib ⁵², S. Haug ¹⁹, R. Hauser ¹⁰⁶, M. Havranek ¹³¹, C.M. Hawkes ²⁰, R.J. Hawkins ³⁶, S. Hayashida ¹¹⁰, D. Hayden ¹⁰⁶, C. Hayes ¹⁰⁵, R.L. Hayes ¹⁶³, C.P. Hays ¹²⁵, J.M. Hays ⁹³, H.S. Hayward ⁹¹, F. He ^{62a}, Y. He ¹⁵³, Y. He ¹²⁶, M.P. Heath ⁵², V. Hedberg ⁹⁷, A.L. Heggelund ¹²⁴, N.D. Hehir ⁹³, C. Heidegger ⁵⁴, K.K. Heidegger ⁵⁴, W.D. Heidorn ⁸⁰, J. Heilman ³⁴, S. Heim ⁴⁸, T. Heim ^{17a}, J.G. Heinlein ¹²⁷, J.J. Heinrich ¹²², L. Heinrich ^{109,ac}, J. Hejbal ¹³⁰, L. Helary ⁴⁸, A. Held ¹⁶⁹, S. Hellesund ¹²⁴, C.M. Helling ¹⁶³, S. Hellman ^{47a,47b}, C. Hensens ³⁶, R.C.W. Henderson ⁹⁰, L. Henkelmann ³², A.M. Henriques Correia ³⁶, H. Herde ¹⁴², Y. Hernández Jiménez ¹⁴⁴, H. Herr ⁹⁹, M.G. Herrmann ¹⁰⁸, T. Herrmann ⁵⁰, G. Herten ⁵⁴, R. Hertenberger ¹⁰⁸, L. Hervas ³⁶, N.P. Hessey ^{155a}, H. Hibi ⁸³, E. Higón-Rodríguez ¹⁶², S.J. Hillier ²⁰, I. Hinchliffe ^{17a}, F. Hinterkeuser ²⁴, M. Hirose ¹²³, S. Hirose ¹⁵⁶, D. Hirschbuehl ¹⁷⁰, T.G. Hitchings ¹⁰⁰, B. Hiti ⁹², J. Hobbs ¹⁴⁴, R. Hobincu ^{27e}, N. Hod ¹⁶⁸, M.C. Hodgkinson ¹³⁸, B.H. Hodgkinson ³², A. Hoecker ³⁶, J. Hofer ⁴⁸, D. Hohn ⁵⁴, T. Holm ²⁴, M. Holzbock ¹⁰⁹, L.B.A.H. Hommels ³², B.P. Honan ¹⁰⁰, J. Hong ^{62c}, T.M. Hong ¹²⁸, Y. Hong ⁵⁵, J.C. Honig ⁵⁴, A. Hönle ¹⁰⁹, B.H. Hooberman ¹⁶¹, W.H. Hopkins ⁶, Y. Horii ¹¹⁰, S. Hou ¹⁴⁷, A.S. Howard ⁹², J. Howarth ⁵⁹, J. Hoya ⁸⁹, M. Hrabovsky ¹²¹, A. Hrynevich ³⁷, T. Hryn'ova ⁴, P.J. Hsu ⁶⁵, S.-C. Hsu ¹³⁷, Q. Hu ^{41,ac}, Y.F. Hu ^{14a,14d,ai}, D.P. Huang ⁹⁵, S. Huang ^{64b}, X. Huang ^{14c}, Y. Huang ^{62a}, Y. Huang ^{14a}, Z. Huang ¹⁰⁰, Z. Hubacek ¹³¹, M. Huebner ²⁴, F. Huegging ²⁴, T.B. Huffman ¹²⁵, M. Huhtinen ³⁶, S.K. Huiberts ¹⁶, R. Hulsken ¹⁰³, N. Huseynov ^{12,a}, J. Huston ¹⁰⁶, J. Huth ⁶¹, R. Hyneman ¹⁴², S. Hyrych ^{28a}, G. Iacobucci ⁵⁶, G. Iakovidis ²⁹, I. Ibragimov ¹⁴⁰, L. Iconomidou-Fayard ⁶⁶, P. Inengo ^{71a,71b}, R. Iguchi ¹⁵², T. Iizawa ⁵⁶, Y. Ikegami ⁸², A. Ilg ¹⁹, N. Ilic ¹⁵⁴, H. Imam ^{35a}, T. Ingebretsen Carlson ^{47a,47b}, G. Introzzi ^{72a,72b}, M. Iodice ^{76a}, V. Ippolito ^{74a,74b}, M. Ishino ¹⁵², W. Islam ¹⁶⁹, C. Issever ^{18,48}, S. Istin ^{21a,ak}, H. Ito ¹⁶⁷, J.M. Iturbe Ponce ^{64a}, R. Iuppa ^{77a,77b}, A. Ivina ¹⁶⁸, J.M. Izen ⁴⁵, V. Izzo ^{71a}, P. Jacka ^{130,131}, P. Jackson ¹, R.M. Jacobs ⁴⁸, B.P. Jaeger ¹⁴¹, C.S. Jagfeld ¹⁰⁸, G. Jäkel ¹⁷⁰, K. Jakobs ⁵⁴, T. Jakoubek ¹⁶⁸, J. Jamieson ⁵⁹, K.W. Janas ^{84a}, G. Jarlskog ⁹⁷, A.E. Jaspán ⁹¹, T. Javůrek ³⁶, M. Javurkova ¹⁰², F. Jeanneau ¹³⁴, L. Jeanty ¹²², J. Jejelava ^{148a,aa}, P. Jenni ^{54,g}, C.E. Jessiman ³⁴, S. Jézéquel ⁴, J. Jia ¹⁴⁴, X. Jia ⁶¹, X. Jia ^{14a,14d}, Z. Jia ^{14c}, Y. Jiang ^{62a}, S. Jiggins ⁵², J. Jimenez Pena ¹⁰⁹, S. Jin ^{14c}, A. Jinaru ^{27b}, O. Jinnouchi ¹⁵³, H. Jivan ^{33g}, P. Johansson ¹³⁸, K.A. Johns ⁷, C.A. Johnson ⁶⁷, D.M. Jones ³², E. Jones ¹⁶⁶, P. Jones ³², R.W.L. Jones ⁹⁰, T.J. Jones ⁹¹, J. Jovicevic ¹⁵, X. Ju ^{17a}, J.J. Junggeburth ³⁶, A. Juste Rozas ^{13,v}, S. Kabana ^{136e}, A. Kaczmarska ⁸⁵, M. Kado ^{74a,74b}, H. Kagan ¹¹⁸, M. Kagan ¹⁴², A. Kahn ⁴¹, A. Kahn ¹²⁷, C. Kahra ⁹⁹, T. Kaji ¹⁶⁷, E. Kajomovitz ¹⁴⁹, N. Kakati ¹⁶⁸, C.W. Kalderon ²⁹, A. Kamenshchikov ¹⁵⁴, N.J. Kang ¹³⁵, Y. Kano ¹¹⁰, D. Kar ^{33g}, K. Karava ¹²⁵, M.J. Kareem ^{155b}, E. Karentzos ⁵⁴, I. Karkanias ¹⁵¹, S.N. Karpov ³⁸, Z.M. Karpova ³⁸, V. Kartvelishvili ⁹⁰, A.N. Karyukhin ³⁷, E. Kasimi ¹⁵¹, C. Kato ^{62d}, J. Katzy ⁴⁸, S. Kaur ³⁴, K. Kawade ¹³⁹, K. Kawagoe ⁸⁸, T. Kawaguchi ¹¹⁰, T. Kawamoto ¹³⁴, G. Kawamura ⁵⁵, E.F. Kay ¹⁶⁴, F.I. Kaya ¹⁵⁷, S. Kazakos ¹³, V.F. Kazanin ³⁷, Y. Ke ¹⁴⁴, J.M. Keaveney ^{33a}, R. Keeler ¹⁶⁴, G.V. Kehris ⁶¹, J.S. Keller ³⁴, A.S. Kelly ⁹⁵,

D. Kelsey ¹⁴⁵, J.J. Kempster ²⁰, J. Kendrick ²⁰, K.E. Kennedy ⁴¹, O. Kepka ¹³⁰,
 B.P. Kerridge ¹⁶⁶, S. Kersten ¹⁷⁰, B.P. Kerševan ⁹², L. Keszezhova ^{28a}, S. Ketabchi Haghghat ¹⁵⁴,
 M. Khandoga ¹²⁶, A. Khanov ¹²⁰, A.G. Kharlamov ³⁷, T. Kharlamova ³⁷, E.E. Khoda ¹³⁷,
 T.J. Khoo ¹⁸, G. Khoriali ¹⁶⁵, J. Khubua ^{148b}, Y.A.R. Khwaira ⁶⁶, M. Kiehn ³⁶,
 A. Kilgallon ¹²², D.W. Kim ^{47a,47b}, E. Kim ¹⁵³, Y.K. Kim ³⁹, N. Kimura ⁹⁵, A. Kirchhoff ⁵⁵,
 D. Kirchmeier ⁵⁰, C. Kirfel ²⁴, J. Kirk ¹³³, A.E. Kiryunin ¹⁰⁹, T. Kishimoto ¹⁵², D.P. Kisliuk ¹⁵⁴,
 C. Kitsaki ¹⁰, O. Kivernyk ²⁴, M. Klassen ^{63a}, C. Klein ³⁴, L. Klein ¹⁶⁵, M.H. Klein ¹⁰⁵,
 M. Klein ⁹¹, U. Klein ⁹¹, P. Klimek ³⁶, A. Klimentov ²⁹, F. Klimpel ¹⁰⁹, T. Klingl ²⁴,
 T. Klioutchnikova ³⁶, F.F. Klitzner ¹⁰⁸, P. Kluit ¹¹³, S. Kluth ¹⁰⁹, E. Kneringer ⁷⁸,
 T.M. Knight ¹⁵⁴, A. Knue ⁵⁴, D. Kobayashi ⁸⁸, R. Kobayashi ⁸⁶, M. Kocian ¹⁴², T. Kodama ¹⁵²,
 P. Kodyš ¹³², D.M. Koeck ¹⁴⁵, P.T. Koenig ²⁴, T. Koffas ³⁴, N.M. Köhler ³⁶, M. Kolb ¹³⁴,
 I. Koletsou ⁴, T. Komarek ¹²¹, K. Köneke ⁵⁴, A.X.Y. Kong ¹, T. Kono ¹¹⁷, N. Konstantinidis ⁹⁵,
 B. Konya ⁹⁷, R. Kopeliansky ⁶⁷, S. Koperny ^{84a}, K. Korcyl ⁸⁵, K. Kordas ¹⁵¹, G. Koren ¹⁵⁰,
 A. Korn ⁹⁵, S. Korn ⁵⁵, I. Korolkov ¹³, N. Korotkova ³⁷, B. Kortman ¹¹³, O. Kortner ¹⁰⁹,
 S. Kortner ¹⁰⁹, W.H. Kostecka ¹¹⁴, V.V. Kostyukhin ¹⁴⁰, A. Kotsokechagia ⁶⁶, A. Kotwal ⁵¹,
 A. Koulouris ³⁶, A. Kourkoumeli-Charalampidi ^{72a,72b}, C. Kourkoumelis ⁹, E. Kourlitis ⁶,
 O. Kovanda ¹⁴⁵, R. Kowalewski ¹⁶⁴, W. Kozanecki ¹³⁴, A.S. Kozhin ³⁷, V.A. Kramarenko ³⁷,
 G. Kramberger ⁹², P. Kramer ⁹⁹, M.W. Krasny ¹²⁶, A. Krasznahorkay ³⁶, J.A. Kremer ⁹⁹,
 T. Kresse ⁵⁰, J. Kretschmar ⁹¹, K. Kreul ¹⁸, P. Krieger ¹⁵⁴, F. Krieter ¹⁰⁸,
 S. Krishnamurthy ¹⁰², A. Krishnan ^{63b}, M. Krivos ¹³², K. Krizka ^{17a}, K. Kroeninger ⁴⁹,
 H. Kroha ¹⁰⁹, J. Kroll ¹³⁰, J. Kroll ¹²⁷, K.S. Krowpman ¹⁰⁶, U. Kruchonak ³⁸, H. Krüger ²⁴,
 N. Krumnack ⁸⁰, M.C. Kruse ⁵¹, J.A. Krzysiak ⁸⁵, A. Kubota ¹⁵³, O. Kuchinskaia ³⁷, S. Kuday ^{3a},
 D. Kuechler ⁴⁸, J.T. Kuechler ⁴⁸, S. Kuehn ³⁶, T. Kuhl ⁴⁸, V. Kukhtin ³⁸, Y. Kulchitsky ^{37,a},
 S. Kuleshov ^{136d,136b}, M. Kumar ^{33g}, N. Kumari ¹⁰¹, M. Kuna ⁶⁰, A. Kupco ¹³⁰, T. Kupfer ⁴⁹,
 A. Kupich ³⁷, O. Kuprash ⁵⁴, H. Kurashige ⁸³, L.L. Kurchaninov ^{155a}, Y.A. Kurochkin ³⁷,
 A. Kurova ³⁷, E.S. Kuwertz ³⁶, M. Kuze ¹⁵³, A.K. Kvam ¹⁰², J. Kvita ¹²¹, T. Kwan ¹⁰³,
 K.W. Kwok ^{64a}, N.G. Kyriacou ¹⁰⁵, C. Lacasta ¹⁶², F. Lacava ^{74a,74b}, H. Lacker ¹⁸,
 D. Lacour ¹²⁶, N.N. Lad ⁹⁵, E. Ladygin ³⁸, B. Laforge ¹²⁶, T. Lagouri ^{136e}, S. Lai ⁵⁵,
 I.K. Lakomic ^{84a}, N. Lalloue ⁶⁰, J.E. Lambert ¹¹⁹, S. Lammers ⁶⁷, W. Lampl ⁷,
 C. Lampoudis ¹⁵¹, A.N. Lancaster ¹¹⁴, E. Lançon ²⁹, U. Landgraf ⁵⁴, M.P.J. Landon ⁹³,
 V.S. Lang ⁵⁴, R.J. Langenberg ¹⁰², A.J. Lankford ¹⁵⁹, F. Lanni ²⁹, K. Lantzsch ²⁴, A. Lanza ^{72a},
 A. Lapertosa ^{57b,57a}, J.F. Laporte ¹³⁴, T. Lari ^{70a}, F. Lasagni Manghi ^{23b}, M. Lassnig ³⁶,
 V. Latonova ¹³⁰, T.S. Lau ^{64a}, A. Laudrain ⁹⁹, A. Laurier ³⁴, S.D. Lawlor ⁹⁴, Z. Lawrence ¹⁰⁰,
 M. Lazzaroni ^{70a,70b}, B. Le ¹⁰⁰, B. Leban ⁹², A. Lebedev ⁸⁰, M. LeBlanc ³⁶, T. LeCompte ⁶,
 F. Ledroit-Guillon ⁶⁰, A.C.A. Lee ⁹⁵, G.R. Lee ¹⁶, L. Lee ⁶¹, S.C. Lee ¹⁴⁷, S. Lee ^{47a,47b},
 T.F. Lee ⁹¹, L.L. Leeuw ^{33c}, H.P. Lefebvre ⁹⁴, M. Lefebvre ¹⁶⁴, C. Leggett ^{17a}, K. Lehmann ¹⁴¹,
 G. Lehmann Miotto ³⁶, W.A. Leight ¹⁰², A. Leisos ^{151,u}, M.A.L. Leite ^{81c}, C.E. Leitgeb ⁴⁸,
 R. Leitner ¹³², K.J.C. Leney ⁴⁴, T. Lenz ²⁴, S. Leone ^{73a}, C. Leonidopoulos ⁵², A. Leopold ¹⁴³,
 C. Leroy ¹⁰⁷, R. Les ¹⁰⁶, C.G. Lester ³², M. Levchenko ³⁷, J. Levêque ⁴, D. Levin ¹⁰⁵,
 L.J. Levinson ¹⁶⁸, M.P. Lewicki ⁸⁵, D.J. Lewis ²⁰, B. Li ^{14b}, B. Li ^{62b}, C. Li ^{62a}, C-Q. Li ^{62c,62d},
 H. Li ^{62a}, H. Li ^{62b}, H. Li ^{14c}, H. Li ^{62b}, J. Li ^{62c}, K. Li ¹³⁷, L. Li ^{62c}, M. Li ^{14a,14d},
 Q.Y. Li ^{62a}, S. Li ^{62d,62c,e}, T. Li ^{62b}, X. Li ¹⁰³, Z. Li ^{62b}, Z. Li ¹²⁵, Z. Li ¹⁰³, Z. Li ⁹¹,
 Z. Liang ^{14a}, M. Liberatore ⁴⁸, B. Liberti ^{75a}, K. Lie ^{64c}, J. Lieber Marin ^{81b}, K. Lin ¹⁰⁶,
 R.A. Linck ⁶⁷, R.E. Lindley ⁷, J.H. Lindon ², A. Linss ⁴⁸, E. Lipeles ¹²⁷, A. Lipniacka ¹⁶,
 A. Lister ¹⁶³, J.D. Little ⁴, B. Liu ^{14a}, B.X. Liu ¹⁴¹, D. Liu ^{62d,62c}, J.B. Liu ^{62a}, J.K.K. Liu ³²,
 K. Liu ^{62d,62c}, M. Liu ^{62a}, M.Y. Liu ^{62a}, P. Liu ^{14a}, Q. Liu ^{62d,137,62c}, X. Liu ^{62a}, Y. Liu ⁴⁸,
 Y. Liu ^{14c,14d}, Y.L. Liu ¹⁰⁵, Y.W. Liu ^{62a}, M. Livan ^{72a,72b}, J. Llorente Merino ¹⁴¹, S.L. Lloyd ⁹³,

E.M. Lobodzinska ^{id48}, P. Loch ^{id7}, S. Loffredo ^{id75a,75b}, T. Lohse ^{id18}, K. Lohwasser ^{id138},
 M. Lokajicek ^{id130,*}, J.D. Long ^{id161}, I. Longarini ^{id74a,74b}, L. Longo ^{id69a,69b}, R. Longo ^{id161},
 I. Lopez Paz ^{id36}, A. Lopez Solis ^{id48}, J. Lorenz ^{id108}, N. Lorenzo Martinez ^{id4}, A.M. Lory ^{id108},
 A. Lösle ^{id54}, X. Lou ^{id47a,47b}, X. Lou ^{id14a,14d}, A. Lounis ^{id66}, J. Love ^{id6}, P.A. Love ^{id90},
 J.J. Lozano Bahilo ^{id162}, G. Lu ^{id14a,14d}, M. Lu ^{id79}, S. Lu ^{id127}, Y.J. Lu ^{id65}, H.J. Lubatti ^{id137},
 C. Luci ^{id74a,74b}, F.L. Lucio Alves ^{id14c}, A. Lucotte ^{id60}, F. Luehring ^{id67}, I. Luise ^{id144},
 O. Lukianchuk ^{id66}, O. Lundberg ^{id143}, B. Lund-Jensen ^{id143}, N.A. Luongo ^{id122}, M.S. Lutz ^{id150},
 D. Lynn ^{id29}, H. Lyons⁹¹, R. Lysak ^{id130}, E. Lytken ^{id97}, F. Lyu ^{id14a}, V. Lyubushkin ^{id38},
 T. Lyubushkina ^{id38}, H. Ma ^{id29}, L.L. Ma ^{id62b}, Y. Ma ^{id95}, D.M. Mac Donell ^{id164}, G. Maccarrone ^{id53},
 J.C. MacDonald ^{id138}, R. Madar ^{id40}, W.F. Mader ^{id50}, J. Maeda ^{id83}, T. Maeno ^{id29}, M. Maerker ^{id50},
 V. Magerl ^{id54}, J. Magro ^{id68a,68c}, H. Maguire ^{id138}, D.J. Mahon ^{id41}, C. Maidantchik ^{id81b},
 A. Maio ^{id129a,129b,129d}, K. Maj ^{id84a}, O. Majersky ^{id28a}, S. Majewski ^{id122}, N. Makovec ^{id66},
 V. Maksimovic ^{id15}, B. Malaescu ^{id126}, Pa. Malecki ^{id85}, V.P. Maleev ^{id37}, F. Malek ^{id60},
 D. Malito ^{id43b,43a}, U. Mallik ^{id79}, C. Malone ^{id32}, S. Maltezos¹⁰, S. Malyukov³⁸, J. Mamuzic ^{id13},
 G. Mancini ^{id53}, G. Manco ^{id72a,72b}, J.P. Mandalia ^{id93}, I. Mandić ^{id92},
 L. Manhaes de Andrade Filho ^{id81a}, I.M. Maniatis ^{id151}, M. Manisha ^{id134}, J. Manjarres Ramos ^{id50},
 D.C. Mankad ^{id168}, K.H. Mankinen ^{id97}, A. Mann ^{id108}, A. Manousos ^{id78}, B. Mansoulie ^{id134},
 S. Manzoni ^{id36}, A. Marantis ^{id151,u}, G. Marchiori ^{id5}, M. Marcisovsky ^{id130}, L. Marcoccia ^{id75a,75b},
 C. Marcon ^{id70a,70b}, M. Marinescu ^{id20}, M. Marjanovic ^{id119}, Z. Marshall ^{id17a}, S. Marti-Garcia ^{id162},
 T.A. Martin ^{id166}, V.J. Martin ^{id52}, B. Martin dit Latour ^{id16}, L. Martinelli ^{id74a,74b}, M. Martinez ^{id13,v},
 P. Martinez Agullo ^{id162}, V.I. Martinez Outschoorn ^{id102}, P. Martinez Suarez ^{id13}, S. Martin-Haugh ^{id133},
 V.S. Martoiu ^{id27b}, A.C. Martyniuk ^{id95}, A. Marzin ^{id36}, S.R. Maschek ^{id109}, L. Masetti ^{id99},
 T. Mashimo ^{id152}, J. Masik ^{id100}, A.L. Maslennikov ^{id37}, L. Massa ^{id23b}, P. Massarotti ^{id71a,71b},
 P. Mastrandrea ^{id73a,73b}, A. Mastroberardino ^{id43b,43a}, T. Masubuchi ^{id152}, T. Mathisen ^{id160},
 A. Matic ^{id108}, N. Matsuzawa¹⁵², J. Maurer ^{id27b}, B. Maček ^{id92}, D.A. Maximov ^{id37}, R. Mazini ^{id147},
 I. Maznas ^{id151}, M. Mazza ^{id106}, S.M. Mazza ^{id135}, C. Mc Ginn ^{id29}, J.P. Mc Gowan ^{id103},
 S.P. Mc Kee ^{id105}, T.G. McCarthy ^{id109}, W.P. McCormack ^{id17a}, E.F. McDonald ^{id104},
 A.E. McDougall ^{id113}, J.A. Mcfayden ^{id145}, G. Mchedlize ^{id148b}, R.P. McKenzie ^{id33g},
 T.C. McLachlan ^{id48}, D.J. McLaughlin ^{id95}, K.D. McLean ^{id164}, S.J. McMahon ^{id133}, P.C. McNamara ^{id104},
 R.A. McPherson ^{id164,y}, J.E. Mdhluli ^{id33g}, S. Meehan ^{id36}, T. Megy ^{id40}, S. Mehlhase ^{id108},
 A. Mehta ^{id91}, B. Meirose ^{id45}, D. Melini ^{id149}, B.R. Mellado Garcia ^{id33g}, A.H. Melo ^{id55},
 F. Meloni ^{id48}, E.D. Mendes Gouveia ^{id129a}, A.M. Mendes Jacques Da Costa ^{id20}, H.Y. Meng ^{id154},
 L. Meng ^{id90}, S. Menke ^{id109}, M. Mentink ^{id36}, E. Meoni ^{id43b,43a}, C. Merlassino ^{id125},
 L. Merola ^{id71a,71b}, C. Meroni ^{id70a}, G. Merz¹⁰⁵, O. Meshkov ^{id37}, J.K.R. Meshreki ^{id140}, J. Metcalfe ^{id6},
 A.S. Mete ^{id6}, C. Meyer ^{id67}, J-P. Meyer ^{id134}, M. Michetti ^{id18}, R.P. Middleton ^{id133}, L. Mijović ^{id52},
 G. Mikenberg ^{id168}, M. Mikesikova ^{id130}, M. Mikuž ^{id92}, H. Mildner ^{id138}, A. Milic ^{id154},
 C.D. Milke ^{id44}, D.W. Miller ^{id39}, L.S. Miller ^{id34}, A. Milov ^{id168}, D.A. Milstead^{47a,47b}, T. Min^{14c},
 A.A. Minaenko ^{id37}, I.A. Minashvili ^{id148b}, L. Mince ^{id59}, A.I. Mincer ^{id116}, B. Mindur ^{id84a},
 M. Mineev ^{id38}, Y. Minegishi¹⁵², Y. Mino ^{id86}, L.M. Mir ^{id13}, M. Miralles Lopez ^{id162},
 M. Mironova ^{id125}, T. Mitani ^{id167}, A. Mitra ^{id166}, V.A. Mitsou ^{id162}, O. Miu ^{id154}, P.S. Miyagawa ^{id93},
 Y. Miyazaki⁸⁸, A. Mizukami ^{id82}, J.U. Mjörnmark ^{id97}, T. Mkrtchyan ^{id63a}, M. Mlynarikova ^{id114},
 M.P. Mlynarski ^{id84a}, T. Moa ^{id47a,47b}, S. Mobius ^{id55}, K. Mochizuki ^{id107}, P. Moder ^{id48}, P. Mogg ^{id108},
 A.F. Mohammed ^{id14a,14d}, S. Mohapatra ^{id41}, G. Mokgatitswane ^{id33g}, B. Mondal ^{id140}, S. Mondal ^{id131},
 K. Möning ^{id48}, E. Monnier ^{id101}, L. Monsonis Romero¹⁶², J. Montejo Berlingen ^{id36}, M. Montella ^{id118},
 F. Monticelli ^{id89}, N. Morange ^{id66}, A.L. Moreira De Carvalho ^{id129a}, M. Moreno Llácer ^{id162},
 C. Moreno Martinez ^{id13}, P. Morettini ^{id57b}, S. Morgenstern ^{id166}, M. Morii ^{id61}, M. Morinaga ^{id152},
 V. Morisbak ^{id124}, A.K. Morley ^{id36}, F. Morodei ^{id74a,74b}, L. Morvaj ^{id36}, P. Moschovakos ^{id36},

B. Moser ³⁶, M. Mosidze^{148b}, T. Moskalets ⁵⁴, P. Moskvitina ¹¹², J. Moss ^{31,o}, E.J.W. Moyses ¹⁰²,
 S. Muanza ¹⁰¹, J. Mueller ¹²⁸, D. Muenstermann ⁹⁰, R. Müller ¹⁹, G.A. Mullier ⁹⁷, J.J. Mullin¹²⁷,
 D.P. Mungo ^{70a,70b}, J.L. Munoz Martinez ¹³, D. Munoz Perez ¹⁶², F.J. Munoz Sanchez ¹⁰⁰,
 M. Murin ¹⁰⁰, W.J. Murray ^{166,133}, A. Murrone ^{70a,70b}, J.M. Muse ¹¹⁹, M. Muškinja ^{17a},
 C. Mwewa ²⁹, A.G. Myagkov ^{37,a}, A.J. Myers ⁸, A.A. Myers¹²⁸, G. Myers ⁶⁷, M. Myska ¹³¹,
 B.P. Nachman ^{17a}, O. Nackenhorst ⁴⁹, A. Nag ⁵⁰, K. Nagai ¹²⁵, K. Nagano ⁸², J.L. Nagle ^{29,aj},
 E. Nagy ¹⁰¹, A.M. Nairz ³⁶, Y. Nakahama ⁸², K. Nakamura ⁸², H. Nanjo ¹²³, R. Narayan ⁴⁴,
 E.A. Narayanan ¹¹¹, I. Naryshkin ³⁷, M. Naseri ³⁴, C. Nass ²⁴, G. Navarro ^{22a},
 J. Navarro-Gonzalez ¹⁶², R. Nayak ¹⁵⁰, P.Y. Nechaeva ³⁷, F. Nechansky ⁴⁸, T.J. Neep ²⁰,
 A. Negri ^{72a,72b}, M. Negrini ^{23b}, C. Nellist ¹¹², C. Nelson ¹⁰³, K. Nelson ¹⁰⁵, S. Nemecek ¹³⁰,
 M. Nessi ^{36,h}, M.S. Neubauer ¹⁶¹, F. Neuhaus ⁹⁹, J. Neundorf ⁴⁸, R. Newhouse ¹⁶³,
 P.R. Newman ²⁰, C.W. Ng ¹²⁸, Y.S. Ng¹⁸, Y.W.Y. Ng ¹⁵⁹, B. Ngair ^{35e}, H.D.N. Nguyen ¹⁰⁷,
 R.B. Nickerson ¹²⁵, R. Nicolaidou ¹³⁴, J. Nielsen ¹³⁵, M. Niemeyer ⁵⁵, N. Nikiforou ³⁶,
 V. Nikolaenko ^{37,a}, I. Nikolic-Audit ¹²⁶, K. Nikolopoulos ²⁰, P. Nilsson ²⁹, H.R. Nindhito ⁵⁶,
 A. Nisati ^{74a}, N. Nishu ², R. Nisius ¹⁰⁹, J-E. Nitschke ⁵⁰, E.K. Nkadimeng ^{33g},
 S.J. Noacco Rosende ⁸⁹, T. Nobe ¹⁵², D.L. Noel ³², Y. Noguchi ⁸⁶, T. Nommensen ¹⁴⁶,
 M.A. Nomura²⁹, M.B. Norfolk ¹³⁸, R.R.B. Norisam ⁹⁵, B.J. Norman ³⁴, J. Novak ⁹², T. Novak ⁴⁸,
 O. Novgorodova ⁵⁰, L. Novotny ¹³¹, R. Novotny ¹¹¹, L. Nozka ¹²¹, K. Ntekas ¹⁵⁹, E. Nurse⁹⁵,
 F.G. Oakham ^{34,ag}, J. Ocariz ¹²⁶, A. Ochi ⁸³, I. Ochoa ^{129a}, S. Oerdek ¹⁶⁰, A. Ogrodnik ^{84a},
 A. Oh ¹⁰⁰, C.C. Ohm ¹⁴³, H. Oide ¹⁵³, R. Oishi ¹⁵², M.L. Ojeda ⁴⁸, Y. Okazaki ⁸⁶,
 M.W. O'Keefe⁹¹, Y. Okumura ¹⁵², A. Olariu^{27b}, L.F. Oleiro Seabra ^{129a}, S.A. Olivares Pino ^{136e},
 D. Oliveira Damazio ²⁹, D. Oliveira Goncalves ^{81a}, J.L. Oliver ¹⁵⁹, M.J.R. Olsson ¹⁵⁹,
 A. Olszewski ⁸⁵, J. Olszowska ^{85,*}, Ö.O. Öncel ⁵⁴, D.C. O'Neil ¹⁴¹, A.P. O'Neill ¹⁹,
 A. Onofre ^{129a,129e}, P.U.E. Onyisi ¹¹, M.J. Oreglia ³⁹, G.E. Orellana ⁸⁹, D. Orestano ^{76a,76b},
 N. Orlando ¹³, R.S. Orr ¹⁵⁴, V. O'Shea ⁵⁹, R. Ospanov ^{62a}, G. Otero y Garzon ³⁰, H. Otono ⁸⁸,
 P.S. Ott ^{63a}, G.J. Ottino ^{17a}, M. Ouchrif ^{35d}, J. Ouellette ^{29,aj}, F. Ould-Saada ¹²⁴, M. Owen ⁵⁹,
 R.E. Owen ¹³³, K.Y. Oyulmaz ^{21a}, V.E. Ozcan ^{21a}, N. Ozturk ⁸, S. Ozturk ^{21d}, J. Pacalt ¹²¹,
 H.A. Pacey ³², K. Pachal ⁵¹, A. Pacheco Pages ¹³, C. Padilla Aranda ¹³, G. Padovano ^{74a,74b},
 S. Pagan Griso ^{17a}, G. Palacino ⁶⁷, A. Palazzo ^{69a,69b}, S. Palazzo ⁵², S. Palestini ³⁶, M. Palka ^{84b},
 J. Pan ¹⁷¹, T. Pan ^{64a}, D.K. Panchal ¹¹, C.E. Pandini ¹¹³, J.G. Panduro Vazquez ⁹⁴, H. Pang ^{14b},
 P. Pani ⁴⁸, G. Panizzo ^{68a,68c}, L. Paolozzi ⁵⁶, C. Papadatos ¹⁰⁷, S. Parajuli ⁴⁴, A. Paramonov ⁶,
 C. Paraskevopoulos ¹⁰, D. Paredes Hernandez ^{64b}, T.H. Park ¹⁵⁴, M.A. Parker ³², F. Parodi ^{57b,57a},
 E.W. Parrish ¹¹⁴, V.A. Parrish ⁵², J.A. Parsons ⁴¹, U. Parzefall ⁵⁴, B. Pascual Dias ¹⁰⁷,
 L. Pascual Dominguez ¹⁵⁰, V.R. Pascuzzi ^{17a}, F. Pasquali ¹¹³, E. Pasqualucci ^{74a}, S. Passaggio ^{57b},
 F. Pastore ⁹⁴, P. Pasuwan ^{47a,47b}, J.R. Pater ¹⁰⁰, J. Patton⁹¹, T. Pauly ³⁶, J. Pearkes ¹⁴²,
 M. Pedersen ¹²⁴, R. Pedro ^{129a}, S.V. Peleganchuk ³⁷, O. Penc ³⁶, C. Peng ^{64b}, H. Peng ^{62a},
 K.E. Pensi ¹⁰⁸, M. Penzin ³⁷, B.S. Peralva ^{81d}, A.P. Pereira Peixoto ⁶⁰, L. Pereira Sanchez ^{47a,47b},
 D.V. Perepelitsa ^{29,aj}, E. Perez Codina ^{155a}, M. Perganti ¹⁰, L. Perini ^{70a,70b,*}, H. Pernegger ³⁶,
 S. Perrella ³⁶, A. Perrevoort ¹¹², O. Perrin ⁴⁰, K. Peters ⁴⁸, R.F.Y. Peters ¹⁰⁰, B.A. Petersen ³⁶,
 T.C. Petersen ⁴², E. Petit ¹⁰¹, V. Petousis ¹³¹, C. Petridou ¹⁵¹, A. Petrukhin ¹⁴⁰, M. Pettee ^{17a},
 N.E. Pettersson ³⁶, A. Petukhov ³⁷, K. Petukhova ¹³², A. Peyaud ¹³⁴, R. Pezoa ^{136f},
 L. Pezzotti ³⁶, G. Pezzullo ¹⁷¹, T. Pham ¹⁰⁴, P.W. Phillips ¹³³, M.W. Phipps ¹⁶¹,
 G. Piacquadio ¹⁴⁴, E. Pianori ^{17a}, F. Piazza ^{70a,70b}, R. Piegaia ³⁰, D. Pietreanu ^{27b},
 A.D. Pilkington ¹⁰⁰, M. Pinamonti ^{68a,68c}, J.L. Pinfeld ², B.C. Pinheiro Pereira ^{129a},
 C. Pitman Donaldson⁹⁵, D.A. Pizzi ³⁴, L. Pizzimento ^{75a,75b}, A. Pizzini ¹¹³, M.-A. Pleier ²⁹,
 V. Plesanovs⁵⁴, V. Pleskot ¹³², E. Plotnikova³⁸, G. Poddar ⁴, R. Poettgen ⁹⁷, L. Poggioli ¹²⁶,
 I. Pogrebnyak ¹⁰⁶, D. Pohl ²⁴, I. Pokharel ⁵⁵, S. Polacek ¹³², G. Polesello ^{72a}, A. Poley ^{141,155a},

R. Polifka ¹³¹, A. Polini ^{23b}, C.S. Pollard ¹²⁵, Z.B. Pollock ¹¹⁸, V. Polychronakos ²⁹,
 D. Ponomarenko ³⁷, L. Pontecorvo ³⁶, S. Popa ^{27a}, G.A. Popeneciu ^{27d},
 D.M. Portillo Quintero ^{155a}, S. Pospisil ¹³¹, P. Postolache ^{27c}, K. Potamianos ¹²⁵, I.N. Potrap ³⁸,
 C.J. Potter ³², H. Potti ¹, T. Poulsen ⁴⁸, J. Poveda ¹⁶², G. Pownall ⁴⁸, M.E. Pozo Astigarraga ³⁶,
 A. Prades Ibanez ¹⁶², M.M. Prapa ⁴⁶, J. Pretel ⁵⁴, D. Price ¹⁰⁰, M. Primavera ^{69a},
 M.A. Principe Martin ⁹⁸, M.L. Proffitt ¹³⁷, N. Proklova ³⁷, K. Prokofiev ^{64c}, G. Proto ^{75a,75b},
 S. Protopopescu ²⁹, J. Proudfoot ⁶, M. Przybycien ^{84a}, J.E. Puddefoot ¹³⁸, D. Pudzha ³⁷,
 P. Puzo ⁶⁶, D. Pyatiizbyantseva ³⁷, J. Qian ¹⁰⁵, Y. Qin ¹⁰⁰, T. Qiu ⁹³, A. Quadt ⁵⁵,
 M. Queitsch-Maitland ¹⁰⁰, G. Rabanal Bolanos ⁶¹, D. Rafanoharana ⁵⁴, F. Ragusa ^{70a,70b},
 J.L. Rainbolt ³⁹, J.A. Raine ⁵⁶, S. Rajagopalan ²⁹, E. Ramakoti ³⁷, K. Ran ^{48,14d}, V. Raskina ¹²⁶,
 D.F. Rassloff ^{63a}, S. Rave ⁹⁹, B. Ravina ⁵⁹, I. Ravinovich ¹⁶⁸, M. Raymond ³⁶, A.L. Read ¹²⁴,
 N.P. Readioff ¹³⁸, D.M. Rebuzzi ^{72a,72b}, G. Redlinger ²⁹, K. Reeves ⁴⁵, J.A. Reidelsturz ¹⁷⁰,
 D. Reikher ¹⁵⁰, A. Reiss ⁹⁹, A. Rej ¹⁴⁰, C. Rembser ³⁶, A. Renardi ⁴⁸, M. Renda ^{27b},
 M.B. Rendel ¹⁰⁹, A.G. Rennie ⁵⁹, S. Resconi ^{70a}, M. Ressegotti ^{57b,57a}, E.D. Resseguie ^{17a},
 S. Rettie ⁹⁵, B. Reynolds ¹¹⁸, E. Reynolds ^{17a}, M. Rezaei Estabragh ¹⁷⁰, O.L. Rezanova ³⁷,
 P. Reznicek ¹³², E. Ricci ^{77a,77b}, R. Richter ¹⁰⁹, S. Richter ^{47a,47b}, E. Richter-Was ^{84b},
 M. Ridel ¹²⁶, P. Rieck ¹¹⁶, P. Riedler ³⁶, M. Rijssenbeek ¹⁴⁴, A. Rimoldi ^{72a,72b}, M. Rimoldi ⁴⁸,
 L. Rinaldi ^{23b,23a}, T.T. Rinn ²⁹, M.P. Rinnagel ¹⁰⁸, G. Ripellino ¹⁴³, I. Riu ¹³, P. Rivadeneira ⁴⁸,
 J.C. Rivera Vergara ¹⁶⁴, F. Rizatdinova ¹²⁰, E. Rizvi ⁹³, C. Rizzi ⁵⁶, B.A. Roberts ¹⁶⁶,
 B.R. Roberts ^{17a}, S.H. Robertson ^{103,y}, M. Robin ⁴⁸, D. Robinson ³², C.M. Robles Gajardo ^{136f},
 M. Robles Manzano ⁹⁹, A. Robson ⁵⁹, A. Rocchi ^{75a,75b}, C. Roda ^{73a,73b}, S. Rodriguez Bosca ^{63a},
 Y. Rodriguez Garcia ^{22a}, A. Rodriguez Rodriguez ⁵⁴, A.M. Rodríguez Vera ^{155b}, S. Roe ³⁶,
 J.T. Roemer ¹⁵⁹, A.R. Roepe-Gier ¹¹⁹, J. Roggel ¹⁷⁰, O. Røhne ¹²⁴, R.A. Rojas ¹⁶⁴,
 B. Roland ⁵⁴, C.P.A. Roland ⁶⁷, J. Roloff ²⁹, A. Romaniouk ³⁷, E. Romano ^{72a,72b},
 M. Romano ^{23b}, A.C. Romero Hernandez ¹⁶¹, N. Rompotis ⁹¹, L. Roos ¹²⁶, S. Rosati ^{74a},
 B.J. Rosser ³⁹, E. Rossi ⁴, E. Rossi ^{71a,71b}, L.P. Rossi ^{57b}, L. Rossini ⁴⁸, R. Rosten ¹¹⁸,
 M. Rotaru ^{27b}, B. Rottler ⁵⁴, D. Rousseau ⁵⁶, D. Rousso ³², G. Rovelli ^{72a,72b}, A. Roy ¹⁶¹,
 A. Rozanov ¹⁰¹, Y. Rozen ¹⁴⁹, X. Ruan ^{33g}, A. Rubio Jimenez ¹⁶², A.J. Ruby ⁹¹,
 V.H. Ruelas Rivera ¹⁸, T.A. Ruggeri ¹, F. Rühr ⁵⁴, A. Ruiz-Martinez ¹⁶², A. Rummler ³⁶,
 Z. Rurikova ⁵⁴, N.A. Rusakovich ³⁸, H.L. Russell ¹⁶⁴, J.P. Rutherford ⁷, E.M. Rüttinger ¹³⁸,
 K. Rybacki ⁹⁰, M. Rybar ¹³², E.B. Rye ¹²⁴, A. Ryzhov ³⁷, J.A. Sabater Iglesias ⁵⁶, P. Sabatini ¹⁶²,
 L. Sabetta ^{74a,74b}, H.F-W. Sadrozinski ¹³⁵, F. Safai Tehrani ^{74a}, B. Safarzadeh Samani ¹⁴⁵,
 M. Safdari ¹⁴², S. Saha ¹⁰³, M. Sahinsoy ¹⁰⁹, M. Saimpert ¹³⁴, M. Saito ¹⁵², T. Saito ¹⁵²,
 D. Salamani ³⁶, G. Salamanna ^{76a,76b}, A. Salnikov ¹⁴², J. Salt ¹⁶², A. Salvador Salas ¹³,
 D. Salvatore ^{43b,43a}, F. Salvatore ¹⁴⁵, A. Salzburger ³⁶, D. Sammel ⁵⁴, D. Sampsonidis ¹⁵¹,
 D. Sampsonidou ^{62d,62c}, J. Sánchez ¹⁶², A. Sanchez Pineda ⁴, V. Sanchez Sebastian ¹⁶²,
 H. Sandaker ¹²⁴, C.O. Sander ⁴⁸, J.A. Sandesara ¹⁰², M. Sandhoff ¹⁷⁰, C. Sandoval ^{22b},
 D.P.C. Sankey ¹³³, A. Sansoni ⁵³, L. Santi ^{74a,74b}, C. Santoni ⁴⁰, H. Santos ^{129a,129b},
 S.N. Santpur ^{17a}, A. Santra ¹⁶⁸, K.A. Saoucha ¹³⁸, J.G. Saraiva ^{129a,129d}, J. Sardain ⁷,
 O. Sasaki ⁸², K. Sato ¹⁵⁶, C. Sauer ^{63b}, F. Sauerburger ⁵⁴, E. Sauvan ⁴, P. Savard ^{154,ag},
 R. Sawada ¹⁵², C. Sawyer ¹³³, L. Sawyer ⁹⁶, I. Sayago Galvan ¹⁶², C. Sbarra ^{23b}, A. Sbrizzi ^{23b,23a},
 T. Scanlon ⁹⁵, J. Schaarschmidt ¹³⁷, P. Schacht ¹⁰⁹, D. Schaefer ³⁹, U. Schäfer ⁹⁹,
 A.C. Schaffer ⁶⁶, D. Schaile ¹⁰⁸, R.D. Schamberger ¹⁴⁴, E. Schanet ¹⁰⁸, C. Scharf ¹⁸,
 V.A. Schegelsky ³⁷, D. Scheirich ¹³², F. Schenck ¹⁸, M. Schernau ¹⁵⁹, C. Scheulen ⁵⁵,
 C. Schiavi ^{57b,57a}, Z.M. Schillaci ²⁶, E.J. Schioppa ^{69a,69b}, M. Schioppa ^{43b,43a}, B. Schlag ⁹⁹,
 K.E. Schleicher ⁵⁴, S. Schlenker ³⁶, K. Schmieden ⁹⁹, C. Schmitt ⁹⁹, S. Schmitt ⁴⁸,
 L. Schoeffel ¹³⁴, A. Schoening ^{63b}, P.G. Scholer ⁵⁴, E. Schopf ¹²⁵, M. Schott ⁹⁹,

J. Schovancova ³⁶, S. Schramm ⁵⁶, F. Schroeder ¹⁷⁰, H-C. Schultz-Coulon ^{63a}, M. Schumacher ⁵⁴,
 B.A. Schumm ¹³⁵, Ph. Schune ¹³⁴, A. Schwartzman ¹⁴², T.A. Schwarz ¹⁰⁵, Ph. Schwemling ¹³⁴,
 R. Schwienhorst ¹⁰⁶, A. Sciandra ¹³⁵, G. Sciolla ²⁶, F. Scuri ^{73a}, F. Scutti ¹⁰⁴, C.D. Sebastiani ⁹¹,
 K. Sedlaczek ⁴⁹, P. Seema ¹⁸, S.C. Seidel ¹¹¹, A. Seiden ¹³⁵, B.D. Seidlitz ⁴¹, T. Seiss ³⁹,
 C. Seitz ⁴⁸, J.M. Seixas ^{81b}, G. Sekhniaidze ^{71a}, S.J. Sekula ⁴⁴, L. Selem ⁴,
 N. Semprini-Cesari ^{23b,23a}, S. Sen ⁵¹, D. Sengupta ⁵⁶, V. Senthilkumar ¹⁶², L. Serin ⁶⁶,
 L. Serkin ^{68a,68b}, M. Sessa ^{76a,76b}, H. Severini ¹¹⁹, S. Sevova ¹⁴², F. Sforza ^{57b,57a}, A. Sfyrla ⁵⁶,
 E. Shabalina ⁵⁵, R. Shaheen ¹⁴³, J.D. Shahinian ¹²⁷, N.W. Shaikh ^{47a,47b}, D. Shaked Renous ¹⁶⁸,
 L.Y. Shan ^{14a}, M. Shapiro ^{17a}, A. Sharma ³⁶, A.S. Sharma ¹⁶³, P. Sharma ⁷⁹, S. Sharma ⁴⁸,
 P.B. Shatalov ³⁷, K. Shaw ¹⁴⁵, S.M. Shaw ¹⁰⁰, Q. Shen ^{62c}, P. Sherwood ⁹⁵, L. Shi ⁹⁵,
 C.O. Shimmin ¹⁷¹, Y. Shimogama ¹⁶⁷, J.D. Shinner ⁹⁴, I.P.J. Shipsey ¹²⁵, S. Shirabe ⁶⁰,
 M. Shiyakova ^{38,x}, J. Shlomi ¹⁶⁸, M.J. Shochet ³⁹, J. Shojaii ¹⁰⁴, D.R. Shope ¹⁴³,
 S. Shrestha ¹¹⁸, E.M. Shrif ^{33g}, M.J. Shroff ¹⁶⁴, P. Sicho ¹³⁰, A.M. Sickles ¹⁶¹,
 E. Sideras Haddad ^{33g}, O. Sidiropoulou ³⁶, A. Sidoti ^{23b}, F. Siegert ⁵⁰, Dj. Sijacki ¹⁵,
 R. Sikora ^{84a}, F. Sili ⁸⁹, J.M. Silva ²⁰, M.V. Silva Oliveira ³⁶, S.B. Silverstein ^{47a}, S. Simion ⁶⁶,
 R. Simoniello ³⁶, E.L. Simpson ⁵⁹, N.D. Simpson ⁹⁷, S. Simsek ^{21d}, S. Sindhu ⁵⁵, P. Sinervo ¹⁵⁴,
 V. Sinetckii ³⁷, S. Singh ¹⁴¹, S. Singh ¹⁵⁴, S. Sinha ⁴⁸, S. Sinha ^{33g}, M. Sioli ^{23b,23a},
 I. Siral ¹²², S.Yu. Sivoklokov ^{37,*}, J. Sjölin ^{47a,47b}, A. Skaf ⁵⁵, E. Skorda ⁹⁷, P. Skubic ¹¹⁹,
 M. Slawinska ⁸⁵, V. Smakhtin ¹⁶⁸, B.H. Smart ¹³³, J. Smiesko ¹³², S.Yu. Smirnov ³⁷,
 Y. Smirnov ³⁷, L.N. Smirnova ^{37,a}, O. Smirnova ⁹⁷, A.C. Smith ⁴¹, E.A. Smith ³⁹,
 H.A. Smith ¹²⁵, J.L. Smith ⁹¹, R. Smith ¹⁴², M. Smizanska ⁹⁰, K. Smolek ¹³¹, A. Smykiewicz ⁸⁵,
 A.A. Snesarev ³⁷, H.L. Snoek ¹¹³, S. Snyder ²⁹, R. Sobie ^{164,y}, A. Soffer ¹⁵⁰,
 C.A. Solans Sanchez ³⁶, E.Yu. Soldatov ³⁷, U. Soldevila ¹⁶², A.A. Solodkov ³⁷, S. Solomon ⁵⁴,
 A. Soloshenko ³⁸, K. Solovieva ⁵⁴, O.V. Solovyanov ³⁷, V. Solovyev ³⁷, P. Sommer ³⁶,
 A. Sonay ¹³, W.Y. Song ^{155b}, A. Sopczak ¹³¹, A.L. Sopio ⁹⁵, F. Sopkova ^{28b}, V. Sothilingam ^{63a},
 S. Sottocornola ^{72a,72b}, R. Soualah ^{115b}, Z. Soumami ^{35e}, D. South ⁴⁸, S. Spagnolo ^{69a,69b},
 M. Spalla ¹⁰⁹, F. Spanò ⁹⁴, D. Sperlich ⁵⁴, G. Spigo ³⁶, M. Spina ¹⁴⁵, S. Spinali ⁹⁰,
 D.P. Spiteri ⁵⁹, M. Spousta ¹³², E.J. Staats ³⁴, A. Stabile ^{70a,70b}, R. Stamen ^{63a},
 M. Stamenkovic ¹¹³, A. Stampekis ²⁰, M. Standke ²⁴, E. Stanecka ⁸⁵, B. Stanislaus ^{17a},
 M.M. Stanitzki ⁴⁸, M. Stankaityte ¹²⁵, B. Stapf ⁴⁸, E.A. Starchenko ³⁷, G.H. Stark ¹³⁵,
 J. Stark ^{101,ab}, D.M. Starko ^{155b}, P. Staroba ¹³⁰, P. Starovoitov ^{63a}, S. Stärz ¹⁰³, R. Staszewski ⁸⁵,
 G. Stavropoulos ⁴⁶, J. Steentoft ¹⁶⁰, P. Steinberg ²⁹, A.L. Steinhebel ¹²², B. Stelzer ^{141,155a},
 H.J. Stelzer ¹²⁸, O. Stelzer-Chilton ^{155a}, H. Stenzel ⁵⁸, T.J. Stevenson ¹⁴⁵, G.A. Stewart ³⁶,
 M.C. Stockton ³⁶, G. Stoicea ^{27b}, M. Stolarski ^{129a}, S. Stonjek ¹⁰⁹, A. Straessner ⁵⁰,
 J. Strandberg ¹⁴³, S. Strandberg ^{47a,47b}, M. Strauss ¹¹⁹, T. Strebler ¹⁰¹, P. Strizenec ^{28b},
 R. Ströhmer ¹⁶⁵, D.M. Strom ¹²², L.R. Strom ⁴⁸, R. Stroynowski ⁴⁴, A. Strubig ^{47a,47b},
 S.A. Stucci ²⁹, B. Stugu ¹⁶, J. Stupak ¹¹⁹, N.A. Styles ⁴⁸, D. Su ¹⁴², S. Su ^{62a},
 W. Su ^{62d,137,62c}, X. Su ^{62a,66}, K. Sugizaki ¹⁵², V.V. Sulin ³⁷, M.J. Sullivan ⁹¹,
 D.M.S. Sultan ^{77a,77b}, L. Sultanaliev ³⁷, S. Sultansoy ^{3b}, T. Sumida ⁸⁶, S. Sun ¹⁰⁵, S. Sun ¹⁶⁹,
 O. Sunneborn Gudnadottir ¹⁶⁰, M.R. Sutton ¹⁴⁵, M. Svatos ¹³⁰, M. Swiatlowski ^{155a},
 T. Swirski ¹⁶⁵, I. Sykora ^{28a}, M. Sykora ¹³², T. Sykora ¹³², D. Ta ⁹⁹, K. Tackmann ^{48,w},
 A. Taffard ¹⁵⁹, R. Tafirout ^{155a}, J.S. Tafoya Vargas ⁶⁶, R.H.M. Taibah ¹²⁶, R. Takashima ⁸⁷,
 K. Takeda ⁸³, E.P. Takeva ⁵², Y. Takubo ⁸², M. Talby ¹⁰¹, A.A. Talyshev ³⁷, K.C. Tam ^{64b},
 N.M. Tamir ¹⁵⁰, A. Tanaka ¹⁵², J. Tanaka ¹⁵², R. Tanaka ⁶⁶, M. Tanasini ^{57b,57a}, J. Tang ^{62c},
 Z. Tao ¹⁶³, S. Tapia Araya ⁸⁰, S. Tapprogge ⁹⁹, A. Tarek Abouelfadl Mohamed ¹⁰⁶, S. Tarem ¹⁴⁹,
 K. Tariq ^{62b}, G. Tarna ^{27b}, G.F. Tartarelli ^{70a}, P. Tas ¹³², M. Tasevsky ¹³⁰, E. Tassi ^{43b,43a},
 A.C. Tate ¹⁶¹, G. Tateno ¹⁵², Y. Tayalati ^{35e}, G.N. Taylor ¹⁰⁴, W. Taylor ^{155b}, H. Teagle ⁹¹,

A.S. Tee ¹⁶⁹, R. Teixeira De Lima ¹⁴², P. Teixeira-Dias ⁹⁴, J.J. Teoh ¹⁵⁴, K. Terashi ¹⁵²,
 J. Terron ⁹⁸, S. Terzo ¹³, M. Testa ⁵³, R.J. Teuscher ^{154,y}, A. Thaler ⁷⁸, O. Theiner ⁵⁶,
 N. Themistokleous ⁵², T. Thevenaux-Pelzer ¹⁸, O. Thielmann ¹⁷⁰, D.W. Thomas ⁹⁴, J.P. Thomas ²⁰,
 E.A. Thompson ⁴⁸, P.D. Thompson ²⁰, E. Thomson ¹²⁷, E.J. Thorpe ⁹³, Y. Tian ⁵⁵,
 V. Tikhomirov ^{37,a}, Yu.A. Tikhonov ³⁷, S. Timoshenko ³⁷, E.X.L. Ting ¹, P. Tipton ¹⁷¹,
 S. Tisserant ¹⁰¹, S.H. Tlou ^{33g}, A. Tnourji ⁴⁰, K. Todome ^{23b,23a}, S. Todorova-Nova ¹³², S. Todt ⁵⁰,
 M. Togawa ⁸², J. Tojo ⁸⁸, S. Tokár ^{28a}, K. Tokushuku ⁸², R. Tombs ³², M. Tomoto ^{82,110},
 L. Tompkins ^{142,q}, P. Tornambe ¹⁰², E. Torrence ¹²², H. Torres ⁵⁰, E. Torró Pastor ¹⁶²,
 M. Toscani ³⁰, C. Toscirci ³⁹, D.R. Tovey ¹³⁸, A. Traet ¹⁶, I.S. Trandafir ^{27b}, T. Trefzger ¹⁶⁵,
 A. Tricoli ²⁹, I.M. Trigger ^{155a}, S. Trincaz-Duvoid ¹²⁶, D.A. Trischuk ¹⁶³, B. Trocmé ⁶⁰,
 A. Trofymov ⁶⁶, C. Troncon ^{70a}, L. Truong ^{33c}, M. Trzebinski ⁸⁵, A. Trzupke ⁸⁵, F. Tsai ¹⁴⁴,
 M. Tsai ¹⁰⁵, A. Tsiamis ¹⁵¹, P.V. Tsiarehsha ³⁷, S. Tsigaridas ^{155a}, A. Tsigiriotis ^{151,u},
 V. Tsiskaridze ¹⁴⁴, E.G. Tskhadadze ^{148a}, M. Tsopoulou ¹⁵¹, Y. Tsujikawa ⁸⁶, I.I. Tsukerman ³⁷,
 V. Tsulaia ^{17a}, S. Tsuno ⁸², O. Tsur ¹⁴⁹, D. Tsybychev ¹⁴⁴, Y. Tu ^{64b}, A. Tudorache ^{27b},
 V. Tudorache ^{27b}, A.N. Tuna ³⁶, S. Turchikhin ³⁸, I. Turk Cakir ^{3a}, R. Turra ^{70a}, T. Turtuvshin ³⁸,
 P.M. Tuts ⁴¹, S. Tzamarias ¹⁵¹, P. Tzani ¹⁰, E. Tzovara ⁹⁹, K. Uchida ¹⁵², F. Ukegawa ¹⁵⁶,
 P.A. Ulloa Poblete ^{136c}, G. Unal ³⁶, M. Unal ¹¹, A. Undrus ²⁹, G. Unel ¹⁵⁹, K. Uno ¹⁵²,
 J. Urban ^{28b}, P. Urquijo ¹⁰⁴, G. Usai ⁸, R. Ushioda ¹⁵³, M. Usman ¹⁰⁷, Z. Uysal ^{21b},
 V. Vacek ¹³¹, B. Vachon ¹⁰³, K.O.H. Vadla ¹²⁴, T. Vafeiadis ³⁶, C. Valderanis ¹⁰⁸,
 E. Valdes Santurio ^{47a,47b}, M. Valente ^{155a}, S. Valentinetti ^{23b,23a}, A. Valero ¹⁶², A. Vallier ^{101,ab},
 J.A. Valls Ferrer ¹⁶², T.R. Van Daalen ¹³⁷, P. Van Gemmeren ⁶, M. Van Rijnbach ^{124,36},
 S. Van Stroud ⁹⁵, I. Van Vulpen ¹¹³, M. Vanadia ^{75a,75b}, W. Vandelli ³⁶, M. Vandenbroucke ¹³⁴,
 E.R. Vandewall ¹²⁰, D. Vannicola ¹⁵⁰, L. Vannoli ^{57b,57a}, R. Vari ^{74a}, E.W. Varnes ⁷,
 C. Varni ^{17a}, T. Varol ¹⁴⁷, D. Varouchas ⁶⁶, L. Varriale ¹⁶², K.E. Varvell ¹⁴⁶, M.E. Vasile ^{27b},
 L. Vaslin ⁴⁰, G.A. Vasquez ¹⁶⁴, F. Vazeille ⁴⁰, T. Vazquez Schroeder ³⁶, J. Veatch ³¹,
 V. Vecchio ¹⁰⁰, M.J. Veen ¹¹³, I. Veliscek ¹²⁵, L.M. Veloce ¹⁵⁴, F. Veloso ^{129a,129c},
 S. Veneziano ^{74a}, A. Ventura ^{69a,69b}, A. Verbytskyi ¹⁰⁹, M. Verducci ^{73a,73b}, C. Vergis ²⁴,
 M. Verissimo De Araujo ^{81b}, W. Verkerke ¹¹³, J.C. Vermeulen ¹¹³, C. Vernieri ¹⁴²,
 P.J. Verschuuren ⁹⁴, M. Vessella ¹⁰², M.L. Vesterbacka ¹¹⁶, M.C. Vetterli ^{141,ag},
 A. Vgenopoulos ¹⁵¹, N. Viaux Maira ^{136f}, T. Vickey ¹³⁸, O.E. Vickey Boeriu ¹³⁸,
 G.H.A. Viehhauser ¹²⁵, L. Vigani ^{63b}, M. Villa ^{23b,23a}, M. Villaplana Perez ¹⁶², E.M. Villhauer ⁵²,
 E. Vilucchi ⁵³, M.G. Vincter ³⁴, G.S. Virdee ²⁰, A. Vishwakarma ⁵², C. Vittori ^{23b,23a},
 I. Vivarelli ¹⁴⁵, V. Vladimirov ¹⁶⁶, E. Voevodina ¹⁰⁹, F. Vogel ¹⁰⁸, P. Vokac ¹³¹, J. Von Ahnen ⁴⁸,
 E. Von Toerne ²⁴, B. Vormwald ³⁶, V. Vorobel ¹³², K. Vorobev ³⁷, M. Vos ¹⁶²,
 J.H. Vossebeld ⁹¹, M. Vozak ¹¹³, L. Vozdecky ⁹³, N. Vranjes ¹⁵, M. Vranjes Milosavljevic ¹⁵,
 M. Vreeswijk ¹¹³, R. Vuillermet ³⁶, O. Vujanovic ⁹⁹, I. Vukotic ³⁹, S. Wada ¹⁵⁶, C. Wagner ¹⁰²,
 W. Wagner ¹⁷⁰, S. Wahdan ¹⁷⁰, H. Wahlberg ⁸⁹, R. Wakasa ¹⁵⁶, M. Wakida ¹¹⁰,
 V.M. Walbrecht ¹⁰⁹, J. Walder ¹³³, R. Walker ¹⁰⁸, W. Walkowiak ¹⁴⁰, A.M. Wang ⁶¹,
 A.Z. Wang ¹⁶⁹, C. Wang ^{62a}, C. Wang ^{62c}, H. Wang ^{17a}, J. Wang ^{64a}, P. Wang ⁴⁴,
 R.-J. Wang ⁹⁹, R. Wang ⁶¹, R. Wang ⁶, S.M. Wang ¹⁴⁷, S. Wang ^{62b}, T. Wang ^{62a},
 W.T. Wang ⁷⁹, W.X. Wang ^{62a}, X. Wang ^{14c}, X. Wang ¹⁶¹, X. Wang ^{62c}, Y. Wang ^{62d},
 Y. Wang ^{14c}, Z. Wang ¹⁰⁵, Z. Wang ^{62d,51,62c}, Z. Wang ¹⁰⁵, A. Warburton ¹⁰³, R.J. Ward ²⁰,
 N. Warrack ⁵⁹, A.T. Watson ²⁰, M.F. Watson ²⁰, G. Watts ¹³⁷, B.M. Waugh ⁹⁵, A.F. Webb ¹¹,
 C. Weber ²⁹, M.S. Weber ¹⁹, S.A. Weber ³⁴, S.M. Weber ^{63a}, C. Wei ^{62a}, Y. Wei ¹²⁵,
 A.R. Weidberg ¹²⁵, J. Weingarten ⁴⁹, M. Weirich ⁹⁹, C. Weiser ⁵⁴, C.J. Wells ⁴⁸, T. Wenaus ²⁹,
 B. Wendland ⁴⁹, T. Wengler ³⁶, N.S. Wenke ¹⁰⁹, N. Wermes ²⁴, M. Wessels ^{63a}, K. Whalen ¹²²,
 A.M. Wharton ⁹⁰, A.S. White ⁶¹, A. White ⁸, M.J. White ¹, D. Whiteson ¹⁵⁹,

L. Wickremasinghe ¹²³, W. Wiedenmann ¹⁶⁹, C. Wiel ⁵⁰, M. Wielers ¹³³, N. Wieseotte ⁹⁹, C. Wiglesworth ⁴², L.A.M. Wiik-Fuchs ⁵⁴, D.J. Wilbern ¹¹⁹, H.G. Wilkens ³⁶, D.M. Williams ⁴¹, H.H. Williams ¹²⁷, S. Williams ³², S. Willocq ¹⁰², P.J. Windischhofer ¹²⁵, F. Winklmeier ¹²², B.T. Winter ⁵⁴, M. Wittgen ¹⁴², M. Wobisch ⁹⁶, A. Wolf ⁹⁹, R. Wölker ¹²⁵, J. Wollrath ¹⁵⁹, M.W. Wolter ⁸⁵, H. Wolters ^{129a,129c}, V.W.S. Wong ¹⁶³, A.F. Wongel ⁴⁸, S.D. Worm ⁴⁸, B.K. Wosiek ⁸⁵, K.W. Woźniak ⁸⁵, K. Wraight ⁵⁹, J. Wu ^{14a,14d}, M. Wu ^{64a}, S.L. Wu ¹⁶⁹, X. Wu ⁵⁶, Y. Wu ^{62a}, Z. Wu ^{134,62a}, J. Wuerzinger ¹²⁵, T.R. Wyatt ¹⁰⁰, B.M. Wynne ⁵², S. Xella ⁴², L. Xia ^{14c}, M. Xia ^{14b}, J. Xiang ^{64c}, X. Xiao ¹⁰⁵, M. Xie ^{62a}, X. Xie ^{62a}, J. Xiong ^{17a}, I. Xiotidis ¹⁴⁵, D. Xu ^{14a}, H. Xu ^{62a}, H. Xu ^{62a}, L. Xu ^{62a}, R. Xu ¹²⁷, T. Xu ¹⁰⁵, W. Xu ¹⁰⁵, Y. Xu ^{14b}, Z. Xu ^{62b}, Z. Xu ¹⁴², B. Yabsley ¹⁴⁶, S. Yacoob ^{33a}, N. Yamaguchi ⁸⁸, Y. Yamaguchi ¹⁵³, H. Yamauchi ¹⁵⁶, T. Yamazaki ^{17a}, Y. Yamazaki ⁸³, J. Yan ^{62c}, S. Yan ¹²⁵, Z. Yan ²⁵, H.J. Yang ^{62c,62d}, H.T. Yang ^{17a}, S. Yang ^{62a}, T. Yang ^{64c}, X. Yang ^{62a}, X. Yang ^{14a}, Y. Yang ⁴⁴, Z. Yang ^{62a,105}, W-M. Yao ^{17a}, Y.C. Yap ⁴⁸, H. Ye ^{14c}, J. Ye ⁴⁴, S. Ye ²⁹, X. Ye ^{62a}, Y. Yeh ⁹⁵, I. Yeletsikh ³⁸, M.R. Yexley ⁹⁰, P. Yin ⁴¹, K. Yorita ¹⁶⁷, C.J.S. Young ⁵⁴, C. Young ¹⁴², M. Yuan ¹⁰⁵, R. Yuan ^{62b,k}, L. Yue ⁹⁵, X. Yue ^{63a}, M. Zaazoua ^{35e}, B. Zabinski ⁸⁵, E. Zaid ⁵², T. Zakareishvili ^{148b}, N. Zakharchuk ³⁴, S. Zambito ⁵⁶, J.A. Zamora Saa ^{136d}, J. Zang ¹⁵², D. Zanzi ⁵⁴, O. Zaplatilek ¹³¹, S.V. Zeibner ⁴⁹, C. Zeitnitz ¹⁷⁰, J.C. Zeng ¹⁶¹, D.T. Zenger Jr ²⁶, O. Zenin ³⁷, T. Ženiš ^{28a}, S. Zenz ⁹³, S. Zerradi ^{35a}, D. Zerwas ⁶⁶, B. Zhang ^{14c}, D.F. Zhang ¹³⁸, G. Zhang ^{14b}, J. Zhang ⁶, K. Zhang ^{14a,14d}, L. Zhang ^{14c}, P. Zhang ^{14a,14d}, R. Zhang ¹⁶⁹, S. Zhang ¹⁰⁵, T. Zhang ¹⁵², X. Zhang ^{62c}, X. Zhang ^{62b}, Z. Zhang ^{17a}, Z. Zhang ⁶⁶, H. Zhao ¹³⁷, P. Zhao ⁵¹, T. Zhao ^{62b}, Y. Zhao ¹³⁵, Z. Zhao ^{62a}, A. Zhemchugov ³⁸, Z. Zheng ¹⁴², D. Zhong ¹⁶¹, B. Zhou ¹⁰⁵, C. Zhou ¹⁶⁹, H. Zhou ⁷, N. Zhou ^{62c}, Y. Zhou ⁷, C.G. Zhu ^{62b}, C. Zhu ^{14a,14d}, H.L. Zhu ^{62a}, H. Zhu ^{14a}, J. Zhu ¹⁰⁵, Y. Zhu ^{62c}, Y. Zhu ^{62a}, X. Zhuang ^{14a}, K. Zhukov ³⁷, V. Zhulanov ³⁷, N.I. Zimine ³⁸, J. Zinsser ^{63b}, M. Ziolkowski ¹⁴⁰, L. Živković ¹⁵, A. Zoccoli ^{23b,23a}, K. Zoch ⁵⁶, T.G. Zorbas ¹³⁸, O. Zormpa ⁴⁶, W. Zou ⁴¹, L. Zwalinski ³⁶.

¹Department of Physics, University of Adelaide, Adelaide; Australia.

²Department of Physics, University of Alberta, Edmonton AB; Canada.

³(^a)Department of Physics, Ankara University, Ankara; (^b)Division of Physics, TOBB University of Economics and Technology, Ankara; Türkiye.

⁴LAPP, Université Savoie Mont Blanc, CNRS/IN2P3, Annecy; France.

⁵APC, Université Paris Cité, CNRS/IN2P3, Paris; France.

⁶High Energy Physics Division, Argonne National Laboratory, Argonne IL; United States of America.

⁷Department of Physics, University of Arizona, Tucson AZ; United States of America.

⁸Department of Physics, University of Texas at Arlington, Arlington TX; United States of America.

⁹Physics Department, National and Kapodistrian University of Athens, Athens; Greece.

¹⁰Physics Department, National Technical University of Athens, Zografou; Greece.

¹¹Department of Physics, University of Texas at Austin, Austin TX; United States of America.

¹²Institute of Physics, Azerbaijan Academy of Sciences, Baku; Azerbaijan.

¹³Institut de Física d'Altes Energies (IFAE), Barcelona Institute of Science and Technology, Barcelona; Spain.

¹⁴(^a)Institute of High Energy Physics, Chinese Academy of Sciences, Beijing; (^b)Physics Department, Tsinghua University, Beijing; (^c)Department of Physics, Nanjing University, Nanjing; (^d)University of Chinese Academy of Science (UCAS), Beijing; China.

¹⁵Institute of Physics, University of Belgrade, Belgrade; Serbia.

¹⁶Department for Physics and Technology, University of Bergen, Bergen; Norway.

- ^{17(a)}Physics Division, Lawrence Berkeley National Laboratory, Berkeley CA;^(b)University of California, Berkeley CA; United States of America.
- ¹⁸Institut für Physik, Humboldt Universität zu Berlin, Berlin; Germany.
- ¹⁹Albert Einstein Center for Fundamental Physics and Laboratory for High Energy Physics, University of Bern, Bern; Switzerland.
- ²⁰School of Physics and Astronomy, University of Birmingham, Birmingham; United Kingdom.
- ^{21(a)}Department of Physics, Bogazici University, Istanbul;^(b)Department of Physics Engineering, Gaziantep University, Gaziantep;^(c)Department of Physics, Istanbul University, Istanbul;^(d)Istinye University, Sariyer, Istanbul; Türkiye.
- ^{22(a)}Facultad de Ciencias y Centro de Investigaciones, Universidad Antonio Nariño, Bogotá;^(b)Departamento de Física, Universidad Nacional de Colombia, Bogotá; Colombia.
- ^{23(a)}Dipartimento di Fisica e Astronomia A. Righi, Università di Bologna, Bologna;^(b)INFN Sezione di Bologna; Italy.
- ²⁴Physikalisches Institut, Universität Bonn, Bonn; Germany.
- ²⁵Department of Physics, Boston University, Boston MA; United States of America.
- ²⁶Department of Physics, Brandeis University, Waltham MA; United States of America.
- ^{27(a)}Transilvania University of Brasov, Brasov;^(b)Horia Hulubei National Institute of Physics and Nuclear Engineering, Bucharest;^(c)Department of Physics, Alexandru Ioan Cuza University of Iasi, Iasi;^(d)National Institute for Research and Development of Isotopic and Molecular Technologies, Physics Department, Cluj-Napoca;^(e)University Politehnica Bucharest, Bucharest;^(f)West University in Timisoara, Timisoara;^(g)Faculty of Physics, University of Bucharest, Bucharest; Romania.
- ^{28(a)}Faculty of Mathematics, Physics and Informatics, Comenius University, Bratislava;^(b)Department of Subnuclear Physics, Institute of Experimental Physics of the Slovak Academy of Sciences, Kosice; Slovak Republic.
- ²⁹Physics Department, Brookhaven National Laboratory, Upton NY; United States of America.
- ³⁰Universidad de Buenos Aires, Facultad de Ciencias Exactas y Naturales, Departamento de Física, y CONICET, Instituto de Física de Buenos Aires (IFIBA), Buenos Aires; Argentina.
- ³¹California State University, CA; United States of America.
- ³²Cavendish Laboratory, University of Cambridge, Cambridge; United Kingdom.
- ^{33(a)}Department of Physics, University of Cape Town, Cape Town;^(b)iThemba Labs, Western Cape;^(c)Department of Mechanical Engineering Science, University of Johannesburg, Johannesburg;^(d)National Institute of Physics, University of the Philippines Diliman (Philippines);^(e)University of South Africa, Department of Physics, Pretoria;^(f)University of Zululand, KwaDlangezwa;^(g)School of Physics, University of the Witwatersrand, Johannesburg; South Africa.
- ³⁴Department of Physics, Carleton University, Ottawa ON; Canada.
- ^{35(a)}Faculté des Sciences Ain Chock, Réseau Universitaire de Physique des Hautes Energies - Université Hassan II, Casablanca;^(b)Faculté des Sciences, Université Ibn-Tofail, Kénitra;^(c)Faculté des Sciences Semlalia, Université Cadi Ayyad, LPHEA-Marrakech;^(d)LPMR, Faculté des Sciences, Université Mohamed Premier, Oujda;^(e)Faculté des sciences, Université Mohammed V, Rabat;^(f)Institute of Applied Physics, Mohammed VI Polytechnic University, Ben Guerir; Morocco.
- ³⁶CERN, Geneva; Switzerland.
- ³⁷Affiliated with an institute covered by a cooperation agreement with CERN.
- ³⁸Affiliated with an international laboratory covered by a cooperation agreement with CERN.
- ³⁹Enrico Fermi Institute, University of Chicago, Chicago IL; United States of America.
- ⁴⁰LPC, Université Clermont Auvergne, CNRS/IN2P3, Clermont-Ferrand; France.
- ⁴¹Nevis Laboratory, Columbia University, Irvington NY; United States of America.
- ⁴²Niels Bohr Institute, University of Copenhagen, Copenhagen; Denmark.

- ^{43(a)}Dipartimento di Fisica, Università della Calabria, Rende; ^(b)INFN Gruppo Collegato di Cosenza, Laboratori Nazionali di Frascati; Italy.
- ⁴⁴Physics Department, Southern Methodist University, Dallas TX; United States of America.
- ⁴⁵Physics Department, University of Texas at Dallas, Richardson TX; United States of America.
- ⁴⁶National Centre for Scientific Research "Demokritos", Agia Paraskevi; Greece.
- ^{47(a)}Department of Physics, Stockholm University; ^(b)Oskar Klein Centre, Stockholm; Sweden.
- ⁴⁸Deutsches Elektronen-Synchrotron DESY, Hamburg and Zeuthen; Germany.
- ⁴⁹Fakultät Physik, Technische Universität Dortmund, Dortmund; Germany.
- ⁵⁰Institut für Kern- und Teilchenphysik, Technische Universität Dresden, Dresden; Germany.
- ⁵¹Department of Physics, Duke University, Durham NC; United States of America.
- ⁵²SUPA - School of Physics and Astronomy, University of Edinburgh, Edinburgh; United Kingdom.
- ⁵³INFN e Laboratori Nazionali di Frascati, Frascati; Italy.
- ⁵⁴Physikalisches Institut, Albert-Ludwigs-Universität Freiburg, Freiburg; Germany.
- ⁵⁵II. Physikalisches Institut, Georg-August-Universität Göttingen, Göttingen; Germany.
- ⁵⁶Département de Physique Nucléaire et Corpusculaire, Université de Genève, Genève; Switzerland.
- ^{57(a)}Dipartimento di Fisica, Università di Genova, Genova; ^(b)INFN Sezione di Genova; Italy.
- ⁵⁸II. Physikalisches Institut, Justus-Liebig-Universität Giessen, Giessen; Germany.
- ⁵⁹SUPA - School of Physics and Astronomy, University of Glasgow, Glasgow; United Kingdom.
- ⁶⁰LPSC, Université Grenoble Alpes, CNRS/IN2P3, Grenoble INP, Grenoble; France.
- ⁶¹Laboratory for Particle Physics and Cosmology, Harvard University, Cambridge MA; United States of America.
- ^{62(a)}Department of Modern Physics and State Key Laboratory of Particle Detection and Electronics, University of Science and Technology of China, Hefei; ^(b)Institute of Frontier and Interdisciplinary Science and Key Laboratory of Particle Physics and Particle Irradiation (MOE), Shandong University, Qingdao; ^(c)School of Physics and Astronomy, Shanghai Jiao Tong University, Key Laboratory for Particle Astrophysics and Cosmology (MOE), SKLPPC, Shanghai; ^(d)Tsung-Dao Lee Institute, Shanghai; China.
- ^{63(a)}Kirchhoff-Institut für Physik, Ruprecht-Karls-Universität Heidelberg, Heidelberg; ^(b)Physikalisches Institut, Ruprecht-Karls-Universität Heidelberg, Heidelberg; Germany.
- ^{64(a)}Department of Physics, Chinese University of Hong Kong, Shatin, N.T., Hong Kong; ^(b)Department of Physics, University of Hong Kong, Hong Kong; ^(c)Department of Physics and Institute for Advanced Study, Hong Kong University of Science and Technology, Clear Water Bay, Kowloon, Hong Kong; China.
- ⁶⁵Department of Physics, National Tsing Hua University, Hsinchu; Taiwan.
- ⁶⁶IJCLab, Université Paris-Saclay, CNRS/IN2P3, 91405, Orsay; France.
- ⁶⁷Department of Physics, Indiana University, Bloomington IN; United States of America.
- ^{68(a)}INFN Gruppo Collegato di Udine, Sezione di Trieste, Udine; ^(b)ICTP, Trieste; ^(c)Dipartimento Politecnico di Ingegneria e Architettura, Università di Udine, Udine; Italy.
- ^{69(a)}INFN Sezione di Lecce; ^(b)Dipartimento di Matematica e Fisica, Università del Salento, Lecce; Italy.
- ^{70(a)}INFN Sezione di Milano; ^(b)Dipartimento di Fisica, Università di Milano, Milano; Italy.
- ^{71(a)}INFN Sezione di Napoli; ^(b)Dipartimento di Fisica, Università di Napoli, Napoli; Italy.
- ^{72(a)}INFN Sezione di Pavia; ^(b)Dipartimento di Fisica, Università di Pavia, Pavia; Italy.
- ^{73(a)}INFN Sezione di Pisa; ^(b)Dipartimento di Fisica E. Fermi, Università di Pisa, Pisa; Italy.
- ^{74(a)}INFN Sezione di Roma; ^(b)Dipartimento di Fisica, Sapienza Università di Roma, Roma; Italy.
- ^{75(a)}INFN Sezione di Roma Tor Vergata; ^(b)Dipartimento di Fisica, Università di Roma Tor Vergata, Roma; Italy.
- ^{76(a)}INFN Sezione di Roma Tre; ^(b)Dipartimento di Matematica e Fisica, Università Roma Tre, Roma; Italy.
- ^{77(a)}INFN-TIFPA; ^(b)Università degli Studi di Trento, Trento; Italy.

- ⁷⁸Universität Innsbruck, Department of Astro and Particle Physics, Innsbruck; Austria.
- ⁷⁹University of Iowa, Iowa City IA; United States of America.
- ⁸⁰Department of Physics and Astronomy, Iowa State University, Ames IA; United States of America.
- ⁸¹(^a) Departamento de Engenharia Elétrica, Universidade Federal de Juiz de Fora (UFJF), Juiz de Fora; (^b) Universidade Federal do Rio De Janeiro COPPE/EE/IF, Rio de Janeiro; (^c) Instituto de Física, Universidade de São Paulo, São Paulo; (^d) Rio de Janeiro State University, Rio de Janeiro; Brazil.
- ⁸²KEK, High Energy Accelerator Research Organization, Tsukuba; Japan.
- ⁸³Graduate School of Science, Kobe University, Kobe; Japan.
- ⁸⁴(^a) AGH University of Science and Technology, Faculty of Physics and Applied Computer Science, Krakow; (^b) Marian Smoluchowski Institute of Physics, Jagiellonian University, Krakow; Poland.
- ⁸⁵Institute of Nuclear Physics Polish Academy of Sciences, Krakow; Poland.
- ⁸⁶Faculty of Science, Kyoto University, Kyoto; Japan.
- ⁸⁷Kyoto University of Education, Kyoto; Japan.
- ⁸⁸Research Center for Advanced Particle Physics and Department of Physics, Kyushu University, Fukuoka ; Japan.
- ⁸⁹Instituto de Física La Plata, Universidad Nacional de La Plata and CONICET, La Plata; Argentina.
- ⁹⁰Physics Department, Lancaster University, Lancaster; United Kingdom.
- ⁹¹Oliver Lodge Laboratory, University of Liverpool, Liverpool; United Kingdom.
- ⁹²Department of Experimental Particle Physics, Jožef Stefan Institute and Department of Physics, University of Ljubljana, Ljubljana; Slovenia.
- ⁹³School of Physics and Astronomy, Queen Mary University of London, London; United Kingdom.
- ⁹⁴Department of Physics, Royal Holloway University of London, Egham; United Kingdom.
- ⁹⁵Department of Physics and Astronomy, University College London, London; United Kingdom.
- ⁹⁶Louisiana Tech University, Ruston LA; United States of America.
- ⁹⁷Fysiska institutionen, Lunds universitet, Lund; Sweden.
- ⁹⁸Departamento de Física Teórica C-15 and CIAFF, Universidad Autónoma de Madrid, Madrid; Spain.
- ⁹⁹Institut für Physik, Universität Mainz, Mainz; Germany.
- ¹⁰⁰School of Physics and Astronomy, University of Manchester, Manchester; United Kingdom.
- ¹⁰¹CPPM, Aix-Marseille Université, CNRS/IN2P3, Marseille; France.
- ¹⁰²Department of Physics, University of Massachusetts, Amherst MA; United States of America.
- ¹⁰³Department of Physics, McGill University, Montreal QC; Canada.
- ¹⁰⁴School of Physics, University of Melbourne, Victoria; Australia.
- ¹⁰⁵Department of Physics, University of Michigan, Ann Arbor MI; United States of America.
- ¹⁰⁶Department of Physics and Astronomy, Michigan State University, East Lansing MI; United States of America.
- ¹⁰⁷Group of Particle Physics, University of Montreal, Montreal QC; Canada.
- ¹⁰⁸Fakultät für Physik, Ludwig-Maximilians-Universität München, München; Germany.
- ¹⁰⁹Max-Planck-Institut für Physik (Werner-Heisenberg-Institut), München; Germany.
- ¹¹⁰Graduate School of Science and Kobayashi-Maskawa Institute, Nagoya University, Nagoya; Japan.
- ¹¹¹Department of Physics and Astronomy, University of New Mexico, Albuquerque NM; United States of America.
- ¹¹²Institute for Mathematics, Astrophysics and Particle Physics, Radboud University/Nikhef, Nijmegen; Netherlands.
- ¹¹³Nikhef National Institute for Subatomic Physics and University of Amsterdam, Amsterdam; Netherlands.
- ¹¹⁴Department of Physics, Northern Illinois University, DeKalb IL; United States of America.
- ¹¹⁵(^a) New York University Abu Dhabi, Abu Dhabi; (^b) University of Sharjah, Sharjah; United Arab

Emirates.

¹¹⁶Department of Physics, New York University, New York NY; United States of America.

¹¹⁷Ochanomizu University, Otsuka, Bunkyo-ku, Tokyo; Japan.

¹¹⁸Ohio State University, Columbus OH; United States of America.

¹¹⁹Homer L. Dodge Department of Physics and Astronomy, University of Oklahoma, Norman OK; United States of America.

¹²⁰Department of Physics, Oklahoma State University, Stillwater OK; United States of America.

¹²¹Palacký University, Joint Laboratory of Optics, Olomouc; Czech Republic.

¹²²Institute for Fundamental Science, University of Oregon, Eugene, OR; United States of America.

¹²³Graduate School of Science, Osaka University, Osaka; Japan.

¹²⁴Department of Physics, University of Oslo, Oslo; Norway.

¹²⁵Department of Physics, Oxford University, Oxford; United Kingdom.

¹²⁶LPNHE, Sorbonne Université, Université Paris Cité, CNRS/IN2P3, Paris; France.

¹²⁷Department of Physics, University of Pennsylvania, Philadelphia PA; United States of America.

¹²⁸Department of Physics and Astronomy, University of Pittsburgh, Pittsburgh PA; United States of America.

¹²⁹(^a)Laboratório de Instrumentação e Física Experimental de Partículas - LIP, Lisboa; (^b)Departamento de Física, Faculdade de Ciências, Universidade de Lisboa, Lisboa; (^c)Departamento de Física, Universidade de Coimbra, Coimbra; (^d)Centro de Física Nuclear da Universidade de Lisboa, Lisboa; (^e)Departamento de Física, Universidade do Minho, Braga; (^f)Departamento de Física Teórica y del Cosmos, Universidad de Granada, Granada (Spain); (^g)Departamento de Física, Instituto Superior Técnico, Universidade de Lisboa, Lisboa; Portugal.

¹³⁰Institute of Physics of the Czech Academy of Sciences, Prague; Czech Republic.

¹³¹Czech Technical University in Prague, Prague; Czech Republic.

¹³²Charles University, Faculty of Mathematics and Physics, Prague; Czech Republic.

¹³³Particle Physics Department, Rutherford Appleton Laboratory, Didcot; United Kingdom.

¹³⁴IRFU, CEA, Université Paris-Saclay, Gif-sur-Yvette; France.

¹³⁵Santa Cruz Institute for Particle Physics, University of California Santa Cruz, Santa Cruz CA; United States of America.

¹³⁶(^a)Departamento de Física, Pontificia Universidad Católica de Chile, Santiago; (^b)Millennium Institute for Subatomic physics at high energy frontier (SAPHIR), Santiago; (^c)Instituto de Investigación Multidisciplinario en Ciencia y Tecnología, y Departamento de Física, Universidad de La Serena; (^d)Universidad Andres Bello, Department of Physics, Santiago; (^e)Instituto de Alta Investigación, Universidad de Tarapacá, Arica; (^f)Departamento de Física, Universidad Técnica Federico Santa María, Valparaíso; Chile.

¹³⁷Department of Physics, University of Washington, Seattle WA; United States of America.

¹³⁸Department of Physics and Astronomy, University of Sheffield, Sheffield; United Kingdom.

¹³⁹Department of Physics, Shinshu University, Nagano; Japan.

¹⁴⁰Department Physik, Universität Siegen, Siegen; Germany.

¹⁴¹Department of Physics, Simon Fraser University, Burnaby BC; Canada.

¹⁴²SLAC National Accelerator Laboratory, Stanford CA; United States of America.

¹⁴³Department of Physics, Royal Institute of Technology, Stockholm; Sweden.

¹⁴⁴Departments of Physics and Astronomy, Stony Brook University, Stony Brook NY; United States of America.

¹⁴⁵Department of Physics and Astronomy, University of Sussex, Brighton; United Kingdom.

¹⁴⁶School of Physics, University of Sydney, Sydney; Australia.

¹⁴⁷Institute of Physics, Academia Sinica, Taipei; Taiwan.

- ¹⁴⁸(^a)E. Andronikashvili Institute of Physics, Iv. Javakhishvili Tbilisi State University, Tbilisi;^(b)High Energy Physics Institute, Tbilisi State University, Tbilisi;^(c)University of Georgia, Tbilisi; Georgia.
- ¹⁴⁹Department of Physics, Technion, Israel Institute of Technology, Haifa; Israel.
- ¹⁵⁰Raymond and Beverly Sackler School of Physics and Astronomy, Tel Aviv University, Tel Aviv; Israel.
- ¹⁵¹Department of Physics, Aristotle University of Thessaloniki, Thessaloniki; Greece.
- ¹⁵²International Center for Elementary Particle Physics and Department of Physics, University of Tokyo, Tokyo; Japan.
- ¹⁵³Department of Physics, Tokyo Institute of Technology, Tokyo; Japan.
- ¹⁵⁴Department of Physics, University of Toronto, Toronto ON; Canada.
- ¹⁵⁵(^a)TRIUMF, Vancouver BC;^(b)Department of Physics and Astronomy, York University, Toronto ON; Canada.
- ¹⁵⁶Division of Physics and Tomonaga Center for the History of the Universe, Faculty of Pure and Applied Sciences, University of Tsukuba, Tsukuba; Japan.
- ¹⁵⁷Department of Physics and Astronomy, Tufts University, Medford MA; United States of America.
- ¹⁵⁸United Arab Emirates University, Al Ain; United Arab Emirates.
- ¹⁵⁹Department of Physics and Astronomy, University of California Irvine, Irvine CA; United States of America.
- ¹⁶⁰Department of Physics and Astronomy, University of Uppsala, Uppsala; Sweden.
- ¹⁶¹Department of Physics, University of Illinois, Urbana IL; United States of America.
- ¹⁶²Instituto de Física Corpuscular (IFIC), Centro Mixto Universidad de Valencia - CSIC, Valencia; Spain.
- ¹⁶³Department of Physics, University of British Columbia, Vancouver BC; Canada.
- ¹⁶⁴Department of Physics and Astronomy, University of Victoria, Victoria BC; Canada.
- ¹⁶⁵Fakultät für Physik und Astronomie, Julius-Maximilians-Universität Würzburg, Würzburg; Germany.
- ¹⁶⁶Department of Physics, University of Warwick, Coventry; United Kingdom.
- ¹⁶⁷Waseda University, Tokyo; Japan.
- ¹⁶⁸Department of Particle Physics and Astrophysics, Weizmann Institute of Science, Rehovot; Israel.
- ¹⁶⁹Department of Physics, University of Wisconsin, Madison WI; United States of America.
- ¹⁷⁰Fakultät für Mathematik und Naturwissenschaften, Fachgruppe Physik, Bergische Universität Wuppertal, Wuppertal; Germany.
- ¹⁷¹Department of Physics, Yale University, New Haven CT; United States of America.
- ^a Also Affiliated with an institute covered by a cooperation agreement with CERN.
- ^b Also at An-Najah National University, Nablus; Palestine.
- ^c Also at Borough of Manhattan Community College, City University of New York, New York NY; United States of America.
- ^d Also at Bruno Kessler Foundation, Trento; Italy.
- ^e Also at Center for High Energy Physics, Peking University; China.
- ^f Also at Centro Studi e Ricerche Enrico Fermi; Italy.
- ^g Also at CERN, Geneva; Switzerland.
- ^h Also at Département de Physique Nucléaire et Corpusculaire, Université de Genève, Genève; Switzerland.
- ⁱ Also at Departament de Física de la Universitat Autònoma de Barcelona, Barcelona; Spain.
- ^j Also at Department of Financial and Management Engineering, University of the Aegean, Chios; Greece.
- ^k Also at Department of Physics and Astronomy, Michigan State University, East Lansing MI; United States of America.
- ^l Also at Department of Physics and Astronomy, University of Louisville, Louisville, KY; United States of America.
- ^m Also at Department of Physics, Ben Gurion University of the Negev, Beer Sheva; Israel.

- ⁿ Also at Department of Physics, California State University, East Bay; United States of America.
- ^o Also at Department of Physics, California State University, Sacramento; United States of America.
- ^p Also at Department of Physics, King's College London, London; United Kingdom.
- ^q Also at Department of Physics, Stanford University, Stanford CA; United States of America.
- ^r Also at Department of Physics, University of Fribourg, Fribourg; Switzerland.
- ^s Also at Department of Physics, University of Thessaly; Greece.
- ^t Also at Department of Physics, Westmont College, Santa Barbara; United States of America.
- ^u Also at Hellenic Open University, Patras; Greece.
- ^v Also at Institutio Catalana de Recerca i Estudis Avancats, ICREA, Barcelona; Spain.
- ^w Also at Institut für Experimentalphysik, Universität Hamburg, Hamburg; Germany.
- ^x Also at Institute for Nuclear Research and Nuclear Energy (INRNE) of the Bulgarian Academy of Sciences, Sofia; Bulgaria.
- ^y Also at Institute of Particle Physics (IPP); Canada.
- ^z Also at Institute of Physics, Azerbaijan Academy of Sciences, Baku; Azerbaijan.
- ^{aa} Also at Institute of Theoretical Physics, Ilia State University, Tbilisi; Georgia.
- ^{ab} Also at L2IT, Université de Toulouse, CNRS/IN2P3, UPS, Toulouse; France.
- ^{ac} Also at Lawrence Livermore National Laboratory, Livermore; United States of America.
- ^{ad} Also at National Institute of Physics, University of the Philippines Diliman (Philippines); Philippines.
- ^{ae} Also at Technical University of Munich, Munich; Germany.
- ^{af} Also at The Collaborative Innovation Center of Quantum Matter (CICQM), Beijing; China.
- ^{ag} Also at TRIUMF, Vancouver BC; Canada.
- ^{ah} Also at Università di Napoli Parthenope, Napoli; Italy.
- ^{ai} Also at University of Chinese Academy of Sciences (UCAS), Beijing; China.
- ^{aj} Also at University of Colorado Boulder, Department of Physics, Colorado; United States of America.
- ^{ak} Also at Yeditepe University, Physics Department, Istanbul; Türkiye.
- * Deceased